Modulation and function of microglial phenotypes

DISSERTATION

ZUR ERLANGUNG DES DOKTORGRADES
DER NATURWISSENSCHAFTEN (DR. RER. NAT.)
DER NATURWISSENSCHAFTLICHEN FAKULTÄT III
BIOLOGIE UND VORKLINISCHE MEDIZIN DER UNIVERSITÄT REGENSBURG

vorgelegt von
Marcus Karlstetter
aus Passau

Februar 2012

Das Promotionsgesuch wurde eingereicht am: 7. Februar 2012

Die Arbeit wurde angeleitet von: Prof. Dr. Thomas Langmann

Unterschrift:

Prüfungsausschuss:

Vorsitzender:	Prof. Dr. Thomas Dresselhaus
Erstgutachter:	Prof. Dr. Thomas Langmann
Zweitgutachter:	Prof. Dr. Stephan Schneuwly
Drittprüfer:	Prof. Dr. Wolf Hayo Castrop

Meinen Eltern

„Das Große kommt nicht allein durch Impuls zustande,
sondern ist eine Aneinanderkettung kleiner Dinge,
die zu einem Ganzen vereint worden sind.“

Vincent van Gogh (1853-1890)

Table of contents

1 General introduction

1.1 The building plan and function of the retina

The mammalian retina represents one of the most complex tissues of the human body. This piece of tissue, embedded in the eyecup, equips us with the most important sense: vision. The complexity of the retina is represented by its unique cellular structure bearing more than 55 different cell types which are each highly specialized (Masland 2001).

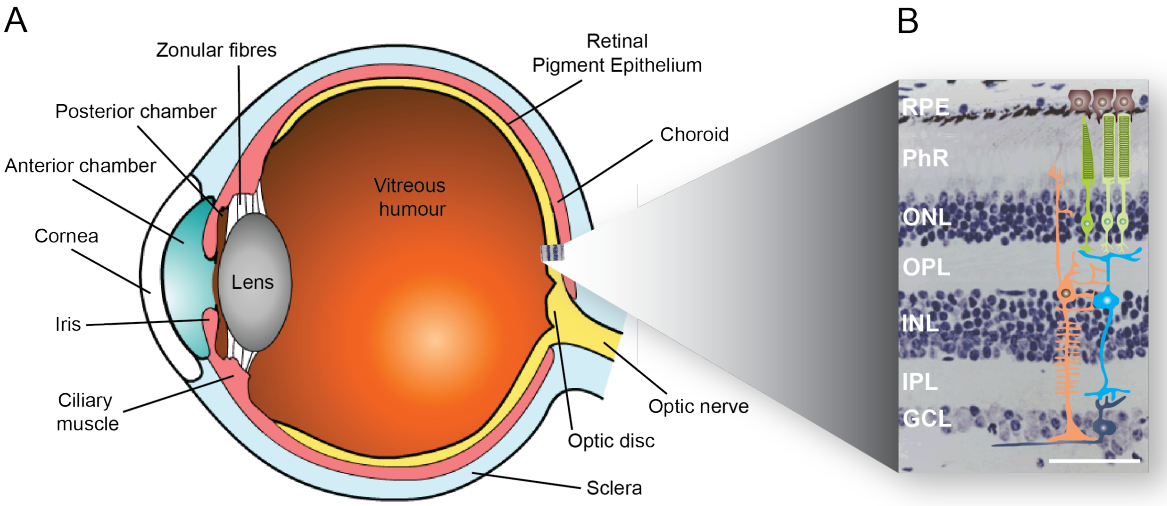

Figure 1 Gross anatomy of the eyeball and detailed cross-section of the human retina. (A) The retina is lining the posterior segment of the eyeball. (B) Stained cross-section through the human retina with schematic cell types for better illustration. Orange: Müller cells; grey: Ganglion cells; blue: bipolar cells; light green: rods; green: cones; brown: retinal pigment epithelial cells; RPE, retinal pigment epithelium; PhR, photoreceptor layer; ONL, outer nuclear layer; OPL, outer plexiform layer; INL, inner nuclear layer; IPL, inner plexiform layer; GCL, ganglion cell layer. The white scale bar represents 100 µm. (Eyeball modified from Campbell et al. 2010); cross section modified from http://www.oculist.net/downaton502/prof/ebook/duanes/pages/v8/v8c013.html).

In detail, the retina is a polarized tissue, organized in layers of different cell types, with a thickness ranging up to 200 µm (Klinke et al. 2003). Light has to pass through all retinal layers in order to reach the light-sensitive cells of the retina, the photoreceptors. The human retina contains approximately 110 million rod- and 6 million cone-photoreceptors (Klinke et al. 2003), ensuring adaptation to day- and night conditions. Cone-photoreceptors are specialized in day- and color vision and enriched in the macular, whereas rod photoreceptors enable us to see during weak light conditions, located predominantly in peripheral areas of the retina.

The photoreceptor layer (Fig. 1, PhR) is embedded in the retinal pigment epithelium (RPE) which phagocytoses old photoreceptor discs, recycles the light sensitive pigment rhodopsin and provides nutrients for photoreceptors. The nuclei of photoreceptors are tightly stacked in the outer nuclear layer (ONL) and connected to the outer segments (OS) by the connecting cilium, which transports proteins from the golgi apparatus towards the OS layer. Absorption of photons by rhodopsin induces the isomerization of 11-cis-retinal to all-trans-retinal and triggers the phototransduction cascade, involving hyperpolarization of the photoreceptor membrane. Nuclei of bipolar and horizontal cells constitute the inner nuclear layer (INL), their synapses are connected to photoreceptors in the outer plexiform layer (OPL). The photoreceptor signal is forwarded to ganglion cells in the ganglion cell layer (GCL) via synapses in the inner plexiform layer (IPL). Amacrine cells in the INL modulate signal transduction between bipolar cells and ganglion cells, whose bundled axons are forming the optic nerve, the retina's connection to the brain (Klinke et al. 2003). Müller glia cells span the entire retina, exerting supportive functions for retinal neurons and signal procession (Bringmann et al. 2006).

1.2 Inherited diseases of the retina and apoptosis

Hereditary eye diseases are a major cause for blindness worldwide. The polarized nature of the retina and the composition of highly specialized cell types represent high susceptibility to genetic defects. To date, the Retnet (Retinal Information Network) database counts 249 genes related to retinal disease. The most prevalent monogenic disorder is *Retinitis Pigmentosa* (RP) with more than 50 different genes described (https://sph.uth.tmc.edu/RetNet/disease.htm). Besides RP, *Age-related Macular Degeneration* (AMD) represents a major cause of vision loss in the industrialized world. Unlike monogenic disorders, AMD is classified as a complex genetic disease. Multiple environmental factors and various genetic variants increase the risk for AMD development and contribute to the pathogenesis of retinal degeneration (Jager et al. 2008; Yuhong Chen 2010; Swaroop et al. 2007).

Due to poor availability of human retinal tissue, numerous animal models of retinal dystrophies have been generated to gain insight into the pathology of degenerative diseases. Although a multitude of diverse factors initiate retinal dystrophies, cell

death represents the common sink in disease progression (Stone et al. 1999). Several studies, investigating the pathology of inherited retinal degeneration in rodent models, observe photoreceptor death. The most prominent apoptotic events occur in the nuclear layers of the retina, independent of the underlying genetic defect (W. Fan et al. 2010; Essner 1979; Sano et al. 2006; Tso et al. 1994; Chang & Hao 1993). Likewise, Retinoschisin-deficient ($Rs1h^{-/Y}$) mice develop massive photoreceptor degeneration very early in postnatal development, accompanied by splitting (schisis) of retinal layers (Weber 2002). In human dystrophic *postmortem* retinas obtained from AMD patients, profound cell death in regions of atrophy indicates a similar role of apoptosis for AMD pathology as seen in the rodent degeneration models (Dunaief et al. 2002).

On the molecular level, apoptosis is a strict series of cellular signaling events, leading to autonomous cell death. Entry into apoptosis is triggered by receptor-induced (extrinsic) or intracellular (intrinsic) signaling pathways. In the extrinsic route, transmembrane death-receptors like *tumor necrosis factor receptor 1* (TNFR1) or CD95 (alias FAS) are activated by their specific ligands (Ashkenazi & Dixit 1998), resulting in the formation of a death-induced signaling complex (DISC), which includes *caspases 8* and *10* (Ashkenazi & Dixit 1998; Chaigne-Delalande et al. 2008). Intrinsic apoptosis is initiated in mitochondria by cellular stressors like DNA damage, ultraviolet light or deprivation of trophic factors (Lo et al. 2011; Brenner & Mak 2009). Subsequent release of *cytochrome c* initiates the formation of the apoptosome, involving initiator *caspase 9* (Brenner & Mak 2009). Both pathways activate effector *caspases 3*, *6* and *7* as downstrean targets (Lavrik 2010). Molecular and histological studies of dystrophic retinas suggest that both types of apoptosis are involved in photoreceptor death (Mohlin et al. 2011; Lohr et al. 2006; Rohrer et al. 2004; Gehrig et al. 2007; Ebert et al. 2009).

1.3 Microglia biology

As unique hematopoetic cell types, macrophages constitute distinct resident populations in diverse tissues, to which they can adapt phenotypically and morphologically (Gordon & Taylor 2005). The phenotypic heterogeneity reflects the importance of macrophages in the maintenance of diverse tissues, a task that is

performed by microglia in the central nervous system (CNS). Based on observations in the brain, Rio-Hortega was the first to hypothesize, that microglia are mobile, macrophage-like cells, being an active part in all inflammatory and necrotic nerve tissues (Rio-Hortega 1939). Hickey and Kimura could confirm Rio-Hortega's hypothesis and showed that microglia are bone-marrow (BM) derived, immune competent cells (Hickey & Kimura 1988). Nowadays we know that microglia perform essential tasks in the healthy and diseased CNS that can be both detrimental and beneficial (Hanisch & Kettenmann 2007).

1.3.1 The origin of microglia

Primitive yolk sac macrophages establish the CNS population of microglia during embryonic development prior to blood brain barrier (BBB) formation (Ginhoux et al. 2010). Although the developmental origin of brain and retinal microglia have been clarified, it is still an open question, how renewal of the adult microglia population is performed. The BBB and respectively the blood retinal barrier (BRB) isolates the CNS and the retina from the periphery. It acts as a selective filter for the influx of molecules like energy substrates (Liebner et al. 2011), simultaneously restricting the intrusion of neurotoxic molecules and blood-derived leukocytes, which could harm the fragile neuronal tissue (Streit 2002). It is questioned whether under homeostatic conditions, blood-derived microglial precursors can cross the BBB/BRB in order to renew the population or if the population is maintained by *in situ* proliferation. Several studies performed in BM-chimeric mice, report donor-derived hematopoetic precursor invasion into the retina and CNS (H. Xu et al. 2007; Kezic & McMenamin 2008; Soulet & Rivest 2008; Mildner et al. 2007). In contradiction, engraftment of blood-derived cells were not, or only to a minor extent, observed in parabiont animal studies (Ginhoux et al. 2010; Ajami et al. 2007), arguing that irradiation during BM-chimera generation might impair BBB permeability and allow artificial blood-cell migration into the CNS (Mildner et al. 2007; Ginhoux et al. 2010). Notably, parabiont animals possess a co-joined blood circulation system, generating blood-chimeras without irradiation, which presents a closer physiological system (Ajami et al. 2007).

1.3.2 Physiological functions of retinal microglia

Pioneering studies in the developing mouse retina have revealed the presence of microglia, distributed in an array of cells throughout distinct regions (Hume 1983). The concept of 'resting' microglia arose from static observations in neuronal tissue, describing immobile microglial cells with long, branched protrusions (Hume 1983; Perry et al. 1985; Perry & Gordon 1988). In fact, novel *in vivo* imaging techniques revealed that the long microglial processes are highly dynamic subcellular structures, which continually survey the integrity of the surrounding environment (Nimmerjahn et al. 2005). In the healthy retina, microglia are distributed throughout the plexiform layers, frequently found at the margin to adjacent nuclear layers (Ebert et al. 2009; Karlstetter et al. 2010b; Eter et al. 2008). Microglial surveillance in the healthy retina is crucial for the maintenance of tissue homeostasis by performing tasks like clearance of cellular debris and apoptotic neurons (e.g. dying photoreceptors), secretion of trophic factors and monitoring synapse function (Streit 2002; Hanisch & Kettenmann 2007; Takahashi 2005; Wake et al. 2009). Neurons produce suppressive ligands like CD200 or CX3CL1 to stimulate essential maintenance tasks in microglia, yet avoiding neurotoxic immune activation. Constitutive ligand-induced receptor signaling via the CD200/CD200R- and CX3CL1/CX3CR1-axis, provides suppressive signals for microglia, preventing harmful activation during tissue homeostasis (Broderick et al. 2002; Hoek 2000; Carter & Dick 2004; Cardona et al. 2006). Simulatenously CD200 and CX3CL1 stimulate microglial migration and protrusion movements, to control the surveillance frequency and vigilance in healthy tissue (Carter & Dick 2004).

1.3.3 Mechanisms of pro-inflammatory microglial activation

The CNS has evolved a tightly controlled innate immune system, to protect fragile neuronal tissue from harmful adaptive immune reactions in response to damage and infection. Apart from the essential role in the healthy retina (see above), classical microglial activation is the result of any kind of subtle tissue damage (Hanisch & Kettenmann 2007). Perturbances in cell-cell communication with neurons and/or triggers from damaged cells, result in microglial activation. Initiation of microglial activation is associated with the release or presentation of soluble factors

from apoptotic cells, so called *damage-associated molecular patterns* (DAMPs). DAMPs are recognized by innate immune receptors on the microglial surface. In this respect, apoptotic neurons realease *high-mobility group protein 1* (HMGB1) which raises a pro-inflammatory response in microglia (Gao et al. 2011) via *toll-like receptor 4* (TLR4) and *toll-like receptor 9* (TLR-9) signaling (Park 2003). In parallel, the P2Y12 receptor mediates microglial activation by binding ATP sequestered from impaired cells (Haynes et al. 2006; Davalos et al. 2005). Both signaling events cause downstream nuclear translocation of *nuclear factor ‚kappa-light-chain-enhancer' of activated B-cells* (NFkB), triggering transcription of pro-inflammatory target gene clusters (Lotze & Tracey 2005; Brambilla et al. 2003).

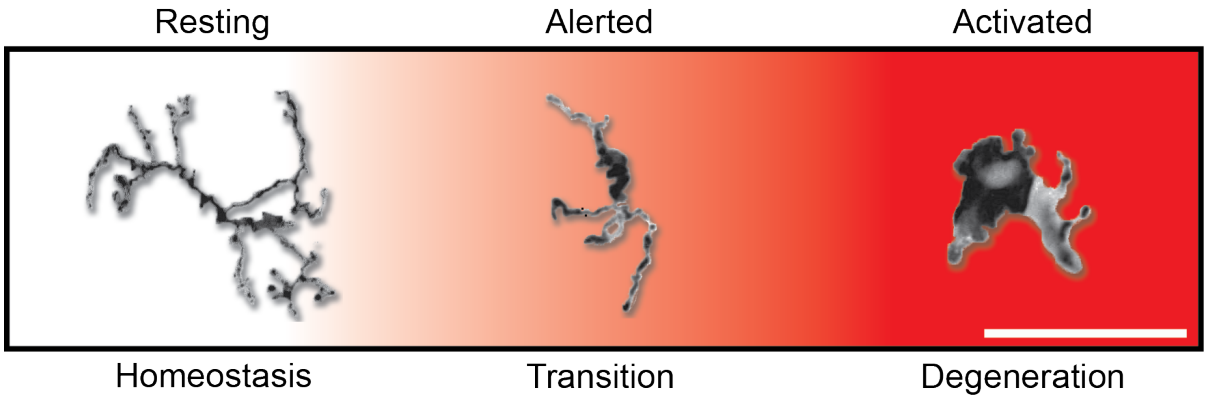

Figure 2 Morphological transition of microglia during the progression of retinal degeneration. Under homeostatic conditions (left), resting microglia build long and branched protrusions and carry out tissue surveillance and maintenance tasks. Perturbance of tissue homeostasis leads to alerted microglia (middle) with less branched protrusions and larger cell bodies. Ongoing apoptotic events during retinal degeneration directs to neurotoxic ('classical') activation of microglia (right), characterized by an amoeboid and bloated cell shape. The progression of retinal degeneration is shown as color gradient. Microglial cell shapes were excised from microphotographs of wholemount preparations from wt Mac Green mouse retinas (resting microglia) (Sasmono 2002) and Rs1h$^{-/Y}$ x Mac Green retinas (alerted and activated microglia). Pictures photographed by Stefanie Ebert. The white scale bar represents 50 µm.

As a consequence of pro-inflammatory activation, ramified microglia morphologically transform into an amoeboid shape and migrate towards the lesion spot (Fig. 2 & 3). Activated microglia express increased levels of *chemokine (C-C) motif ligand 2* (CCL2), a modulator of microglial migration and proliferation (Hinojosa et al. 2011), building a chemoattractant gradient at the lesion spot to attract further cells and shield the adjacent tissue environment from neurotoxic substances (Ambrosini & Aloisi 2004). Activated microglia sequester effector cytokines like *interleukin-6* (IL-6) and *interleukin-1β* (IL-1β) leading to paracrine activation of migrating microglia

(Krady et al. 2008; Ferreira et al. 2010). Clearance of damaged cells involves release of *nitric oxide* (NO) and *reactive oxygen species* (ROS) from microglia, followed by phagocytosis of cellular debris (Langmann 2007). During the resolution of inflammation, tissue homeostasis is reconstituted to prevent secondary damage of healthy surrounding tissue. As part of this, microglia exit the inflammatory program based on intrinsic feed-back regulators, that are induced during activation (J. Yang et al. 2005; Karlstetter et al. 2010a).

1.3.4 Microglial activation in retinal degeneration

Retinal degenerative diseases mostly affect broad areas of the retina and create a major imbalance of tissue homeostasis, perpetuating neuronal inflammation. Irrespective of the causative genetic defect and the subsequent pathomechanism, studies from retinal degeneration models report the early occurrence of amoeboid, activated microglia, predominantely in regions of photoreceptor loss, the ONL (Thanos 1991; Essner 1979; Zeiss 2004; Gehrig et al. 2007; Combadière et al. 2007; Ebert et al. 2009). In accordance with this, dystrophic retinas from human AMD and RP patients (Gupta et al. 2003; Penfold et al. 1985) reveal the appearance of activated microglia in the ONL, bearing engulfed fragments from apoptotic photoreceptors (Gupta et al. 2003). Laser-induced damage in mouse retinas shows an immediate microglial reaction, involving activation and migration to the lesion spot *in vivo* (Eter et al. 2008; J. E. Lee et al. 2008). Resting microglia in the proximity of the lesion site, start directed remodelling of their protrusions within minutes after laser-damage (J. E. Lee et al. 2008). One hour after damage, activated microglia accumulate at the damage site (Eter et al. 2008). Due to the rapid progression of degeneration, the $Rs1h^{-/Y}$ mouse model (Fig. 3) allows staging of microglial activation in respect to degenerative processes at high resolution. Migration of activated microglia into the INL of very young $Rs1h^{-/Y}$ retinas can be observed even before the occurence of signs of apoptosis (Ebert et al. 2009; Gehrig et al. 2007). In detail, time-dependent assessment of the global $Rs1h^{-/Y}$ retinal transcriptome has identified immune-/microglia-related transcript expression from postnatal day 12 (P12) onwards, prior to the rise of cell-death related transcripts, suggesting early microglial activation as a key event preceding/triggering photoreceptor death

(Gehrig et al. 2007; Langmann 2007). A similar expression profile was observed in the *Rd* mouse model. Microglial activation markers were expressed from P8 onwards peaking at P14, whereas the climax of apoptosis was seen towards P16 (Zeng et al. 2005). In addition to resident microglia, ongoing damage of the retina allows the recruitment of peripheral macrophages. In the retinal microenvironment, recruited macrophages transform phenotypically into microglia-like cells and actively contribute to the inflammatory processes (Kaneko et al. 2008).

To sum up, early microglial activation represents a mutual phenotype in retinal dystrophies and a starting point for loss of retinal neurons and impairment of physiological properties.

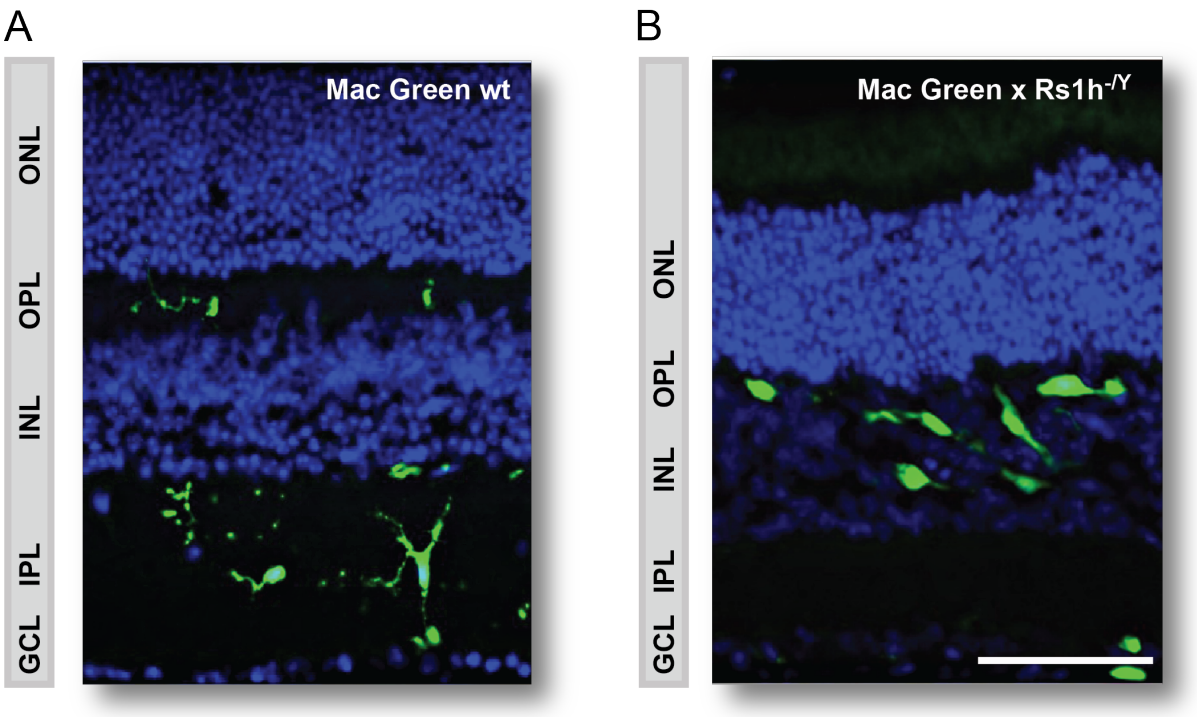

Figure 3 Location and morphology of microglia in the healthy and degenerating retina. Cross-sections of $EGFP^{+}$ microglia (A) in the wt Mac Green murine retina (P18). Ramified microglia are localized in the plexiform layers in the healthy retina. During severe retinal degeneration, microglia migrate to the INL (B) in the $Rs1h^{-/Y}$ x Mac Green retina (P18) and are transformed into amoeboid, bloated microglial cells. Notably, the degenerated retinal layers are thinner compared to the healthy wt-retina. The white scale bar represents 50 µm. Pictures modified from (Karlstetter et al. 2010b). GCL, ganglion cell layer; IPL, inner plexiform layer; INL, inner nuclear layer; OPL, outer plexiform layer; ONL, outer nuclear layer.

1.3.5 Microglial phenotypes in retinal degeneration

Microglia are facing a multitude of stimuli which appear during imbalance of tissue homeostasis. Depending on the extent and progression of degeneration, microglia

are exposed to various molecules of different quantity, quality at different time points of disease. Due to the plasticity of myeloid cells, microglia possess a tremendous heterogeneity, allowing them to respond accurately to the stimuli landscape (Lawson et al. 1990).

Integration of macrophage biology can also serve as a guide for the classification of microglia activation phenotypes. Macrophage phenotypes are roughly classified into ‘classically’ (M1) and ‘alternatively’ (M2) activated macrophages (Ransohoff & Perry 2009). In response to profound TLR4 stimulation, microglia trigger a ‘classical’ activation program, associated with pro-inflammatory cytokine expression and NO-production (Michelucci et al. 2009), generating a toxic environment for photoreceptors (Dirscherl et al. 2010). In contrast, the cytokines *interleukine-10* (IL-10) and *interleukine-4* (IL-4) induce neuroprotective ‘alternative’ activation, characterized by the markers *arginase 1* (ARG1) and *triggering receptor expressed on myeloid cells-2* (TREM2) (Takahashi 2005). Alternatively activated microglia show an enhanced phagocytic capacity (Michelucci et al. 2009). A study investigating microglial activation in a spinal chord injury model reports the co-existence of M1-like and M2-like microglia. Notably at the site of injury, M2-microglia are overrun by an extensive and persistent M1-population resulting in impaired tissue regeneration (Kigerl et al. 2009). The same study reports M2-like microglia to be beneficial for axonal regeneration, whereas M1 microglia have the opposite effect (Kigerl et al. 2009). Likewise, retina-invading M2-primed macrophages increase photoreceptor survival and slow down the course of retinal degeneration (Sasahara et al. 2008). Genome-wide expression profiling of the Rs1h-deficient mouse retina has also revealed co-expression of classical and alternative marker genes suggesting the same concept of co-existing microglia phenotypes in retinal degeneration (Gehrig et al. 2007).

1.4 Strategies for modulation of microglial phenotypes

Pro-inflammatory microglial activation is a common theme in the development of retinal dystrophies, yet distinct populations of activated microglia may exert neuroprotective features on retinal cells. This suggests that reprogramming of microglia could be a potential approach for broad therapeutic intervention in retinal

diseases. Several modulation strategies have been described involving endogenous mechanisms, natural compounds, dietary supplements or immune-modulating substances that are already in clinical use.

1.4.1 Endogenous microglial factors

Microglia and macrophages have evolved endogenous mechanisms to prevent excessive over-activation and to ensure reversion to the 'resting' state after clearance of insult. As one example, the small RNAs miRNA-124 and miRNA-147 have been described to act suppressively on microglia/macrophage activation *in vitro* and *in vivo* (Liu et al. 2009; Ponomarev et al. 2010). Furthermore, whey acidic domain proteins (WAPs) represent a family of secreted innate immune peptides bearing several unique immuno-modulatory features in one molecule (Bingle & Vyakarnam 2008). The best studied whey acidic protein, *secretory leukocyte protease inhibitor* (SLPI) is expressed in multiple tissues including activated microglia (Dirscherl et al. 2010; Mueller et al. 2008). SLPI has a tripartite function with anti-bacterial, anti-inflammatory and protease-inhibitory potential (Bingle & Vyakarnam 2008). SLPI is secreted during microglial activation and exerts its anti-inflammatory function by inhibiting NFkB-binding to promoters of pro-inflammatory target genes (Taggart et al. 2005; F. Y. Jin et al. 1997). Thus, over-expression of SLPI prevents pro-inflammatory activation of myeloid cells (Zhu et al. 1999).

1.4.2 Natural compounds

Herbal plants and their natural active compounds serve as traditional medicine since ancient times, especially due to their antioxidant and anti-inflammatory features (Choi et al. 2011). Most of the plant molecules belong to the chemical class of polyphenols and are characterized by good bioavailability, absorption and biosafety (Choi et al. 2011). General health benefits have been described for numerous compounds including Curcumin, Resveratrol and Luteolin. The latter belongs to the most abundant class of polyphenols, the flavonoids (Ross & Kasum 2002). Luteolin is enriched in spices and vegetables like parsley, celery or sage (Seelinger et al. 2008) and has high impact on microglial activation due to its anti-oxidant and radical scavenging features (Harris et al. 2006). Luteolin directly inhibits intracellular

signaling pathways mediated by the transcription factors NFkB and *activator protein 1* (AP-1) (C. Chen et al. 2007), preventing induction of pro-inflammatory IL-6 expression and sequestration of NO (J. Kim et al. 2006). Luteolin treatment attenuates microglial activation and induces a neuroprotective phenotype (Dirscherl et al. 2010; H.-Q. Chen et al. 2008).

Curcumin is derived from the plant *Curcuma longa*, and has been extensively studied due to its pleiotropic anti-oxidant and anti-inflammatory features, known from traditional chinese medicine (Jagetia & Aggarwal 2007). Like Luteolin, Curcumin antagonizes inflammatory microglial activation involving downregulation of NO- and inflammagen-production coupled with increased phagocytic capacity (K. K. Jung et al. 2006; C.-Y. Jin et al. 2007a). Curcumin treated activated microglia are neuroprotective and can rescue neurons from apoptosis *in vitro* (S. Yang et al. 2008).

Docosahexaenoic acid (DHA) is an essential long chain fatty acid and can be administered by consumption of fish or commercially available capsules. DHA supplementation has beneficial effects on infant neurodevelopment, general mental health and neuroinflammatory conditions (Davis-Bruno & Tassinari 2011; Cole et al. 2010). DHA is highly abundant in the CNS and retina, and serves as a precursor of *neuroprotectin D1*, which is a trophic factor for photoreceptors (Mukherjee et al. 2007). Treatment of activated microglia with DHA reduces IL-6 production and increases the M2-marker genes Il-10- and Arg1. DHA-induced M2 microglia are beneficial for survival and differentiation of neuronal progenitor cells (Antonietta Ajmone-Cat et al. 2011), and DHA supplementation can inhibit the progression of retinal degeneration in mice (Ebert et al. 2009).

1.4.3 Approved pharmaceuticals and potential new candidates

Clinically used immuno-suppressing drugs are promising tools for modulation of microglia, because biosafety, toxicity and side effects have been evaluated during their approval. Recombinant type I interferons are routinely used to treat *Multiple Sclerosis* (MS), a demyelinating autoimmune disorder involving microglial activation (Benveniste 1997). Selective depletion of the complementary *interferon-α/β receptor* (IFNAR) on microglia in a mouse model for MS, reveals a profound worsening of disease progression. These findings suggest a major impact of type I interferon

signaling on modulation of the microglial phenotype. Notably, type I interferon (IFN-β) stimulation of microglia induces a unique phenotype, showing characteristics for both M1- and M2- microglial activation without inducing neuronal apoptosis *in vitro* (S. Jin et al. 2007b; Prinz et al. 2008).

Ligands for mitochondrial translocator protein (18 kD) (TSPO) have been extensively studied and used for treatment of anxiety disorders (Rupprecht et al. 2009). Increased expression of TSPO has been reported in response to injury and during progression of various neurological diseases (Girard et al. 2012). In this context, TSPO was found to be predominantely expressed by activated microglia and selected TSPO ligands are capable of modulating microglial activation. TSPO ligand PK11195 was shown to modulate microglial action by inhibition of pro-inflammatory cyclooxygenase-2 (Cox2) expression (Hong et al. 2006). PK11195-treated mice with primed inflammation in the hippocampus, reveal a decreased number of microglia in the inflamed tissue and less apoptotic neurons, compared to controls (Veiga et al. 2007). Due to their pleiotropic effects, IFN-β and TSPO ligands are interesting candidates for the modulation of microglial activation.

1.5 Aim of the thesis

The aim of this work was to investigate the therapeutic potential of microglial modulators and their regulatory potential in respect to neurotoxic microglial activation. Microglial activation is a mutual event in all retinal dystrophies and is thought to promote the progression of degenerative processes. Thus, attenuation of pro-inflammatory activation represents a promising approach to mitigate retinal degeneration. In one part of this work (Chapter 1), the functional characterization of the novel whey acidic protein AMWAP should provide insights into the transcriptional regulation of the AMWAP gene during retinal degeneration. Furthermore, it should be clarified whether AMWAP has modulatory potential on microglial activation with a special focus on anti-inflammatory, neuroprotective features. Another attempt of this thesis was to test the therapeutic potential of the plant-derived polyphenolic compounds Curcumin (Chapter 2) and Luteolin (Chapter 3). As part of a novel screening pipeline, genome-wide transcript profiling was performed, to obtain a comprehensive view on transcriptomic changes upon microglial modulation by

Luteolin and Curcumin. This approach was aimed to identify novel genes and pathways for subsequent functional analyses.

2 Results

2.1 Chapter 1 – AMWAP (Karlstetter et al. 2010a)

The novel Activated Microglia/Macrophage WAP Domain Protein, AMWAP, acts as a counter-regulator of pro-inflammatory response

Marcus Karlstetter, Yana Walczak, Karin Weigelt, Stefanie Ebert,
Jan Van den Brulle, Heinz Schwer, Rudolf Fuchshofer, and Thomas Langmann

Published in the Journal of Immunology. 2010 Sep 15;185(6):3379-90.

Abstract

Microgliosis is a common phenomenon in neurodegenerative disorders including retinal dystrophies. To identify candidate genes involved in microglial activation, we used DNA-microarray analysis of retinal microglia from wild-type and retinoschisin-deficient ($Rs1h^{-/Y}$) mice, a prototypic model for inherited retinal degeneration. Thereby we cloned a novel 76 amino acid protein encoding a *microglia/macrophage-restricted whey acidic protein* (WAP) termed activated microglia/macrophage WAP domain protein (AMWAP). The gene consists of three exons and is located on mouse chromosome 11 in proximity to a chemokine gene cluster. mRNA expression of AMWAP was detected in microglia from $Rs1h^{-/Y}$ retinas, brain microglia, and other tissue macrophages. AMWAP transcription was rapidly induced in BV-2 microglia upon stimulation with multiple TLR ligands and IFN-γ. The TLR-dependent expression of AMWAP was dependent on NFkB while its microglia/macrophage-specific transcription was regulated by PU.1. Functional characterization showed that AMWAP over-expression reduced the pro-inflammatory cytokines Il-6 and Il-1β and concomitantly increased expression of the alternative activation markers *arginase 1* and Cd206. Conversely, siRNA knock-down of AMWAP lead to higher Il-6, Il-1β, and Ccl2 transcript levels while diminishing *arginase 1* and Cd206 expression. Moreover, AMWAP expressing cells had less migratory capacity and showed increased adhesion in a trypsin-protection assay indicating anti-serine protease activity. In agreement with findings from other WAP proteins, micromolar concentrations of recombinant AMWAP exhibited significant growth inhibitory activity against *E. coli*, *P. aeruginosa* and *B. subtilis*. Taken together, we propose that AMWAP is a counter-regulator of pro-inflammatory microglia/macrophage activation and a potential modulator of innate immunity in neurodegeneration.

Introduction

Microglial cells, the resident phagocyte population of the nervous system, exert several important functions in immune surveillance (Hanisch 2002; Hanisch & Kettenmann 2007) and neuronal homeostasis (Streit 2002; Streit 2005). In the healthy brain and the retina, ramified microglia serve as highly motile patrolling cells constantly surveying their microenvironment (Nimmerjahn et al. 2005). There is an

ongoing debate whether resident microglia in the CNS and the retina are replenished by *in situ* proliferation and/or recruitment of myeloid cells from the bloodstream (Soulet & Rivest 2008; Graeber & Streit 2009; Ransohoff & Perry 2009). Accumulating evidence now suggests that experimental confounds including alterations of the blood-retina barrier could have biased earlier results from bone-marrow chimeras (Ransohoff 2007). Thus, parabiosis studies demonstrated that microglia in the healthy or experimentally damaged brain are poorly replenished from the bloodstream (Ajami et al. 2007). Moreover, Mildner et al. (Mildner et al. 2007) showed that irradiation is essential for infiltration of circulating microglial precursors into the brain in chimerism experiments.

Microglia communicate with other glial cells and neurons which regulate their activation status, their capacity for phagocytosis of cellular debris, and secretion of neurotrophic factors (Dick 2003). Key regulatory signals from neurons and glia are transmitted to microglia cells through various soluble factors including nucleotides (Inoue et al. 2007), the chemokine fractalkine (Ransohoff et al. 2007), transforming growth factor beta (Paglinawan et al. 2003), and nerve growth factor (De Simone et al. 2007). Control of microglial activation and function is further regulated by direct neuron-microglia cross-talk including Cd200/Cd200 receptor ligation (Hoek 2000) and complex formation of triggering receptors expressed on myeloid cells with different ligands on neurons (Klesney-Tait et al. 2006).

Activated microglia can elicit both protective and deleterious functions. In the early phase of neurodegeneration, microglia evoke potent tissue remodeling programs (Streit 2005) and initiate repair mechanisms such as glial scar formation (Muzio et al. 2007). However, excessive or prolonged microglial activation in the CNS and the retina can lead to chronic inflammation with severe pathological side effects often resulting in irreversible neuronal loss (Hanisch 2002; Langmann 2007; Schuetz & Thanos 2004). In eye research, various animal models have demonstrated that microglial activation is tightly associated with and mostly precedes retinal degeneration and photoreceptor apoptosis (Zeng et al. 2005; Zeiss 2004; Gehrig et al. 2007). Functional and phenotypic characterization of microglia populations in the diseased retina could be of high relevance to reveal signaling events that trigger their activation. However, like other tissue macrophages (Hume 2008), activated microglia

comprise a continuum of diverse functional phenotypes with a broad spectrum of activation markers (Schwartz et al. 2006).

Our laboratory has employed large-scale transcriptional phenotyping to identify characteristic gene signatures of LPS and chondroitin sulphate proteoglycan-disaccharide (CSPG-DS) stimulated BV-2 microglia as clearly polarized cell populations (Ebert et al. 2008). Moreover, we have profiled primary retinal microglia from wild-type and retinoschisin-deficient ($Rs1h^{-/Y}$) mice (Weigelt et al. 2007), a prototypic model for rapid retinal apoptosis and degeneration (Weber 2002). In contrast to LPS and CSPG-DS treated microglia, expression profiles of retinal $Rs1h^{-/Y}$ microglia indicated overlapping transcript clusters reminiscent of both pro- and anti-inflammatory macrophage activation (Weigelt et al. 2007; Ebert et al. 2009; Langmann et al. 2009). Finally, several transcripts previously not linked to microglial activation have been identified in these genome-wide expression studies, including high levels of the adaptor protein STAP-1 (Stoecker et al. 2009) and the uncharacterized whey acidic protein (WAP) motif bearing protein AMWAP.

WAP domain proteins have originally been described as low molecular weight proteins with ‘defensin-like’ properties involved in immune homeostasis (Bingle & Vyakarnam 2008). Their counter-regulatory role on inflammatory mediators is mainly ascribed to the anti-protease and anti-microbial activities of the WAP domain (Hiemstra et al. 1996; Ranganathan et al. 1999; Williams et al. 2006). This 40-50 amino acid motif contains eight conserved cysteins which form four defined disulfide bonds. *Secretory leukocyte protease inhibitor* (SLPI) and elafin are the best studied WAP proteins in humans and mice (Moreau et al. 2008). SLPI is constitutively produced at many mucosal surfaces and is also produced by lung epithelial cells, neutrophils, and macrophages (Doumas et al. 2005). SLPI expression in macrophages is induced by bacterial endotoxin leading to the suppression of NO and TNF secretion (J. Yang et al. 2005). Elafin is mainly present in epithelia of the skin, oral cavity, vagina and lung to fulfill distinct anti-microbial and immuno-modulatory functions (Molhuizen & Schalkwijk 1995).

In this study, we identified a novel *microglia/macrophage-restricted WAP domain protein*, AMWAP, in activated primary retinal microglia. AMWAP expression is rapidly induced by ligands for TLRs2/4/9 and IFN-γ in the BV-2 cell line. AMWAP

over-expression reduces pro-inflammatory cytokine expression and concurrently induces markers for alternative macrophage activation. We therefore propose that AMWAP is a novel modulator of microglial activation in neurodegenerative disorders.

Materials and Methods

Animals

Retinoschisin knockout ($Rs1h^{-/Y}$) mice have been described previously (Weber 2002) and C57BL/6 mice were purchased from Charles River Laboratories. Mice were kept in an air-conditioned barrier environment at constant temperature of 20-22°C on a 12-h light-dark schedule, and had free access to food and water. The health of the animals was regularly monitored, and all procedures were approved by the University of Regensburg animal rights committee and complied with the German Law on Animal Protection and the Institute for Laboratory Animal Research Guide for the Care and Use of Laboratory Animals, 1999.

Isolation and culture of primary cells

Retinal microglia were isolated and cultured as described earlier (Weigelt et al. 2007). Briefly, retinal tissue from wild-type and $Rs1h^{-/Y}$ mice at postnatal days 14 and 18 was isolated from eye bulbs and purified from contaminating vitreous body and retinal pigment epithelium/choriocapillaris. Pools of 4-6 retinas each were cut into small pieces and incubated for 40 min at 37°C in 1 ml of PBS with 1 mg/ml collagenase type I (Sigma), 0.3 mg/ml DNase I (Roche) and 0.2 mg/ml hyaluronidase (Sigma). The cell suspension was filtered through a 70 µm cell strainer (Becton Dickinson). Cells were washed twice with 10 ml DMEM/10% FCS and finally subjected to Ficoll density gradient centrifugation for 20 min at 2000 rpm (690 x g, without brake) in a Heraeus centrifuge for the isolation of mononuclear cells. The interphase was carefully removed and washed with 10 ml DMEM/FCS. The cells were cultured for 11 days in 75 cm^2 flasks containing DMEM/10% FCS supplemented with 50 ng/ml recombinant human M-CSF (R&D Systems) and phase contrast micrographs were taken with a Nikon Eclipse TE2000-S microscope.

Brain microglia were isolated from the brains of 4 weeks old wild type mice. Each brain was dissected, cut into small pieces in 520 µl PBS, and incubated for 40 min at 37°C with vigorous shaking (800 rpm) containing the same dissolving solution described above. The single cell suspension was filtered through a 70 µm cell strainer (Becton Dickinson), washed twice with 10 ml DMEM/10% FCS followed by

centrifugation at 1600 rpm for 5 min at room temperature. The pellet was resuspended in 10 ml DMEM/10% FCS supplemented with 50 ng/ml recombinant human M-CSF (R&D Systems) and cultured in 75 cm^2 cell culture flasks. Non adherent cells were removed after four days by washing with culture medium. After 11 days of culture 100 ng/ml LPS was added where indicated and total RNA was isolated after 24 h of stimulation.

Bone marrow macrophages were isolated from bone marrow of adult wild-type animals. Femur and tibia were dissected from the surrounding muscle tissue and both ends were cut. Bone marrow was flushed with 2 ml DMEM/10% FCS with a 27 G syringe and cell clumps were separated by pipetting. The cell suspension was centrifuged for 10 min at 1200 rpm at room temperature. The supernatant was discarded and the pellet was dissolved in 2 ml Red Blood Cell lysis buffer (Sigma) and incubated for 7 min at room temperature. Then incubation was stopped with 5 ml DMEM/10% FCS followed by centrifugation. The cell pellet was resuspended in 10 ml DMEM/10% FCS supplemented with 50 ng/ml recombinant M-CSF (R&D Systems). Cell culture medium was removed at days 4 and 8. After 10 days in culture, bone marrow macrophages were stimulated with 100 ng/ml LPS where indicated and total RNA was isolated after 24 h.

Dissected spleen tissue of adult wild-type animals was disintegrated by scissors in 520 µl PBS, passed through a wire mesh and washed with 10 ml DMEM/10% FCS. Cells were filtered through a 40 µm cell strainer and processed as described above for bone marrow macrophage isolation.

Immature bone marrow dendritic cells were isolated as described previously (Lutz et al. 1999). For maturation, dendritic cells were collected after 10 days, and resuspended in culture medium containing 100 U/ml rmGM-CSF and 1 µg/ml LPS. Total RNA was collected after 24 h of maturation.

Cell lines and reagents

RAW264.7 cells were received from the American Type Culture Collection (Manassas, VA, USA) and BV-2 cells were kindly provided by Professor Ralph Lucius (Clinic of Neurology, Christian Albrechts University, Kiel, Germany). RAW264.7 macrophages were kept in DMEM supplemented with 10% FCS, 100 U/ml penicillin

and 100 µg/ml streptomycin. BV-2 cells were cultured in RPMI/5% FCS supplemented with 2mM L-Glutamine and 195 nM β-mercaptoethanol. Culture and treatment of tamoxifen-inducible PUER cells has been described elsewhere (Weigelt et al. 2009). Lipopolysaccharide (LPS), interferon-g (IFN-γ), and cycloheximide (CHX) were purchased from Sigma. PAM3CSK4 was purchased from Invitrogen. The phosphorothioate CpG oligonucleotide (5'-tccatgacgttcctgatgct-3') and control oligonucleotide (5'-tccatgaggttcctgatgct-3') were synthesized by Metabion (Martinsried, Germany). Caffeic acid phenethyl ester (CAPE) was purchased from Tocris Bioscience (Ellisville, MO, USA). For activation experiments, cells were exposed to LPS, IFN-γ, CpG oligonucleotides, or PAM3CSK4 in various doses for different time points. For inhibition of NFkB and protein synthesis, BV-2 cells were pre-treated with 15 µg/ml CAPE for 2 h or 5 µg/ml CHX for 1h, respectively. Cells were then washed with culture medium prior to stimulation with 50 ng/ml LPS, 1 µg/ml CpG oligonucleotides, or 1 µg/ml PAM3CSK4 for 4 h.

RNA isolation, Reverse Transcription and 5'-RLM-RACE

Total RNA was extracted using the RNeasy Mini Kit (Qiagen). Purity and integrity of the RNA was assessed on the Agilent 2100 bioanalyzer with the RNA 6000 Nano LabChip® reagent kit (Agilent Technologies). The RNA was quantified spectrophotometrically and stored at -80°C. cDNAs were generated using the RevertAid™ H Minus First Strand cDNA Synthesis Kit (Fermentas).

To identify and clone full-length AMWAP transcripts, 5'RNA ligase mediated RACE-PCR was carried out using RNA from RAW264.7 cells activated with 100ng/ml LPS and the Ambion FirstChoice® RLM-RACE Kit according to the manufacturer´s instructions. AMWAP-specific reverse primers were designed on the incomplete database entry Mm.24097. The first 5'-RLM-RACE PCR was carried out with the AMWAP-specific reverse primer 5'-GGG CAG GAT CCA TCT CCT-3' and the 5'-RACE outer primer 5'-GCT GAT GGC GAT GAA TGA ACA CTG-3'. The nested 5'-RLM-RACE PCR was conducted with the AMWAP-specific reverse primer 5'-TTT GCA GAC ATG ACC ACA GC-3' and the inner 5' RACE primer 5'-CGC GGA TCC GAA CAC TGC GTT TGC TGG CTT TGA TG-3'. PCR products were analyzed on 2% agarose gels and individual bands were extracted, cloned into the pCR2.1

Topo TA vector (Invitrogen) and sequenced. The full-length AMWAP sequence was submitted to Genbank under accession number FJ007372 (http://www.ncbi.nlm.nih.gov/Genbank).

Quantitative real-time RT-PCR

Relative transcript levels were assessed by amplifications of 50 ng cDNA in a 7900HT real-time PCR detection system (Invitrogen Life Technologies). The 20 µl reaction volumes contained 1x TaqMan Gene Expression Master Mix (Invitrogen Life Technologies), 200 nM primers (Supplementary table 1) and 0.25 µl dual-labelled probe (Roche Universal Probe Library). The PCR reaction parameters were as follows: 2-min 50 °C hold, 30-min 60 °C hold, and 5-min 95 °C hold, followed by 45 cycles of 20-s 94 °C melt and 1-min 60 °C anneal/extension. The results were analyzed using the ΔΔCt method for relative quantification (Mauerer et al. 2009).

Chromatin immunoprecipitation (ChIP)

ChIP experiments of RAW264.7 cells coupled to Affymetrix Promoter Arrays have been described elsewhere (44). For ChIP-PCR with microglia, 10 million BV-2 cells were treated with 1% formaldehyde for 15 min and lyzed with SDS, Empigen and NP-40 (supplemented with 1 mM PMSF, 1 µg/ml aprotinin and 1 µg/ml pepstatin A). The nuclear pellet was homogenized by sonication twice at 30% amplitude for 10 s. Immunoprecipitation was performed on the lysate with 2.5 µg of anti-PU.1 antibody (Santa Cruz Biotechnology) anti-di-acetylated (K9 and K14) histone H3 (Upstate Biotechnology), anti-p300 clone RW128 (Upstate Biotechnology), anti-CBP (Upstate Biotechnology), or anti-IgG antibody (Santa Cruz Biotechnology). After washing and elution steps, cross-links were reversed at 65°C overnight. The immunoprecipitated DNA was purified using the QIAquick PCR purification kit (Qiagen) and analyzed by PCR using the forward primer 5'-CCC CTC GAG CTG GAA AAA GGA ACC TGG TG-3′ and the reverse primer 5′-CCC AAG CTT TCA TCC CCA CAG TGA TCA AA-3′ specific for the AMWAP proximal promoter region −114/+68.

Over-expression of AMWAP in BV-2 cells

The full-length coding sequence of mouse AMWAP was RT-PCR amplified from RAW264.7 RNA with primer pair forward 5'-CCC AGC TTC CCA ACA TGA AGA CAG CCA CA-3' and reverse 5'-CCC CTC GAG TAA AAG ACA GGA GTT TTG CAG AC-3'. PCR products were sequenced and cloned into the HindIII/XhoI site of a pCEP1.4 vector in-frame with a C-terminal rhodopsin (Rho)-1D4 tag (Stoehr et al. 2004) to generate pAMWAP-1D4. A fusion protein of milk fat globule protein 8 with a C-terminal rhodopsin (Rho)-1D4 tag (pMFG-1D4) was cloned as positive control. The AMWAP-GFP-fusion protein (pAMWAP-GFP) was created by cloning the AMWAP open reading frame into the pcDNA/CT-GFP-TOPO vector using RT-PCR with primer pair forward 5'-CCC GGT ACC CCA ACA TGA AGA CAG CCA CA-3' and reverse 5'-CCC GAT ATC TAA AGA CAG GAG TTT TGC AGA C-3', containing restriction sites for KpnI and EcoRV, respectively. BV-2 cells were transfected with 2µg of endotoxin-free plasmid using transIT-LT1 transfection reagent (Mirus Bio) following the manufacturer's recommendations. Stable BV-2 cell transformants expressing GFP or AMWAP-GFP were created by neomycin selection. Successful expression of GFP and AMWAP-GFP was monitored by GFP fluorescence.

siRNA knock-down of AMWAP in BV-2 cells

Target sequences for murine AMWAP were based on the longest transcript obtained from the 5' RLM-RACE-PCR (Accession Nr. FJ007372.1). siRNAs were designed with the Ambion siRNA target finder and synthesized with the siRNA construction kit (Ambion, Austin, TX, USA). AMWAP siRNA was synthesized using sense primer 5'-AAA GGA TCC ATC TCC TGA GCA CCT GTC TC-3' and antisense primer 5'-AAT GCT CAG GAG ATG GAT CCT CCT GTC TC-3'. BV-2 cells were transfected with 33 nM AWMAP siRNA or scrambled siRNA (Ambion) using lipofectamine 2000 (Invitrogen). Twenty four hours after transfection, cells were stimulated with 5 ng/ml LPS for 24 h before isolation of total RNA.

Western blotting

Cells were grown in 10 cm dishes and lysed in 1 ml boiling lysis buffer (PBS, 1% SDS). Equal amounts of protein samples were separated with NuPAGE Bis-Tris 4-12% gels (Invitrogen) and subsequently transferred to a Hybond ECL membrane (Amersham Biosciences). For determination of protein size, PageRuler^{TM} prestained protein standard (Fermentas) was used. The membranes were blocked in 5% milk powder in PBS and probed with either anti-Rhodopsin-1D4 mouse monoclonal antibody (1:10000) (a generous gift of Robert S. Molday, Department of Biochemistry and Molecular Biology, Centre for Macular Research, University of British Columbia, Vancouver, Canada) or anti-His-Penta mouse monoclonal antibody (Qiagen, 1:10000). A HRP-conjugated secondary antibody against mouse Ig (Cell signaling Technology) and the ECL Plus system (Amersham Biosciences) were used for detection.

Immunocytochemistry

BV-2 cells were plated overnight on coverslips, fixed with 4% paraformaldehyde for 10 min at 37°C, permeabilized with 0.2% Triton X-100, blocked with 5% non-fat milk in 0.2% Triton X-100, and stained with anti-GFP-antibody (Abcam). Nuclei were stained with DAPI for 10 min (0.1 µg/ml in PBS, 4'6-diamidino-2-phenylindol, Molecular Probes). Coverslips were mounted on glass slides and visualized with an Axioskop 2 fluorescence microscope equipped with an Eclipse digital analyzer (Carl Zeiss).

Wound healing and transwell migration assays

Stably pAMWAP-GFP and pGFP expressing BV-2 cells were grown in 6-well plates as 80% confluent monolayers and were wounded with a sterile pipette tip. Cell migration into the open scar was documented with microphotographs at time points 0 h and 24 h after wounding. As an independent method, the Costar Transwell System (8 µm pore size polycarbonate membrane) was used to evaluate cell migration. BV-2 cells (1×10^6 cells in 1.5 ml serum-free medium) were added to the upper well, and 2.6 ml serum-free medium was added to the lower chamber. 50 ng/ml LPS or ethanol as solvent control were added to the lower chamber medium.

At the end of the 24 h incubation, cells on the top of the membrane were removed by swiping with a damp cotton swab, and cells that had migrated to the lower surface were fixed in methanol for 15 minutes at room temperature and stained with 1% crystal violet. The migration activity was quantified by counting the migrated cells on the lower surface of the membrane using light microscopy.

Trypsin protease protection assay

Stably AMWAP-GFP and GFP-expressing BV-2 cells were cultured in 24-well plates overnight until 80% confluence was reached. The culture medium was removed and 0.25% trypsin in PBS was added to the cells for the indicated time points. Complete medium containing 10% FCS was added to the cells to stop trypsin activity. The cells were washed three times and stained with 0.2% crystal violet in PBS for 10 min. After additional washing steps, cell-associated crystal violet was extracted with 10% acetic acid and the optical density was assessed on a microplate reader at 600 nm. OD values were normalized to untreated control cells.

Ccl2 luciferase reporter assay

The murine Ccl2 promoter (-988/+113) was PCR amplified from genomic DNA using the primers forward 5'-CCC CTC GAG CAT GCT ACA GAA AGC CCA AAA-3' and reverse 5'-CCC AGA TCT GGC CCA GAA GCA TGA CAG-3'. The PCR product was cut with restriction enzymes XhoI and BglII and cloned into the pGL4.10 vector (Promega). BV-2 cells were co-transfected with the luciferase construct and a pTK-Hyg vector (Clontech, CA, USA) for selection of stable clones with Hygromycin B (PAA). BV-2 cells stably expressing the Ccl2 luciferase reporter were transiently transfected with 2 µg of pAMWAP-GFP or pGFP vectors. Transfected cells were harvested after 24 h and luciferase activity was determined with the Luciferase assay system (Promega) on a FLUOstar Optima plate reader (BMG Labtech).

Bacterial expression and purification of recombinant AMWAP

The AMWAP cDNA sequence was codon-optimized and *de novo* synthesized for recombinant expression in *E. coli* (Sloning Biotechnology), resulting in an increased codon adaption index from 0.7 to 0.91 (Fig. S1) (46). Signal-sequence lacking and

codon-optimized AMWAP was PCR amplified from pSlo1.0-AMPWAP with forward primer 5'-CCC CAT ATG ACC TAT GTG GTG TCC TGT CC-3' and reverse primer 5'-CCC AAG CTT AAA CAC CGG GGT TTT GC-3'. The PCR product was inserted with NdeI and HindIII into the pET21a(+) vector (Novagen) in-frame with an N-terminal His-tag sequence.

E. coli BL21α-DE3 cells transformed with pAMWAP-His were grown in 500 ml of LB-medium until an OD_{600} of 0.7 was reached. Isopropyl-β-D-thiogalactoside was added to a final concentration of 1 mM and culture was continued at 37°C for 4 h. Cells were harvested, the cell pellet was resuspended in 7 ml lysis buffer (300 mM NaCl, 50 mM sodium phosphate, pH 8.0) containing 7 mg lysozyme, and the sample was incubated for 30 min at 4°C. Thereafter, the cell suspension was sonicated and stirred on ice with 5 µg/ml DNase I for 15 min. The crude lysate was centrifuged at 10,000 x g for 30 min at 4°C and the supernatant was loaded onto Protino Ni-TED Columns (Macherey-Nagel). Three fractions were eluted in buffer containing 250 mM imidazole and concentrated in Amicon Ultra-4 Ultracel 5kDa tubes (Millipore) by centrifugation. The protein was dialysed four times against PBS, the concentration of each fraction was determined by Bradford assay and purified recombinant protein was stored at -80°C.

Antimicrobial assay

The bacterial strains *E.coli* (ATCC25922), *P. aeruginosa* (ATCC27853) and *B. subtilis* (ATCC6633) were grown in LB medium at 37°C to an OD_{600} of 1.0. Bacteria were then diluted in MT-LB medium (16 mM disodium hydrogen phosphate, 5 mM sodium dihydrogen phosphate, 150 mM sodium chloride and 1% LB medium) to a concentration of 1 x 10^4 colony forming units/ml. 50µl of bacterial suspensions were incubated with PBS as control or 10 µM, 20 µM, or 30 µM AMWAP-His protein for 2 h at 37°C. Subsequently, appropriate serial dilutions were plated on LB agar plates, incubated over night at 37°C and colony-forming units were determined.

Statistical analyses

The Student's t test or Mann-Whitney-U test were used for the comparison of experimental groups as indicated. $p<0.05$ was considered significant.

Microarray datasets used in this study

The microarray datasets cited in this study are available at the NCBI Gene Expression Omnibus as series records GSE5581 ($Rs1h^{-/Y}$ vs. wild-type retinas), GSE9011 (PU.1 ChIP-Chip), and GSE13125 (PUER cells) at (http://www.ncbi.nlm.nih.gov/geo/).

Results

AMWAP is strongly induced in activated retinal microglia

To identify novel genes involved in the activation of microglia, we have previously performed DNA-microarray analysis of isolated retinal microglia from degenerating Rs1h$^{-/Y}$ and *wild-type* retinas (Gehrig et al. 2007; Weigelt et al. 2007; Ebert et al. 2009). Nine previously uncharacterized transcripts showed a significantly different expression pattern in activated Rs1h$^{-/Y}$ versus non-activated *wild-type* microglia (data not shown). Among these, a more than 7-fold induction of a predicted gene with the UniGene entry Mm.24097 was detected in activated retinal microglia. Here, we confirmed these microarray findings by quantitative real-time RT-PCR assays with RNA samples from independently isolated retinal microglia from Rs1h$^{-/Y}$ and wild-type mice were performed. AMWAP transcript levels were increased in microglia from postnatal day 14 (P14) Rs1h$^{-/Y}$ retinas and were further substantially induced in P18 Rs1h$^{-/Y}$ microglia (Fig. 4A). We have previously shown that microglia activation starts at P14 in the retina of retinoschisin-deficient mice, a time point where neuronal apoptosis and degeneration is not yet evident (Gehrig et al. 2007).

For a more precise refinement of the temporal expression profile of AMWAP in relation to the inflammatory process, mRNA levels were quantified in retinal tissue of postnatal stages (P)11, 12, 14, 18, 21, 24, and 28 (Fig. 4B). The highest AMWAP expression was noted at P18 and P21 and thereafter declined to intermediate levels (Fig. 4B). The AMWAP transcript profile is in good accordance with the time kinetics of the known early activation markers *lysozyme* (Lyzs) (Fig. 4C) and *secreted phosphoprotein 1* (SPP1, alias *osteopontin*) (Fig. 4D). This implicates that high AMWAP expression is already present at the very early stage of retinal microglial activation and declines in the chronic and resultion phase of neuroinflammation. The deduced protein sequence contains a whey acidic protein (WAP) domain and together with the data on its specific expression pattern, this gene was named AMWAP for **A**ctivated **M**icroglia/Macrophage **WAP** Domain Protein.

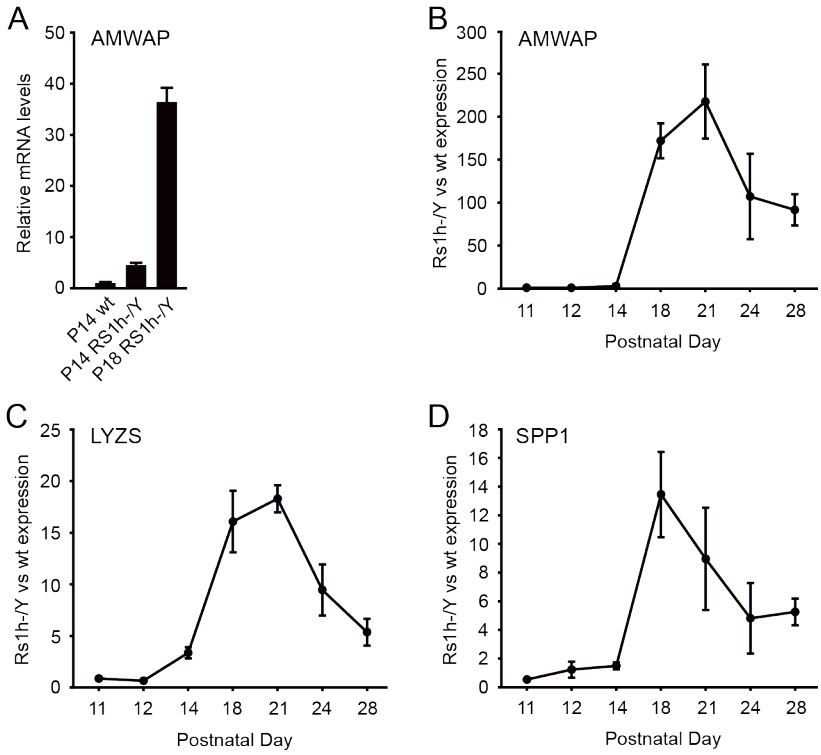

Figure 4 Temporal qRT-PCR expression profile of AMWAP during early retinal microglia activation. (A) AMWAP mRNA expression in primary retinal microglia isolated from postnatal day 14 (P14) and P18 wild-type (wt) and retinoschisin-deficient (Rs1h$^{-/Y}$) mice. Temporal expression profiles of AMWAP (B), lysozyme (C), and secreted phosphoprotein 1 (D) in early postnatal retinas of Rs1h$^{-/Y}$ mice compared to age-matched wild-type mice. Data represent means ± SD of two independent microglia preparations (A) or the means ± SD of three independent retina preparations analyzed in triplicates (B-D), respectively.

AMWAP is exclusively expressed in activated microglia and macrophages

We next addressed the question whether AMWAP is also expressed in brain microglia and macrophages outside of the CNS. Primary brain microglia, spleen macrophages, bone-marrow-derived macrophages, and bone-marrow-derived dendritic cells were isolated and stimulated with LPS to induce a pro-inflammatory state. AMWAP transcripts were already present in the four different types of macrophages but stimulation with LPS further up-regulated AMWAP gene expression (Fig. 5). Examination of AMWAP transcript levels in public domain Affymetrix microarray data (BioGPS, http://biogps.gnf.org and http://macrophages.com) further revealed a macrophage-restricted expression of probeset 1436530_at, which specifically and exclusively targets the AMWAP mRNA (Fig. S2). In the BioGPS database, high abundance of AMWAP transcripts was detected in microglia, bone-marrow-derived macrophages, peritoneal macrophages, and osteoclasts, but not in

any of the other studied mouse tissues or cell types (Fig. S2). Consistent with our qRT-PCR data, these comprehensive expression profiles indicate that AMWAP is a microglia/macrophage-specific transcript induced by pro-inflammatory activation.

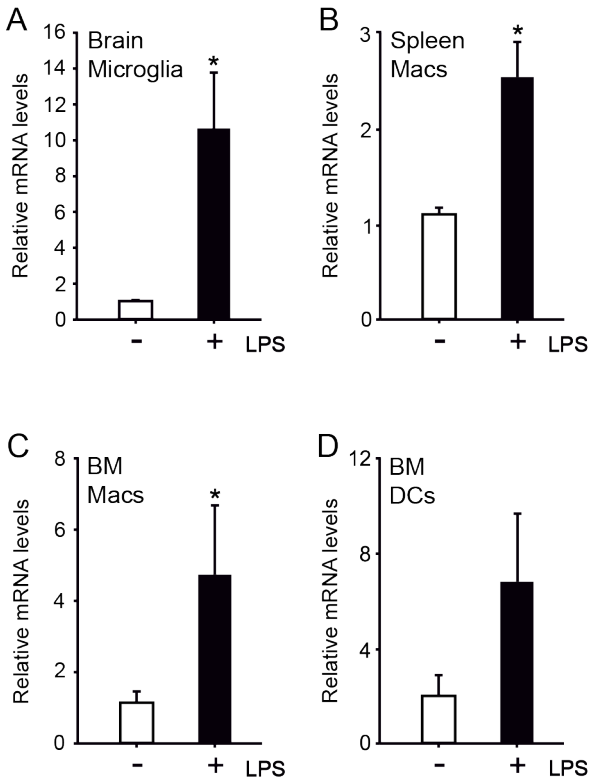

Figure 5 AMWAP is expressed and LPS-inducible in brain microglia and other tissue macrophages. Brain microglia (A), spleen macrophages (B), bone-marrow-derived macrophages (C), and bone-marrow-derived dendritic cells (D) were cultured in the absence or presence of 100 ng/ml LPS for 24 h. Total RNA was isolated and AMWAP transcript levels were determined by qRT-PCR. Data points represent the means ± SD of three independent cell preparations analyzed in triplicates. *, $p<0.05$; Student's t test.

Multiple TLR ligands and IFN-γ rapidly trigger AMWAP transcription in microglia

We next analyzed AMWAP expression and regulation in the BV-2 microglial cell line as an independent in vitro model system. AMWAP mRNA was present in BV-2 cells, but transcript levels were markedly elevated after pro-inflammatory stimulation with TLR ligands and IFN-γ (Fig. 6). Specifically, treatment of BV-2 cells with LPS as TLR4 ligand (Fig. 6A, B), CpG oligonucleotides as TLR9 ligand (Fig. 6C, D), PAM3SCK4 as TLR2 ligand (Fig. 6E, F), and IFN- γ (Fig. 6G, H) evenly up-regulated AMWAP expression in a time- and dose-dependent manner.

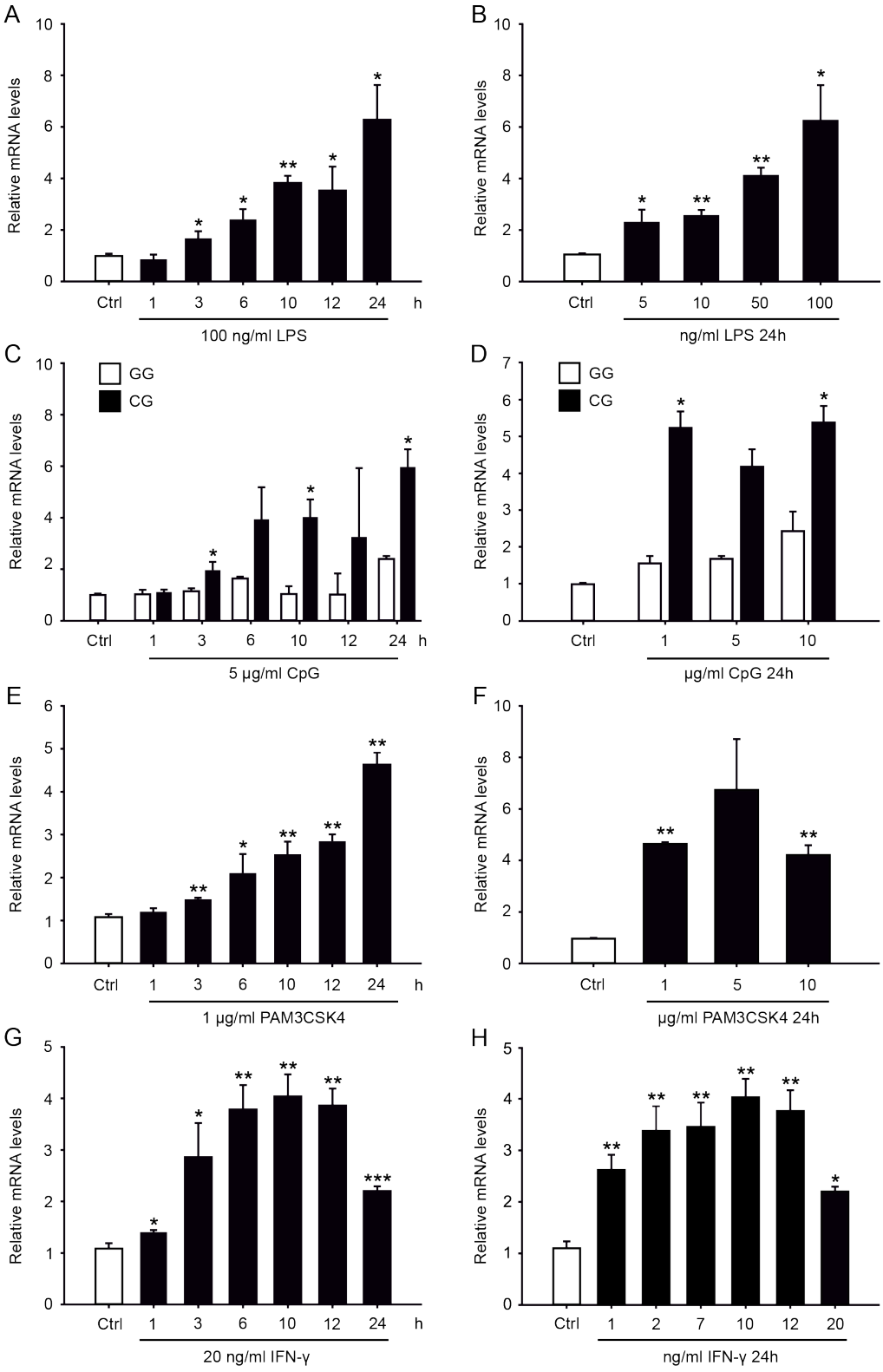

Figure 6 AMWAP is up-regulated by multiple TLR ligands and IFN-γ in BV-2 microglia in a time- and dose-dependent manner. Time-course (A, C, E, G) and dose-response (B, D, F, H) of BV-2 cells treated with the indicated concentrations for the given time periods of LPS (A, B), CpG oligonucleotides or control GG oligonucleotides (C, D), PAM3SCK4 (E, F), or IFN-γ (G, H). qRT-PCR was performed to determine AMWAP levels. Values represent the means ± SD of three independent cell cultures analyzed in triplicates. *, $p<0.05$; **, $p<0.01$; ***, $p<0.001$; Student's t test.

The shortest time of treatment (1 h) and the lowest concentration of each compound were sufficient to induce significant increases in AMWAP levels. These data suggest that AMWAP transcription is very sensitive to pro-inflammatory stimulation of BV-2 microglial cells.

We then examined whether AMWAP induction by TLR ligands depends on the transcription factor NFkB. BV-2 cells were pre-treated with the specific NFkB inhibitor CAPE before exposure to LPS, PAM3SCK4, or CpG oligonucleotides. CAPE completely prevented TLR-dependent AMWAP up-regulation in all three stimulatory conditions (Fig. 7A), indicating that NFkB is absolutely required for AMWAP induction. Next, we pre-treated BV-2 cells with cycloheximide (CHX), a protein synthesis inhibitor, to study whether newly synthesized proteins may be involved in this process. We found that TLR-dependent expression of AMWAP was diminished by CHX pre-treatment (Fig. 7B).

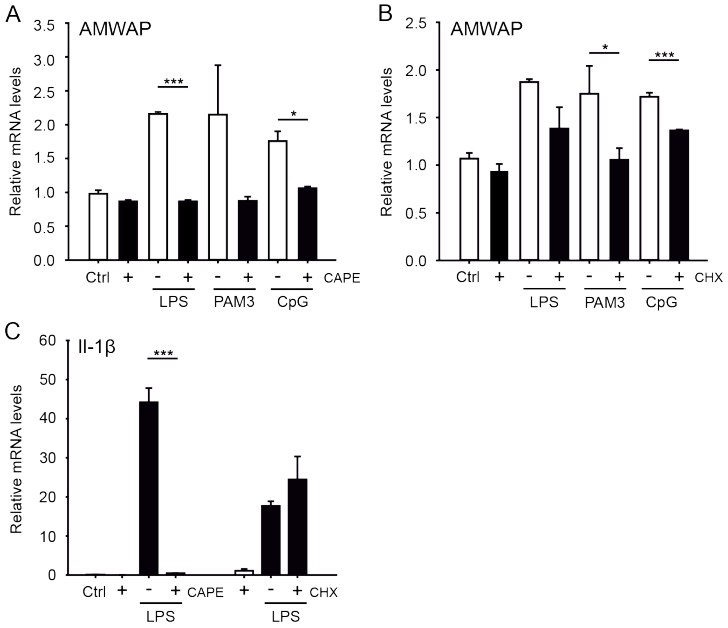

Figure 7 AMWAP up-regulation by TLR ligands requires NFkB and new protein synthesis. To block NFkB, BV-2 cells were pre-treated with 15 µg/ml caffeic acid phenethyl ester (CAPE) for 2 h and cells were thereafter stimulated with 50 ng/ml LPS, 1 µg/ml CpG oligonucleotides, or 1 µg/ml PAM3SCK4 for 4 h (A, C). To block new protein synthesis, BV-2 cells were pre-treated with 5 µg/ml cycloheximide (CHX) for 1 h and were thereafter stimulated with 50 ng/ml LPS, 1 µg/ml CpG oligonucleotides, or 1 µg/ml PAM3SCK4 for 4 h (B, C). qRT-PCR was performed to determine mRNA levels of AMWAP (A, B) and IL-1β as NFkB-dependent control gene (C). Values represent the means ± SD of three independent cell cultures analyzed in triplicates. *, $p<0.05$; ***, $p<0.001$; Student's t test.

This suggests that new protein synthesis is necessary and that additional factors may be relevant for AMWAP induction by TLR-ligands. As a positive control, the LPS-

induced expression of Il-1β was critically dependent on NFkB, but required no protein synthesis (Fig. 7C).

Cloning and genomic structure of AMWAP

The previous database entry of Mm.24097 (Genbank Accession No. BC089618) was complete at the 3'-end including the polyA tail, but contained only nine nucleotides upstream of the start codon. We therefore performed 5'-RLM-RACE with RNA from LPS-stimulated RAW264.7 cells (Fig. 8A).

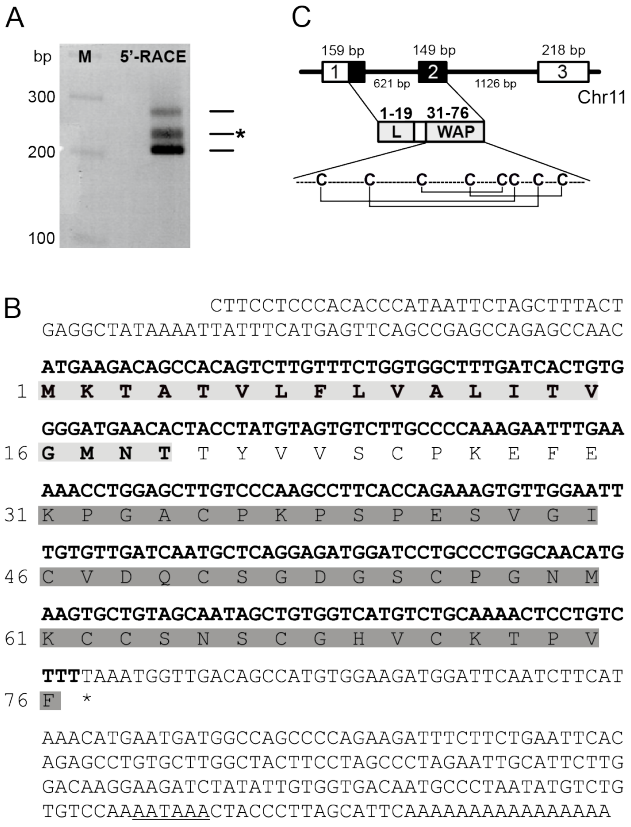

Figure 8 AMWAP full-length cDNA, genomic structure and protein domains. (A) Distinct 5'-RLM-RACE-PCR products generated with template cDNA from LPS-activated RAW264.7 cells and a reverse primer located in the second exon. Specific bands are indicated by arrows and the asterisk denotes a double band. (B) Full-length AMWAP cDNA sequence deposited in Genbank under Accession No. FJ007372. The open reading frame and translated amino acids are given in bold letters. The potential signal sequence is shaded in light gray and the WAP domain is marked in dark grey. The position of the stop codon is indicated by an asterisk and the polyadenylation signal is underlined. (C) Genomic organization of the AMWAP gene (top), predicted protein domains (middle panel), and eight cysteine-residues forming four putative disulfide bonds (bottom).

Three major 5'-RLM-RACE-PCR products were amplified and sequencing after cloning of the individual products identified four different transcripts with the longest variant extending 68 bp further upstream (Fig. 8A).

The 526-bp full-length AMWAP cDNA encodes for a 76 amino acid polypeptide. After predicted cleavage of the 19 amino acid signal sequence, the mature AMWAP polypeptide should consist of a 58 amino acids single WAP motif (Fig. 8B). BLAST analysis against DNA databases resulted in the identification of the AMWAP gene on mouse chromosome 11, consisting of three exons and two introns (Fig. 8C). The N-terminal signal peptide is encoded by exon one, whereas exon two completely codes for the C-terminal WAP domain with eight cysteines presumably forming four disulfide bonds (Fig. 8C). The four-disulfide core domain and its genomic structure as single exon are characteristic features of all WAP proteins (Laslo et al. 2006).

Microglia/macrophage-specific AMWAP expression depends on PU.1 binding to its proximal promoter

Because of the microglia/macrophage-restricted expression of AMWAP, we sought to investigate the relevant cis-regulatory elements. A comparison of mouse and rat AMWAP promoter sequences and their closest rodent homologue Expi revealed a highly conserved TATA-box, proximal PU.1 sites, a STAT motif and an overlapping IRF/PU.1 sequence (Fig. 9A). Our information from 5' RLM-RACE identified the existence of four alternative transcription start sites (Fig. 9A, arrows). Since the longest AMWAP transcript includes the TATA-motif and extends 40 bp upstream, a nearby PU.1 site could function in the formation of the transcription preinitiation complex and thus regulate AMWAP gene activity (Fig. 9A).

To determine whether PU.1 is directly involved in the macrophage-specific expression of the AMWAP gene, recent PU.1-related large scale genomic data from our group were used as resource for further analyses. In the first dataset, a genome-wide discovery of PU.1 target genes in RAW264.7 macrophages was performed using chromatin immunoprecipitation coupled to microarrays (ChIP-Chip) (Weigelt et al. 2008). In the second dataset, PU.1$^{-/-}$ progenitors and PUER cells with restored PU.1 activity were analyzed with exon-specific microarrays to identify PU.1 regulated genes (Weigelt et al. 2009). Results from the ChIP-Chip experiments revealed that the proximal AMWAP promoter strongly bound macrophage PU.1 in vivo, indicated by the specific enrichment of probes in the immediate upstream region (Fig. 9B, black bars). In full agreement with these data, restored PU.1 activity in

PUER cells and differentiation along the macrophage lineage caused a significant increase of AMWAP transcript levels, as shown by specific hybridization signals to all three AMWAP exons (Fig. 9B, red bars).

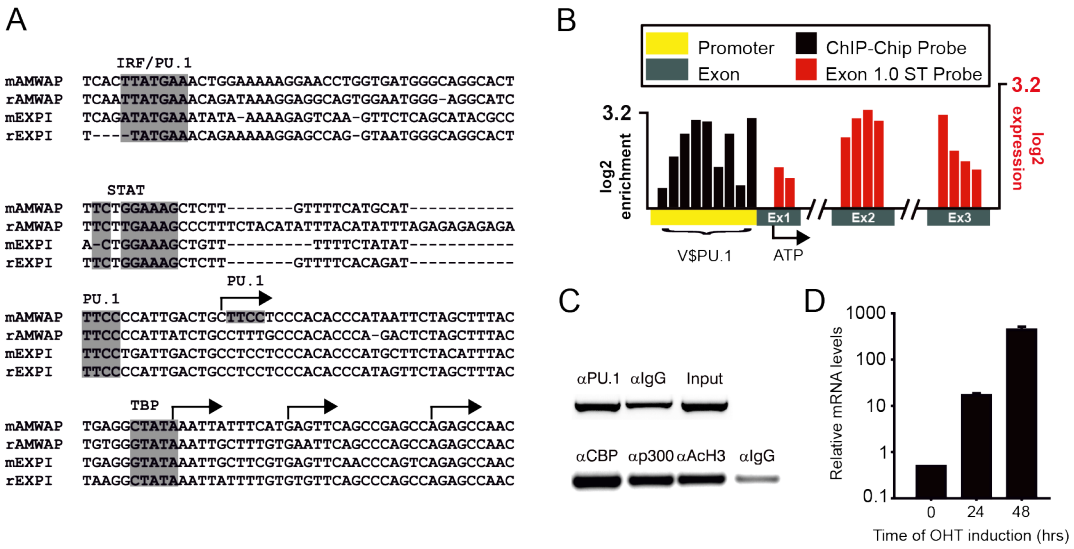

Figure 9 PU.1 regulates the macrophage/microglia-specific expression of AMWAP. (A) Alignment of proximal promoter sequences of rodent AMWAP and Expi. Predicted transcription factor binding matrices are shaded. Arrows indicate transcription start sites experimentally verified by 5'-RLM-RACE. (B) Genomic structure of the AMWAP gene and log2 enrichment/expression values of tiled probes spanning the promoter and all three exons. Significant probes of PU.1 vs. IgG ChIP-Chip analysis of RAW264.7 cells are shown in black and differentially expressed probes in exon array analyses of 24 h OHT-treated PUER cells versus untreated PUER cells are depicted in red. (C) Chromatin immunoprecipitation analysis of PU.1 and co-activator binding to the AMWAP promoter. Agarose gel analysis of AMWAP-specific PCR products generated from BV-2 DNA after chromatin immunoprecipitation with anti-PU.1, anti-Cbp, anti-p300, anti-AcH3, or anti-IgG-control antibodies. Input DNA was used as positive control in the PCR reaction. (D) Time kinetics of AMWAP transcript expression before and after OHT treatment of PUER cells to induce macrophage differentiation. Error bars indicate the standard deviation of the mean from two independent experiments performed in duplicates.

To recapitulate the findings from PU.1 ChIP-Chip experiments with RAW264.7 macrophages also in microglial cells, ChIP-PCR assays were performed with BV-2 microglia. The proximal −114/+68 AMWAP promoter region harbouring the conserved PU.1 site was specifically enriched in PU.1-precipitated DNA compared to the IgG control (Fig. 9C, upper panel). Moreover, ChIP-PCR products were obtained with precipitated DNA from antibodies directed against the transcriptional co-activators p300 and Cbp (Fig. 9C, lower panel), factors known to be involved in chromatin relaxation via histone acetyltransferase activity and RNA polymerase II recruitment to transcription start sites. The −114/+68 AMWAP promoter DNA was

also enriched in anti-AcH3 antibody precipitated DNA (Fig. 9C, lower panel), indicating open chromatin and active AMWAP gene expression in BV-2 cells.

We then aimed to validate the microarray findings of increased AMWAP mRNA expression in differentiated PUER cells by real-time qRT-PCR. In this tuneable system the PU.1-estrogen receptor binding domain fusion protein PUER is conditionally activated in myeloid progenitors upon addition of 4-hydroxy-tamoxifen (OHT), leading to rapid cell cycle arrest and differentiation into macrophages (Weigelt et al. 2009; Laslo et al. 2006). Quantitative RT-PCR analysis of independent RNAs from a time series of OHT-treated PUER cells showed very low AMWAP mRNA levels in PU.1$^{-/-}$ progenitors and a steep increase of AMWAP transcripts in OHT-differentiated cells (Fig. 9D). These data strongly support the hypothesis that AMWAP expression in macrophages as well as in microglia is critically dependent on PU.1 binding to its proximal promoter region.

AMWAP reduces pro-inflammatory gene expression and triggers alternative activation markers in microglia

To further investigate the immunological functions of AMWAP in microglia cells, the full-length open reading frame was over-expressed in BV-2 cells. A C-terminally 1D4-rhodopsin-epitope-tagged variant of AMWAP was transiently expressed in BV-2 cells. The rhodopsin epitope is not endogenously expressed in BV-2 cells, as shown by the absence of a Western blot band using a monoclonal anti-1D4 antibody (Fig. 10A). A specific band of 10 kDa was detected in cells transfected with the pAMWAP-1D4 construct, demonstrating successful over-expression of AMWAP in BV-2 cells (Fig. 10A). A milk fat globule protein-1D4 fusion protein was used as positive control and produced the expected band size of 15 kDa (Fig. 10A). To verify these findings and to visualize AMWAP within cells, BV-2 transformants expressing AMWAP-GFP or only GFP as control were generated. GFP-immunofluorescence confirmed that recombinant AMWAP was expressed in BV-2 cells (Fig. 10B). AMWAP-GFP was localized in perinuclear structures and in some cells in dome-shaped structures with a polarity that resembled the Golgi apparatus (Fig. 10B, arrows in left panel). In constrast, GFP alone was broadly expressed in the cytoplasmic region (Fig. 10B, right panel). This finding is consistent with proteins that

are processed through the endoplasmic reticulum and Golgi for extracellular transport.

Because AMWAP transcription was regulated by pro-inflammatory activation and the related WAP protein SLPI modifies inflammatory responses (Nakamura et al. 2003; Taggart et al. 2005), the effect of AMWAP on macrophage/microglia activation marker expression was studied. The immune-regulatory potential of AMWAP was addressed under basal and LPS-treated conditions. Enhanced AMWAP-GFP expression in non-stimulated and LPS-treated BV-2 cells reduced transcripts for Il1-β, Il-6, and Ccl2, three typical markers for pro-inflammatory activation of macrophages (Fig. 10C-E). In the same cells, the alternative macrophage activation markers *arginase 1* and Cd206 were substantially increased (Fig. 10F-G). These effects were not due to different growth conditions of the cells or varying transfection efficiencies (data not shown). To investigate if AMWAP is also a direct suppressor of pro-inflammatory gene transcription, we determined its effect on Ccl2 promoter activity. A stable BV-2 cell line was generated with a luciferase reporter under the control of the murine Ccl2 promoter region. In these cells, transient co-transfection of AMWAP strongly decreased Ccl2 promoter activity compared to mock transfected cells (Fig. 10H).

We next studied the role of physiological AMWAP levels in the modulation of microglial activation. Knock-down experiments with specific AMWAP siRNA or control siRNA were performed and marker transcripts were determined in transiently transfected BV-2 cells. A 30 % knock-down of AMWAP expression was achieved in both the basal and LPS-activated state (Fig. 11A). AMWAP silencing resulted in significantly de-repressed transcript levels of Il1-β, Il-6, and Ccl2 (Fig. 11B-D) and markedly reduced *arginase 1* and Cd206 expression (Fig. 11E, F). These data suggest that AMWAP acts as negative regulator of pro-inflammatory gene expression and may support alternative activation of microglial cells.

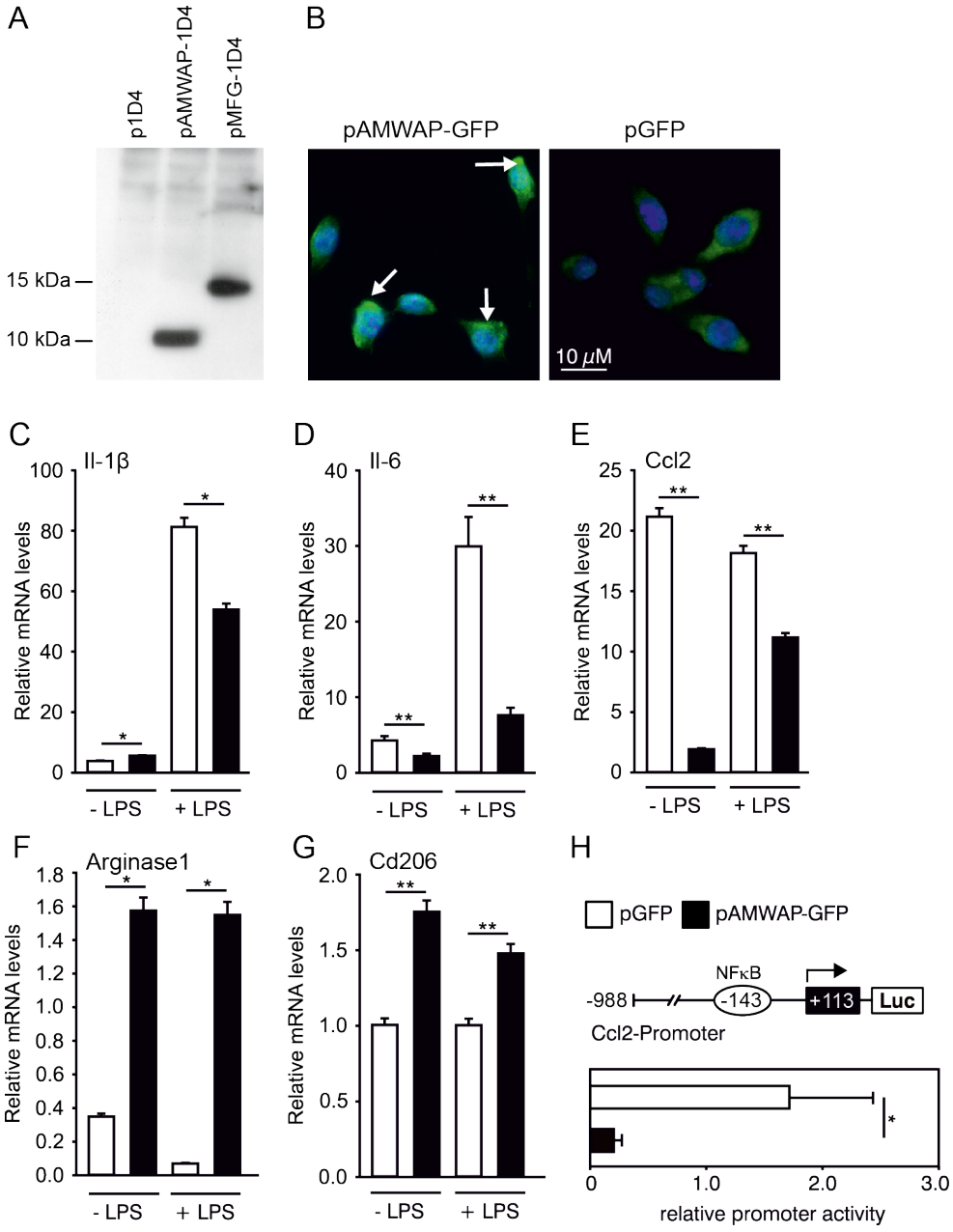

Figure 10 AMWAP over-expression reduces pro-inflammatory gene expression and up-regulates alternative activation markers in BV-2 microglia. (A) BV-2 cells were transiently transfected with an AMWAP-Rhodopsin 1D4 tag fusion protein, empty 1D4 mock vector, or a milk fat globule (MFG)-1D4 control protein, respectively. Cells were then analyzed by Western blot with anti-1D4-antibody. (B) BV-2 cells were transiently transfected with an AMWAP-GFP fusion protein or GFP vector alone. Intracellular GFP was detected by immunofluorescence microscopy. Dome-shaped Golgi regions are indicated by arrows. *(C-G)* qRT-PCR analysis of Il-6-, Il-1β- and Ccl2-transcripts as pro-inflammatory markers (C-E) and arginase 1 and Cd206 levels as alternative activation markers (F, G) in AMWAP-GFP versus GFP over-expressing BV-2 cells under basal and LPS-stimulated conditions. (H) Luciferase assays of BV-2 microglia containing a stable Ccl2-promoter-luciferase-construct. BV-2 cells stably expressing the Ccl2 reporter were transiently transfected with either AMWAP-GFP or GFP control vector. 24 h after transfection luciferase acitvity was determined. Bar graphs represent means ± SD of three independent cell cultures analyzed in triplicates. *, $p<0.05$; **, $p<0.01$; Student's t test.

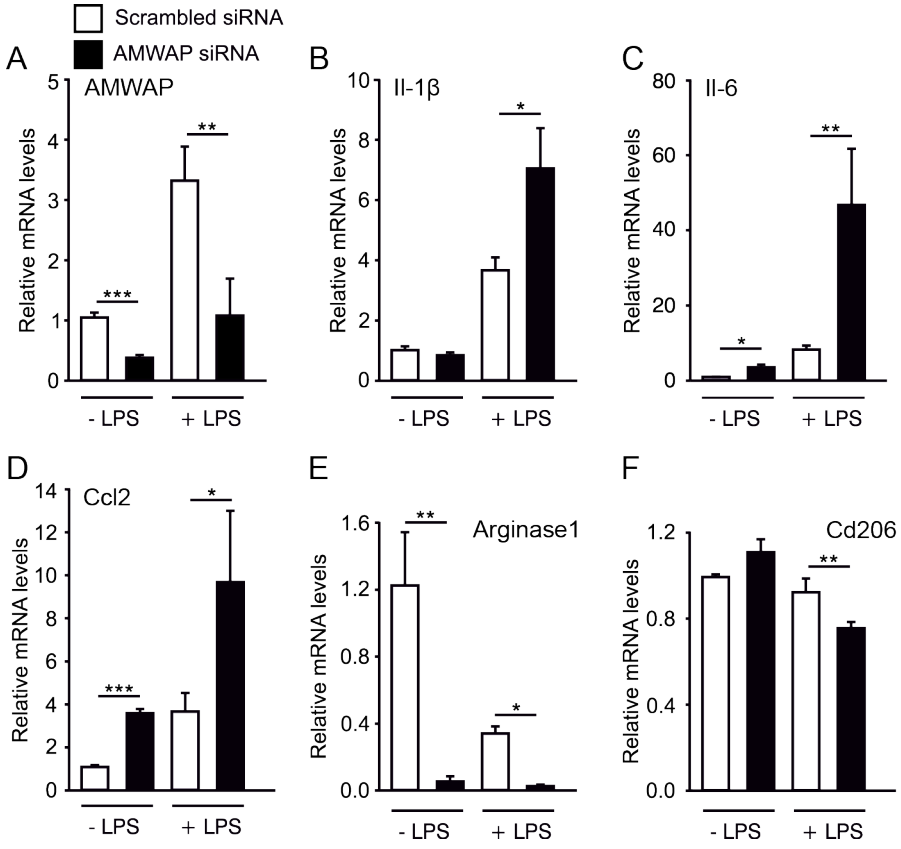

Figure 11 AMWAP knock-down leads to increased pro-inflammatory gene expression and impairs expression of alternative activation markers in BV-2 microglia. BV-2 cells were transiently transfected with 33 nM of each AMWAP-specific siRNA or non-targeting (scrambled) siRNA for 24 h. Thereafter, cells were left untreated or were further stimulated with 5 ng/ml LPS for 24 h. mRNA levels for AMWAP (A), Il1-β (B), Il6 (C), Ccl2 (D), arginase 1 (E), and Cd206 (F) were determined by qRT-PCR. Bar graphs represent means ± SD of three independent cell cultures analyzed in triplicates. *, $p<0.05$; **, $p<0.01$; ***, $p<0.001$; Student's t test.

AMWAP blocks microglial migration and acts as serine-protease inhibitor

To assess whether AMWAP influences the motility of microglia as a functional parameter, in vitro wound-healing assays and transwell migration experiments were performed. A cell-free zone was created in confluent monolayers of stably transfected BV-2 cells by scraping cells off with a pipette tip. The repopulation of the cell-free zone was then monitored by microscopy. In GFP control cells, migration into the wounded area was completed after 24 h (Fig. 12A, left panels). In contrast, AMWAP-GFP expressing cells showed a clearly reduced capacity to repopulate the cleared area, indicating diminished migratory potential (Fig. 12A, right panels).

To rule out the possibility that the reduced microglial migration in the scratch assays was due to different proliferation rates of stably transfected BV-2 cells, we tested their

LPS-induced chemotactic migration in transwell chambers. In this system, stable AMWAP over-expression reduced the LPS-induced transwell migration of BV-2 cells to 50% compared to GFP expressing cells (Fig. 12B). In contrast, transient siRNA knock-down of AMWAP significantly promoted chemotactic migration of BV-2 microglial cells compared to cells transfected with non-targeting control siRNA (Fig. 12C). These findings implicate that modulation of AMWAP expression levels in microglia directly influences their migration capacity.

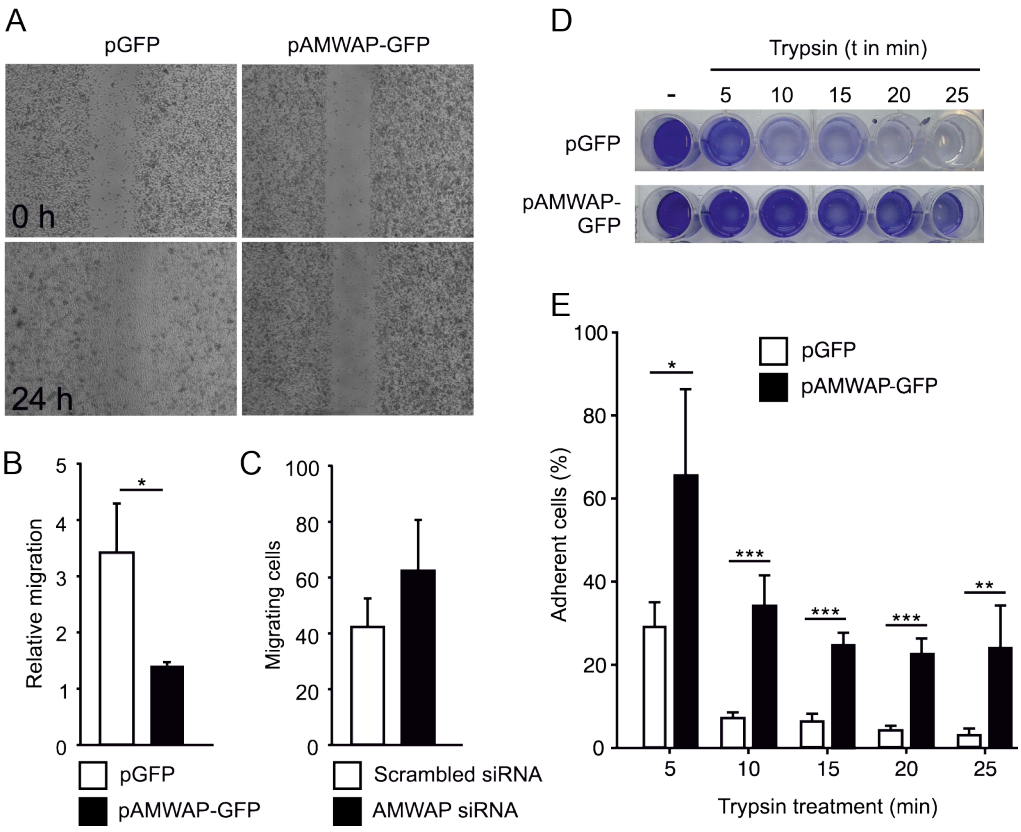

Figure 12 AMWAP attenuates microglial migration and exerts anti-serine protease activity. (A) Wound-healing assay in BV-2 microglia stably expressing AMWAP-GFP or GFP as control. AMWAP-GFP and GFP expressing BV-2 microglia were grown to comparable cell density, wounded with a pipette tip and microphotographs from wounded areas were taken immediately and after 24 hours. (B) Relative LPS-induced transwell chamber migration of stably transfected AMWAP-GFP versus GFP expressing BV-2 microglia. (C) BV-2 microglia were transiently transfected with AMWAP-specific siRNA or non-targeting (scrambled) siRNA for 24 h. Thereafter, the lower wells of transwell chambers were treated with LPS for further 24 h and the absolute numbers of migrating cells were counted. (D) Trypsin protease protection assay. Stable AMWAP-GFP and GFP expressing BV-2 microglia were treated with 0.25% trypsin for the indicated time points. Residing attached cells were stained with crystal violet, washed with PBS and photomicrographs were taken. (E) Quantitative analysis of anti-protease activity in AMWAP-GFP and GFP expressing BV-2 microglia. Optical densities were normalized to untreated cells. Bars represent the percentage of adherent cells after different time points of trypsin incubation. Data are expressed as mean ± SD of duplicate measurements from three independent biological replicates. *, $p<0.05$; **, $p<0.01$; ***$p<0.001$; Student's t test.

Since SLPI and other WAP proteins are potent serine protease inhibitors (Weldon et al. 2007), we investigated a similar function of AMWAP in a trypsin-protection assay. In this test system, the adhesive capacity of cells is monitored in the presence of trypsin in a time course (Nukumi et al. 2007). The rate of adherent cells after trypsinization for 5 min was significantly higher in AMWAP-expressing cultures than GFP control cells (Fig. 12D, E). This difference persisted at all time points analyzed up to 25 min trypsin incubation, indicating that AMWAP confers protease resistance and increases microglial adhesion. In agreement with the wound-healing assays, the transwell chemotaxis tests and the Ccl2 expression data, these results indicate an immuno-modulatory role of AMWAP by limiting microglial migration.

Recombinant AMWAP has anti-bacterial activity

As anti-bacterial activity is a major feature of WAP domain proteins, we studied the effect of recombinant AMWAP on different bacterial strains. Initially, we only achieved low recombinant expression of AMWAP in E. coli (data not shown). Therefore, codon-optimized AMWAP (Fig. S1) was synthesized, expressed in *E.coli*, and purified via an N-terminal His-tag sequence by affinity chromatography. Western blot analysis of the recombinant protein via an anti-His antibody detected a single specific band at the expected molecular mass of ~10 kDa (Fig. 13A). To study the anti-bacterial potential of AMWAP, the target bacteria *E. coli* (ATCC25922, Gram-negative rod), *P. aeruginosa* (ATCC27853, Gram-negative rod), and *B. subtilis* (ATCC6633, Gram-positive rod) were incubated in the presence of recombinant AMWAP for 2 h. After overnight growth on plates, colony forming units were counted to assess the number of viable bacteria. AMWAP showed a relatively weak (IC_{50} of 30 µM) but significant bactericidal activity against *E. coli* (Fig. 13B). Growth of *P. aeruginosa* (Fig. 13C) and *B. subtilis* (Fig. 13D) was significantly inhibited at lower micromolar concentrations (IC_{50} of 16 µM). Thus, the anti-bacterial potential of AMWAP increased dose-dependently and reached similar IC_{50} values as those of other WAP motif proteins including SLPI (Hiemstra et al. 1996) and elafin (Simpson et al. 1999).

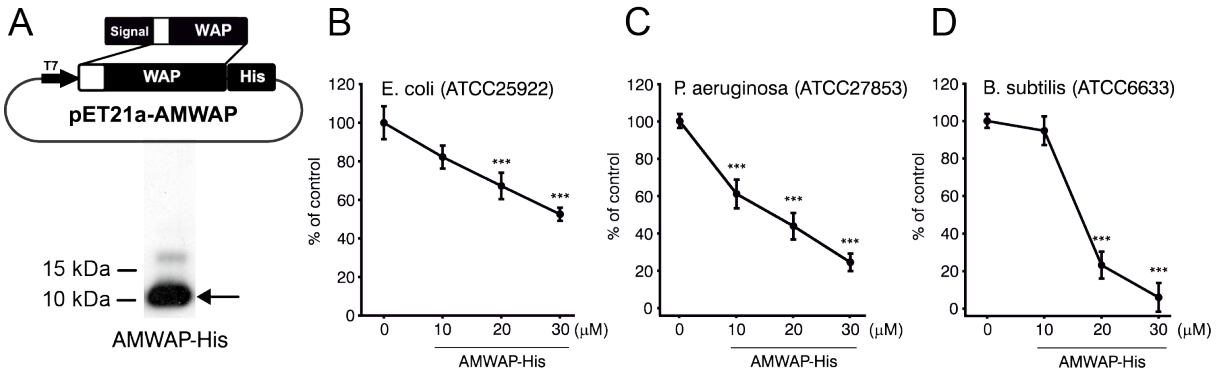

Figure 13 Expression, purification and anti-microbial activity of recombinant AMWAP. (A) Schematic presentation of the pET21a-AMWAP expression construct. Codon-optimized AMWAP cDNA sequence lacking the signal peptide was cloned into pET21a(+) vector in frame with a His-tag. Expression in E. coli BL21(DE3) was induced by 1 mM isopropyl-β-D-thiogalactoside and AMWAP-His was purified from the soluble fraction of the bacterial lysate using Ni-TED columns. Purified recombinant AMWAP-His was separated by SDS-PAGE and detected with Anti-His antibody. (B-D) Growth inhibitory activity of different concentrations of recombinant AMWAP-His on E. coli (B), P. aeruginosa (C) and B. subtilis (D). Log-phase bacterial cultures were incubated with the indicated concentrations of AMWAP-His in MT-LB medium for 2h at 37°C. Bacteria were then plated over-night and the number of colony-forming-units was determined by counting colonies. Cells incubated with PBS were set as 100%. Data are expressed as mean ± SD of duplicate measurements from three independent biological replicates. ***p<0.001; Mann-Whitney-U test.

Discussion

This study is part of an ongoing effort to characterize known and novel transcripts involved in the activation and regulation of microglia during retinal degeneration. We identified the novel mouse protein AMWAP and investigated its specific expression and function in activated microglia and macrophages. AMWAP attenuates pro-inflammatory cytokine and chemokine expression, while promoting expression of alternative activation markers. AMWAP also regulates microglial migration and chemotaxis and it directly exerts anti-bacterial activity.

Although initially identified in early activated microglia from retinoschisin-deficient retinas, induced AMWAP transcript levels were also detected in activated microglia stimulated with multiple TLR ligands including LPS, CpG oligonucleotides, PAM3SCK4 as well as IFN-γ. Up-regulation of AMWAP by these pro-inflammatory stimuli was critically dependent on NFkB but also involves new protein synthesis. AMWAP mRNA expression was highly enriched in microglia and other tissue macrophages, but transcripts were absent in all other mouse tissues studied so far. These findings on TLR-dependent and microglia/macrophage-restricted expression correlate well with the major influence of NFkB and PU.1 in the transcriptional control of the AMWAP gene. PU.1 is a key transcription factor in myeloid cells, with high expression levels in activated retinal microglia (Weigelt et al. 2007; Walton et al. 2000). Although the precise mechanisms underlying the activation-dependent induction of AMWAP are not fully understood, we postulate that PU.1 plays a critical role in AMWAP expression by direct binding to the proximal promoter.

Immune-related genes including cytokines and chemokines, as well as their receptors are often organized in chromosomal clusters or miniclusters (Rowell et al. 2008; Colobran et al. 2007; Zlotnik et al. 2006). In agreement with this concept, the murine AMWAP gene is located in close proximity to a cluster of the chemokine genes Ccl3, Ccl4, Ccl5, Ccl6, and Ccl9. On the other side, the AMWAP gene is flanked by the WAP protein extracellular peptidase inhibitor precursor (Expi), which shares 83% sequence homology possibly suggesting a gene duplication event. Our ChIP-Chip and ChIP-PCR assays have revealed that the AMWAP promoter, but not the Expi region are bound by PU.1 and the co-activators Cbp and p300. These

findings are consistent with microglia/macrophage-restricted expression of AMWAP and the ubiquitous expression of Expi (D. Jung et al. 2004). Likely, the different expression patterns and regulation of both genes coincides with different cellular functions. In line with this, Expi was identified as a protein over-expressed in non-metastatic mammary cancer cells (Dear et al. 1989; Dear et al. 1988) and ectopic expression of Expi resulted in induced apoptosis of mammary epithelial cells (D. Jung et al. 2004).

Together with SLPI (Mueller et al. 2008), the best studied WAP protein so far, AMWAP is the only other WAP family member expressed and regulated in microglia. SLPI transcript levels were markedly increased in experimental autoimmune encephalomyelitis and a role for SLPI in the promotion of tissue repair was discussed (Mueller et al. 2008). SLPI can be secreted by activated macrophages and acts as a suppressor of LPS response (F. Y. Jin et al. 1997). The inhibition of LPS-induced NO and TNF production in macrophage cell lines by SLPI is independent of its anti-protease function (J. Yang et al. 2005). Intracellular SLPI also competes with NFkB for binding sites in the promoters of pro-inflammatory cytokines (Taggart 2002) and blocks LPS-induced IκBα-degradation (Rubartelli & Lotze 2007). Both mechanisms may also be relevant for AMWAP function. Support for the hypothesis that AMWAP similar to SLPI interferes with NFkB signaling comes from our finding that Ccl2 promoter activity was directly repressed by AMWAP.

Two major questions relate to why and how AMWAP expression is induced during microglia activation in retinal degeneration. Since no obvious infection is present in the gene mutation-based model of retinoschisin-deficient retinas, we speculate that AMWAP is induced by damage-associated-molecular-patterns (DAMPs) (Oppenheim & D. Yang 2005) and/or alarmins (Scheibner et al. 2006). Our data on the rapid induction of AMWAP in early retinal degeneration and the TLR-dependent up-regulation in BV-2 cells support the assumption that AMWAP may respond very sensitive to DAMPs. Innate immune cells are often recruited to injured areas by matrix degradation products (Klune et al. 2008) or actively secreted alarmin molecules like HMGB1 (Odaka et al. 2003), consequently initiating tissue remodeling and repair. Related to this, a secreted and a non-secreted intracellular form of SLPI were both induced in mouse macrophages after exposure to apoptotic cells

(Sheehan et al. 2007), indicating that SLPI may promote clearance of dying cells in the absence of inflammation. AMWAP may have a similar “alarmin-like” function in the degenerating retina and thereby may limit microglial activation.

A hallmark of retinal degeneration in the retinoschisin-deficient mouse model is the rapid migration of activated microglia into the photoreceptor and ganglion cell layer (Ebert et al. 2009). Ccl2, an important chemoattractant is strongly expressed in $Rs1h^{-/Y}$ retinas (Gehrig et al. 2007) and we demonstrated that AMWAP over-expression down-regulated Ccl2 transcripts in microglia. Furthermore, AMWAP diminished BV-2 cell migration and inhibited the serine protease trypsin. Recent data indicated that Ccl2 is proteolytically activated by the serine protease plasmin and that plasmin-deficient mice were resistant to excitotoxic neurodegeneration (Shai 2002). Thus, in addition to its effect on Ccl2 gene expression, AMWAP may impair Ccl2-mediated migration of microglia by limiting proteolytic processing of Ccl2.

Our study also suggests that recombinant AMWAP has a potent anti-microbial activity. Most bactericidal proteins have a cationic surface that bind negatively charged phospholipids and thereby disturb the integrity of bacterial membranes (Hagiwara et al. 2003). Although AMWAP has a lower predicted positive charge than SLPI and elafin (Moreau et al. 2008), we detected significant antimicrobial activity against *E. coli*, *P. aeruginosa* and *B. subtilis* at micromolar concentrations. The domain signature of AMWAP is related to the anti-microbial single-WAP-domain proteins SWAM1 and SWAM2 (Hagiwara et al. 2003). We therefore speculate that local positive charges on the 3D protein surface of AMWAP could be important for antibacterial activity (Zasloff 2002).

Although the precise mechanisms remain to be determined, the data described in this study suggest that AMWAP induction by neuronal degeneration and inflammatory signals is an important counter-regulatory response in microglial and macrophage activation. Moreover, AMWAP seems to actively support alternative activation of microglia and macrophages. AMWAP could be a potential candidate for modulating the homeostasis of microglia and thereby limit neurotoxicity and apoptotic degeneration. AMWAP-deficient mice will be a valuable tool to further characterize the *in vivo* role of this novel WAP protein in microglia and macrophage function.

Acknowledgments

We thank Bernhard Weber and Joost Oppenheim for critical reading of the manuscript and David Hume for helpful discussions. We also thank Johann Röhrl for providing the bacterial strains *P. aeruginosa* and *B. subtilis*.

2.2 Chapter 2 – Curcumin (Karlstetter et al. 2011)

Curcumin is a potent modulator of microglial gene expression and migration

Marcus Karlstetter*, Elena Lippe*, Yana Walczak*, Christoph Moehle,
Alexander Aslanidis, Myriam Mirza, and Thomas Langmann

* Authors contributed equally to this work

Published in the Journal of Neuroinflammation. 2011 Sep 29;8:125.

Abstract

Background

Microglial cells are important effectors of the neuronal innate immune system with a major role in chronic neurodegenerative diseases. Curcumin, a major component of tumeric, alleviates pro-inflammatory activities of these cells by inhibiting nuclear factor kappa B (NFkB) signaling. To study the immuno-modulatory effects of Curcumin on a transcriptomic level, DNA-microarray analyses were performed with resting and LPS-challenged microglial cells after short-term treatment with Curcumin.

Methods

Resting and LPS-activated BV-2 cells were stimulated with Curcumin and genome-wide mRNA expression patterns were determined using DNA-microarrays. Selected qRT-PCR analyses were performed to confirm newly identified Curcumin-regulated genes. The migration potential of microglial cells was determined with wound healing assays and transwell migration assays. Microglial neurotoxicity was estimated by morphological analyses and quantification of caspase 3/7 levels in 661W photoreceptors cultured in the presence of microglia-conditioned medium.

Results

Curcumin treatment markedly changed the microglial transcriptome with 49 differentially expressed transcripts in a combined analysis of resting and activated microglial cells. Curcumin effectively triggered anti-inflammatory signals as shown by induced expression of *Interleukin 4* and *Peroxisome proliferator activated receptor* α. Several novel Curcumin-induced genes including *Netrin G1*, *Delta-like 1*, *Platelet endothelial cell adhesion molecule 1*, and *Plasma cell endoplasmic reticulum protein 1*, have been previously associated with adhesion and cell migration. Consequently, Curcumin treatment significantly inhibited basal and activation-induced migration of BV-2 microglia. Curcumin also potently blocked gene expression related to pro-inflammatory activation of resting cells including *Toll-like receptor 2* and *Prostaglandin-endoperoxide synthase 2.* Moreover, transcription of *NO synthase 2* and *Signal transducer and activator of transcription 1* was reduced in LPS-triggered microglia. These transcriptional changes in Curcumin-treated LPS-primed microglia

also lead to decreased neurotoxicity with reduced apoptosis of 661W photoreceptor cultures.

Conclusions

Collectively, our results suggest that Curcumin is a potent modulator of the microglial transcriptome. Curcumin attenuates microglial migration and triggers a phenotype with anti-inflammatory and neuroprotective properties. Thus, Curcumin could be a nutraceutical compound to develop immuno-modulatory and neuroprotective therapies for the treatment of various neurodegenerative disorders.

Background

Microglial cells are resident macrophages of the nervous system with pivotal roles in innate immune regulation and neuronal homeostasis (Hanisch & Kettenmann 2007; Streit 2002). They are cells of the mononuclear phagocyte lineage but their unique localization within the nervous system and their morphological features clearly distinguish them from other macrophage populations (Giulian et al. 1995). Ramified microglial cells actively scan their environment with their long protrusions (Davalos et al. 2005; Nimmerjahn et al. 2005) and continuous inhibitory signals from neurons prevent microglial toxicity (Broderick et al. 2002; Cardona et al. 2006). Disconnection of the microglia-neuron cross-talk (Dick 2003), local danger signals such as released ATP (Haynes et al. 2006), or neurotransmitter gradients (Ransohoff & Perry 2009) can lead to a functional transformation of microglial populations with a variety of effector functions. Consequently, alarmed microglia and reactive microgliosis have been identified in a variety of neurodegenerative diseases including *Alzheimer's disease* (Khoury & Luster 2008), *Parkinson's disease* (Orr et al. 2002), *amyotrophic lateral sclerosis* (Sargsyan et al. 2005), *multiple sclerosis* (Raivich & Banati 2004), and inherited photoreceptor dystrophies (Langmann 2007). The concept of a microglia-targeted pharmacotherapy to prevent neurodegeneration in the brain and the retina is therefore a promising approach under active investigation (Schuetz & Thanos 2004; Schwartz 2007).

There is a growing interest in the identification of natural compounds that limit neuroinflammation and simultaneously support neuronal survival (Zhang et al. 2009;

Jang & Johnson 2010). Among the naturally occuring immuno-modulators, Curcumin ((E,E)-1,7-bis(4-hydroxy-3-methoxyphenyl)-1,6-heptadiene-3,5-dione), a major constituent of tumeric, is a herbal medicine used for centuries in India and China (Ammon & Wahl 1991). Curcumin has a wide range of pharmacological activities including anti-inflammatory, anti-microbial, antioxidant, and anti-tumor effects (Maheshwari et al. 2006). Curcumin is a particularly potent immuno-regulatory agent that can modulate the activation and function of T-cells, B-cells, neutrophils, natural killer cells and macrophages (Jagetia & Aggarwal 2007).

Curcumin treatment effectively inhibits the activation of microglial cells by diminishing the production of nitric oxide (K. K. Jung et al. 2006) and reducing the secretion of pro-inflammatory cytokines such as Il1β, Il6 and TNF (C.-Y. Jin et al. 2007a). Moreover, Curcumin blocks the LPS-mediated induction of cyclooxygenase-2 (COX2) via inhibition of the transcription factors nuclear factor kappa B (NFkB), activator protein 1 (AP1), and signal transducers and activators of transcription (STATs) (Kang et al. 2004; H. Kim et al. 2003). Recent experiments have also demonstrated that Curcumin protects dopaminergic neurons against microglia-mediated neurotoxicity (He et al. 2010), limits brain inflammation (S. Yang et al. 2008), and rescues retinal cells from stress-induced cell death (Mandal et al. 2009).

The inhibitory role of Curcumin on pro-inflammatory gene expression in microglia is well documented. However, this information is limited to only a few well-studied examples including pro-inflammatory cytokines, Nos2 and COX2. In a genome-wide search for target genes, we investigated the transcriptomic effects of Curcumin in resting and LPS-activated BV-2 microglial cultures using DNA-microarrays. Furthermore, we validated the Curcumin-regulated expression of microglial transcripts with qRT-PCR and studied the related microglial migration and neurotoxicity.

Methods

Reagents

Curcumin and *E.coli* 0111:B4 lipopolysaccharide were purchased from Sigma Aldrich (Steinheim, Germany). Curcumin was dissolved in DMSO and added in concentrations that did not exceed 0.05% of the total volume in any of the cell culture experiments.

Cell culture

BV-2 microglia-like cells were provided by Professor Ralph Lucius (Clinic of Neurology, Christian Albrechts University, Kiel, Germany). BV-2 cells were cultured in RPMI/5% FCS supplemented with 2mM L-Glutamine and 195 nM β-mercaptoethanol. BV-2 cells were stimulated with 100 ng/ml LPS, 20 µM of Curcumin, or DMSO as control for 6 h. These stimulation conditions were adapted from previously published experiments (C.-Y. Jin et al. 2007a; Dirscherl et al. 2010). MTT assays revealed that 100 ng/ml LPS, 20 µM Curcumin, or a combination of both had no cytotoxic effects on BV-2 cells (data not shown). 661W photoreceptor-like cells were a gift from Prof. Muayyad Al-Ubaidi (University of Illinois, Chicago, IL) and the culture conditions have been described elsewhere (Ebert et al. 2008).

Scratch assay

500.000 BV-2 cells were grown in 6-well plates as 80% confluent monolayers and were wounded with a sterile 100 µl pipette tip. Thereafter, the cells were stimulated with 100 ng/ml LPS, 20 µM of Curcumin, 100 ng/ml LPS + 20 µM of Curcumin, or DMSO as solvent control. Migration into the open scar was documented with microphotographs at different time points after wounding. The number of migrating cells was quantified by counting all cells within a 0.4 mm^2 region in the center of each scratch. A minimum of 5 individual cultures was used to calculate the mean migratory capacity of each cell culture condition.

Transwell migration assay

The Costar Transwell System (8-µm pore size polycarbonate membrane) was used to evaluate vertical cell migration. 1 Mio BV-2 cells in 1.5 ml serum-free medium were added to the upper well, and 2.6 ml serum-free medium was added to the lower chamber. 100 ng/ml LPS, 20 µm Curcumin, 100 ng/ml LPS + 20 µm Curcumin, or DMSO as solvent control were added to the lower chamber medium. At the end of a 24 h incubation period, cells that had migrated to the lower surface were quantified by counting the migrated cells on the lower surface of the membrane using microscopy.

661W co-culture in microglia-conditioned medium and apoptosis assay

To test microglial neurotoxicity, a culture system of 661W photoreceptors with microglia conditioned medium was established. 661W cells were incubated for 48 h either in their own medium or with culture supernatants from unstimulated, 100 ng/ml LPS, 20 µM Curcumin, or 100 ng/ml LPS + 20 µM Curcumin treated microglial cells. The 661W cell morphology was assessed by phase contrast microscopy and apoptotic cell death was determined with the Caspase-Glo® 3/7 Assay (Promega). Cells were lysed and incubated with a luminogenic caspase-3/7 substrate, which contains the tetrapeptide sequence DEVD. Luminescence was then generated by addition of recombinant luciferase and was proportional to the amount of caspase activity present. The luminescent signal was read on a BMG FluoStar Optima plate reader (Labtech, Offenburg, Germany). A blank reaction was used to measure background luminescence associated with the cell culture system and Caspase-Glo® 3/7 Reagent. The value for the blank reaction was subtracted from all experimental values. Negative control reactions were performed to determine the basal caspase activity of 661W cells. Relative luciferase units (RLU) reflect the level of apoptotic cell death in the different 661W cell cultures.

RNA isolation and reverse transcription

Total RNA was extracted from cultured microglial cells according to the manufacturer's instructions using the RNeasy Protect Mini Kit (Qiagen, Hilden, Germany). Purity and integrity of the RNA was assessed on the Agilent 2100 bioanalyzer with the RNA 6000 Nano LabChip® reagent set (Agilent Technologies, Böblingen, Germany).

The RNA was quantified spectrophotometrically and then stored at −80 °C. First-strand cDNA synthesis was performed with RevertAid™ H Minus First Strand cDNA Synthesis Kit (Fermentas, St. Leon-Rot, Germany).

DNA-microarray analysis

4x44K microarrays (014868) (Agilent Technologies) were used for hybridization with three independent RNAs from non-stimulated BV-2 microglial cells or cultures treated for 6 h with 20 µM Curcumin, 100 ng/ml LPS, or 20 µM Curcumin + 100 ng/ml LPS, respectively. Briefly, 200 ng of total RNA were labeled with Cy3 using the Agilent Quick-Amp Labeling Kit - 1 color according to the manufacturer´s instructions. cRNA was purified with the RNeasy Mini Kit (Qiagen) and labeling efficiency was determined with a NanoDrop ND-1000 photometer (PeqLab). The arrays were incubated with cRNAs in Agilent SureHyb chambers for 17 hours at 65°C while rotating. After washing, scanning was done with the Agilent G2565CA Microarray Scanner System and the resulting TIFF files were processed with Agilent Feature Extraction software (10.7.). Minimum information about a microarray experiment (MIAME) criteria were met (Brazma et al. 2001). The microarray dataset of this study is publicly available at the National Center for Biotechnology Information Gene Expression Omnibus (http://www.ncbi.nlm.nih.gov/geo/) as series record GSE23639.

Bioinformatic data analysis

Integrative analysis of genome-wide expression activities from BV-2 cells was performed with the Gene Expression Dynamics Inspector (GEDI), a Matlab (Mathworks, Natick, MA) freeware program which uses self-organizing maps (SOMs) to translate high-dimensional data into a 2D mosaic (Eichler et al. 2003). Each tile of the mosaic represents an individual SOM cluster and is color-coded to represent high or low expression of the cluster's genes, thus identifying the underlying pattern. The Partek Genomics Suite (Partek Inc.) was used for ANOVA analysis and hierarchical clustering of normalized expression values. Differentially regulated transcripts in Curcumin-stimulated versus non-treated and Curcumin + LPS versus LPS-treated BV-2 cells, respectively, were retrieved with the Genomatix ChipInspector program (Genomatix Software GmbH, Munich, Germany), applying the Significance Analysis of Microarray (SAM) algorithm using a false-discovery rate of 0.1%.

Quantitative real-time RT-PCR

Amplifications of 50 ng cDNA were performed with an ABI7900HT machine (Applied Biosystems) in triplicates in 10 µl reaction mixtures containing 1×TaqMan Universal PCR Master Mix (Applied Biosystems), 200nM of primers and 0.25 µl dual-labeled probe (Roche Probe Library). The reaction parameters were as follows: 2-min 50 °C hold, 30-min 60 °C hold, and 5-min 95 °C hold, followed by 45 cycles of 20-s 94 °C melt and 1-min 60 °C anneal/extension. Measurements were performed in triplicate. Results were analyzed with an ABI sequence detector software version 2.3 using the ΔΔCt method for relative quantitation. A Ct (cycle threshold) <35 was used as cutoff for estimating significantly expressed transcripts and cDNA samples with values >35 were marked with n.e. for not expressed. Ct-values between 35 and 40 were solely used for calculation of relative expression differences in treated cells versus control cells. Primer sequences and Roche Library Probe numbers are listed in Table 1.

Table 1 Primer pairs and Roche library probes for real-time qRT-PCR validation

Gene	F-Primer (5'-3')	R-Primer (5'-3')	Roche Library Probe
Atp5b	ggcacaatgcaggaaagg	tcagcaggcacatagatagcc	77
C3	accttacctcggcaagtttct	ttgtagagctgctggtcagg	76
Ccl2	catccacgtgttggctca	gatcatcttgctggtgaatgagt	62
Dll1	ttcaactgtgagaagaagatggat	gccgaggtccacacactt	103
Egr2	ctacccggtggaagacctc	aatgttgatcatgccatctcc	60
Il4	catcggcattttgaacgag	cgagctcactctctgtggtg	2
Il6	gatggatgctaccaaactggat	ccaggtagctatggtactccaga	6
Nos2	ctttgccacggacgagac	tcattgtactctgagggctga	13
Ntng1	aggggcaagagaccaagg	agggatggtgtctatcgtcct	103
Pecam1	cggtgttcagcgagatcc	cgacaggatggaaatcacaa	45
Perp1	tcatatgccggctcacct	atccactggcgtctggagt	110
Pparα	ccgagggctctgtcatca	gggcagctgactgaggaa	11
Ptgs2	gatgctcttccgagctgtg	ggattggaacagcaaggattt	45
Stat1	aaatgtgaaggatcaagtcatgtg	catcttgtaattcttctagggtcttga	15
Tlr2	accgaaacctcagacaaagc	cagcgtttgctgaagagga	49

Statistical analyses

Statistical analyses were performed on ΔΔCt data using the Mann-Whitney Rank Sum test and quantitative expression data are expressed as mean ± SD plotted at a logarithmic scale. Gene expression levels in control BV-2 cells were used as calibrators. The Student´s t test or Mann-Whitney Rank Sum test were used for the

comparison of experimental groups in cell migration assays and apoptosis assays as indicated. $p<0.05$ was considered significant.

Results

Curcumin has a major impact on the microglial transcriptome

To determine the transcriptional profiles of resting and LPS-activated BV-2 microglial cells after treatment with 20 µM Curcumin for 6 h, we performed DNA-microarray analyses from three independent stimulations. We first applied the Gene Expression Dynamics Inspector (GEDI) on the complete dataset to visualize the global patterns of gene expression in the four different conditions, untreated, Curcumin-treated, LPS-treated, and Curcumin + LPS-treated cells. GEDI uses self-organizing maps to capture genome-wide transcriptome activity via 'gestalt' recognition (Eichler et al. 2003). GEDI facilitates the identification of genome-wide patterns with each mosaic tile in the map representing a gene cluster that is expressed at similar levels. The four GEDI maps, with blue color indicating low and red color high mRNA expression levels, show a dynamic regulation of gene transcription in the cultured microglial cells (Fig. 14A).

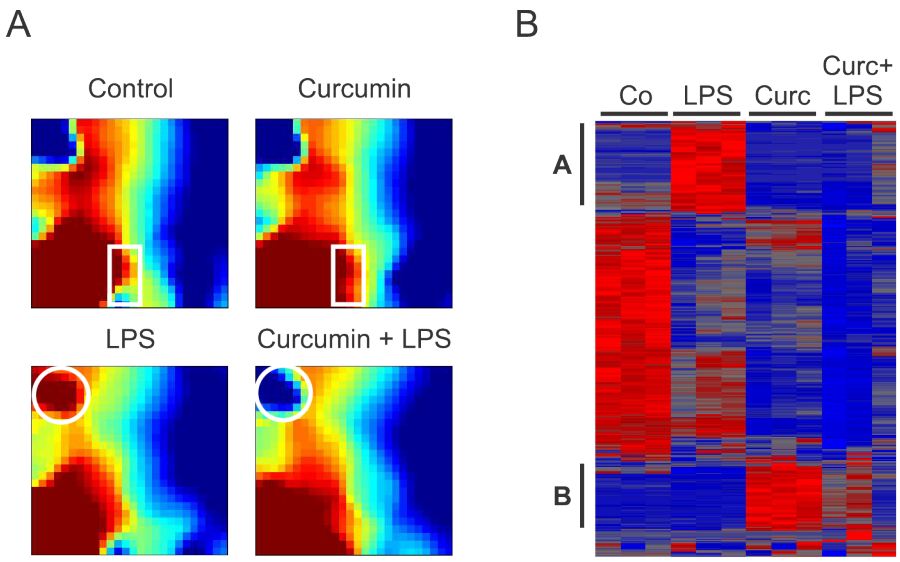

Figure 14 Curcumin influences global gene expression in resting and LPS-activated BV-2 microglial cells. (A) Gene Expression Dynamics Inspector (GEDI) analysis of the complete DNA-microarray dataset from control BV-2 cells or cells treated with 20 µM Curcumin, 100 ng/ml LPS, or 20 µM Curcumin + 100 ng/ml LPS for 6 hours. The white rectangles and circles denote the most prominent expression changes in corresponding gene clusters. (B) Hierarchical clustering of normalized expression levels after one-way ANOVA at $p<0.01$. Triplicate microarrays were analyzed for each condition and the pseudo-color scale indicates high (red) or low (blue) expression levels. LPS and Curcumin-related clusters are marked with A and B, respectively.

The major difference between Curcumin-treated resting microglial cells and control cells was a region with higher expression at the bottom of the map (Fig. 14A, white rectangles). In the LPS-treated condition, mimicking a highly activated state, elicited a largely converse expression pattern with a pronounced area of weakly expressed genes (Fig. 14A, white circles). These data indicate that Curcumin stimulates gene expression in resting, non-activated cells but mainly dampens activation-associated transcriptional programs in LPS-primed microglia.

We next calculated hierarchical clusters of each individual microarray dataset after filtering for significantly altered gene expression using one way ANOVA at $p<0.01$. This analysis showed a clear separation of the four different conditions with their own characteristic gene expression profiles (Fig. 14B). The clustering revealed two distinct groups of inversely regulated genes. Group A (Fig. 14B) contains LPS-induced genes, which are no longer up-regulated in the presence of Curcumin. Group B (Fig. 14B) represents genes selectively up-regulated by Curcumin treatment of resting microglial cells. Together with the GEDI analysis, these results demonstrate that stimulation with Curcumin impacts distinct patterns of gene expression in resting and LPS-activated microglial cells, respectively.

To narrow down the identified global gene clusters to a subset of genes with significantly different mRNA expression in the different Curcumin-treated conditions, we used the Genomatix ChipInspector tool applying the Significance Analysis of Microarray (SAM) algorithm at a false discovery rate of 0.1% and a minimum fold change of 2.0 (Weigelt et al. 2009). Thereby, 35 significantly regulated transcripts were identified in Curcumin-treated versus resting microglial cells (Table 2) and 30 differentially expressed genes were detected in Curcumin + LPS versus LPS-stimulated cells (Table 3). Comparison of the total numer of differentially expressed transcripts and considering overlapping gene sets revealed that Curcumin affects both resting and LPS-activated BV-2 cells.

Table 2 Differentially expressed transcripts after 6 h stimulation of BV-2 cells with 20µM Curcumin

Nr	ID	Symbol	Gene Name	FC
UP-REGULATED				
1	80883	Ntng1	Netrin G1	313.0
2	18613	Pecam1	Platelet/endothelial cell adhesion molecule 1	42.8
3	13388	Dll1	Delta-like 1	35.5
4	12824	Col2a1	Collagen, type II, alpha 1	21.6
5	14103	Fasl	Fas ligand (TNF superfamily, member 6)	12.8
6	12653	Chgb	Chromogranin B	11.9
7	66184	Rps4y2	Ribosomal protein S4, Y-linked 2	9.7
8	69816	Perp1	RIKEN cDNA 2010001M09 gene	9.7
9	16992	Lta	Lymphotoxin A	9.4
10	19206	Ptch1	Patched homolog 1	5.9
11	19013	Ppara	Peroxisome proliferator activated receptor alpha	4.6
12	109685	Hyal3	Hyaluronoglucosaminidase 3	4.5
13	20997	T	Brachyuri	4.2
14	17246	Mdm2	Transformed mouse 3T3 cell double minute 2	3.1
15	14102	Fas	Fas	2.8
16	14183	Fgfr2	Fibroblast growth factor receptor 2	2.7
17	13645	Egf	Epidermal growth factor	2.2
18	14179	Fgf8	Fibroblast growth factor 8	2.1
19	20655	Sod1	Superoxide dismutase 1	2.1
20	14526	Gcg	Glucagon	2.0
DOWN-REGULATED				
1	24088	Tlr2	Toll-like receptor 2	-6.9
2	18505	Pax3	Paired box gene 3	-6.6
3	14281	Fos	FBJ osteosarcoma oncogene	-4.4
4	11622	Ahr	Aryl-hydrocarbon receptor	-4.1
5	16835	Ldlr	Low density lipoprotein receptor	-3.8
6	13654	Egr2	Early growth response 2	-3.5
7	68010	Bambi	BMP and activin membrane-bound inhibitor	-3.3
8	12048	Bcl2l1	BCL2-like 1	-3.3
9	19225	Ptgs2	Prostaglandin-endoperoxide synthase 2	-3.0
10	20296	Ccl2	Chemokine (C-C motif) ligand 2	-2.8
11	12393	Runx2	Runt related transcription factor 2	-2.8
12	17311	Kitl	Kit ligand	-2.4
13	16869	Lhx1	LIM homeobox protein 1	-2.4
14	12977	Csf1	Colony stimulating factor 1	-2.4
15	20528	Slc2a4	Solute carrier family 2, member 4	-2.2

Significance analysis of triplicate microarrays was performed with a false discovery rate of 0.1%. ID, Entrez Gene ID; FC: Fold change.

Table 3 Differentially expressed transcripts after 6 h stimulation with 20 µM Curcumin + 100 ng/ml LPS versus 100 ng/ml LPS

Nr	ID	Symbol	Gene Name	FC
UP-REGULATED				
1	80883	Ntng1	Netrin G1	86.2
2	18613	Pecam1	Platelet/endothelial cell adhesion molecule 1	11.7
3	12824	Col2a1	Collagen, type II, alpha 1	9.0
4	12653	Chgb	Chromogranin B	8.1
5	14103	Fasl	Fas ligand (TNF superfamily, member 6)	6.9
6	19206	Ptch1	Patched homolog 1	6.5
7	69816	Perp1	RIKEN cDNA 2010001M09 gene	5.4
8	14526	Gcg	Glucagon	5.0
9	109685	Hyal3	Hyaluronoglucosaminidase 3	4.1
10	16189	Il4	Interleukin 4	3.8
11	20655	Sod1	Superoxide dismutase 1	3.5
12	19013	Ppara	Peroxisome proliferator activated receptor alpha	3.1
13	20997	T	Brachyuri	2.6
14	640627	Gm9789	ENSMUSG00000044227	2.6
15	16147	Ihh	Indian hedgehog homolog	2.6
16	17246	Mdm2	Transformed mouse 3T3 cell double minute 2	2.5
17	99439	Duox1	Dual oxidase 1	2.3
18	257956	Olfr1307	Olfactory receptor 1307	2.3
19	14179	Fgf8	Fibroblast growth factor 8	2.1
DOWN-REGULATED				
1	16193	Il6	Interleukin 6	-93.1
2	18126	Nos2	Nitric oxide synthase 2	-55.7
3	19225	Ptgs2	Prostaglandin-endoperoxide synthase 2	-17.6
4	20296	Ccl2	Chemokine (C-C motif) ligand 2	-14.7
5	12266	C3	Complement C3	-9.1
6	20846	Stat1	Signal transducers and activator of transcription 1	-7.4
7	12048	Bcl2l1	BCL2-like 1	-5.4
8	14281	Fos	FBJ osteosarcoma oncogene	-4.6
9	16835	Ldlr	Low density lipoprotein receptor	-4.1
10	16992	Lta	Lymphotoxin A	-3.5
11	17395	Mmp9	Matrix metallopeptidase 9	-2.2

Significance analysis of triplicate microarrays was performed with a false discovery rate of 0.1%. ID, Entrez Gene ID; FC: Fold change.

qRT-PCR confirmation of novel Curcumin target genes in microglial cells

To validate selected differentially expressed genes identified by DNA-microarrays, real-time qRT-PCR assays were performed with RNA samples from three Independent BV-2 stimulation series. We especially focused ongenes which have not been

previously shown to be Curcumin targets. In the first set of experiments, mRNA levels of genes highly up-regulated by Curcumin compared to control cells were assessed (Fig. 15). Transcripts of *Netrin G1* (Ntng1), *Platelet endothelial cell adhesion* molecule 1 (Pecam1), *Delta-like 1* (Dll1), *Plasma cell endoplasmic reticulum protein 1* (Perp1), *Peroxisome proliferator activated receptor alpha* (PPARα), and *Interleukin 4* (Il4) were all significantly increased by stimulation with Curcumin (Fig. 15).

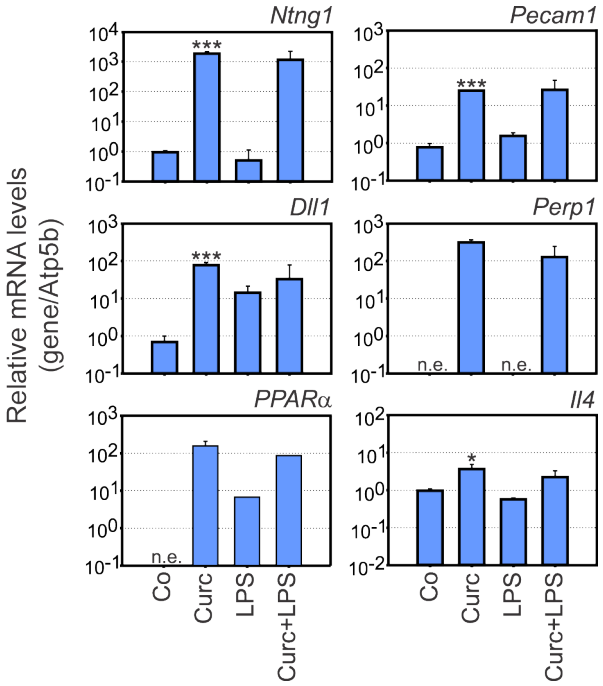

Figure 15 Curcumin induces genes related to adhesion and anti-inflammatory response. Real-time qRT-PCR validation of transcripts in BV-2 microglia stimulated with 20 µM Curcumin, 100 ng/ml LPS, or 20 µM Curcumin + 100 ng/ml LPS for 6 hours. Relative mRNA levels were quantified for Netrin G1 (Ntng1), Platelet endothelial call adhesion molecule 1 (Pecam1), Delta-like 1 (Dll1), Plasma cell induced endoplasmic reticulum protein 1 (Perp1), Peroxisome proliferator activated receptor α (PPARα), and Interleukin 4 (Il4). Expression was normalized to the control gene Atp5b and mRNA levels (+/- SD) are graphed relative to control cells. Results are calculated from three independent experiments performed in triplicate measurements. * $p \leq 0.05$, *** $p \leq 0.001$ for Curcumin vs. control, Mann-Whitney Rank Sum test. n.e., not expressed.

Ntng1 showed the strongest expression difference with a change of more than 1800-fold. Perp1 and PPARα transcripts were not significantly expressed in resting microglia and were switched on to intermediate levels after Curcumin treatment (Fig. 15). All six transcripts after combined LPS/Curcumin treatment remained similarly high as after Curcumin stimulation alone, indicating that the effects of Curcumin persist in activated microglial cells.

In the next series of qRT-PCR experiments, down-regulated transcripts known to be involved in pro-inflammatory activation of microglial cells were analyzed. *Toll-like receptor 2* (Tlr2), *Early growth response 2* (Egr2), *Prostaglandin endoperoxide synthase 2* (Ptgs2, alias Cox2), and *Chemokine (C-C-motif) ligand 2* (Ccl2, alias Mcp1) showed diminished transcript levels in Curcumin-treated resting BV-2 cells (Fig. 16A).

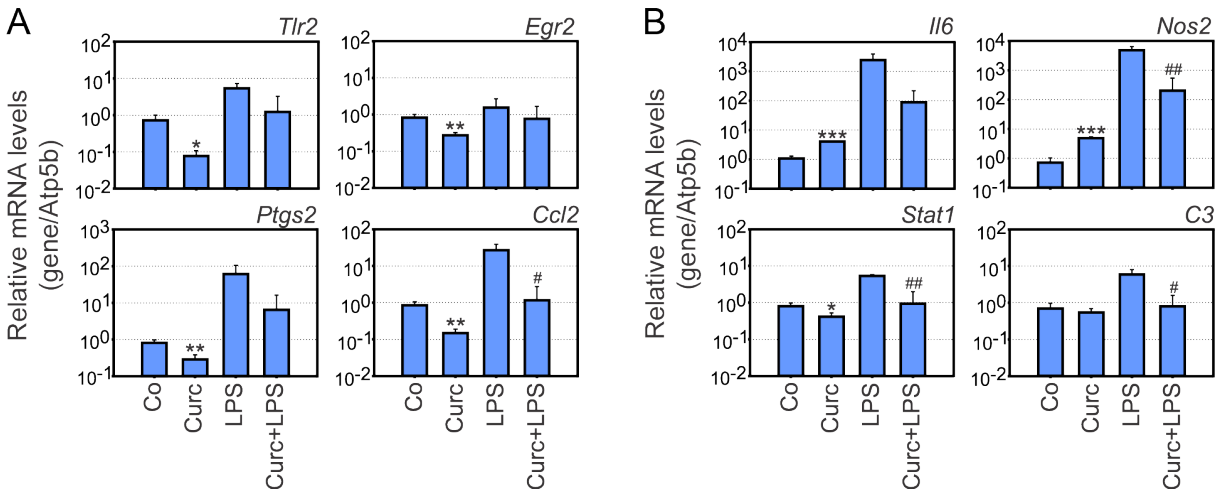

Figure 16 Real-time qRT-PCR validation of transcripts in BV-2 microglia stimulated with 20 µM Curcumin, 100 ng/ml LPS, or 20 µM Curcumin + 100 ng/ml LPS for 6 hours. Relative mRNA levels were quantified for (A) Toll-like receptor 2 (*Tlr2*), Early growth response 2 (*Egr2*), Prostaglandin endoperoxide synthase 2 (*Ptgs2*), Chemokine ligand 2 (*Ccl2*), and (B) Interleukin 6 (*Il6*), Nitric oxide synthase 2 (*Nos2*, alias *iNos*), Signal transducer and activator of transcription 1 (*Stat1*), Complement C3 (*C3*). Expression was normalized to the control gene Atp5b and mRNA levels (+/- SD) are graphed relative to control cells. Results are calculated from three independent experiments performed in triplicate measurements. * $p \leq 0.05$, ** $p \leq 0.01$, *** $p \leq 0.001$ for Curcumin vs. control, and # $p \leq 0.05$, ## $p \leq 0.01$ for Curcumin + LPS vs. LPS, Mann-Whitney Rank Sum test.

In the activated state, microglial cells also had the tendency to expressed lower amounts of these transcript but only Ccl2 levels reached the level of statistical significance. When LPS-activated BV-2 cells were incubated in the presence of Curcumin, transcription of *Interleukin 6* (Il6), *nitric oxide synthase 2* (Nos2, alias iNos), *Signal transducer and activator of transcription 1* (Stat1), and *Complement factor C3* (C3) were all repressed (Fig. 16B).

Curcumin has an inhibitory effect on microglial migration

The induction of several transcripts related to cell motility and adhesion (Ntng1, Pecam1, and Perp1) prompted us to study the effect of Curcumin on microglial migration. We first cultured BV-2 microglia on plastic dishes until 80%

confluence and then created a scratch with a pipette tip. 12 hours after stimulation of resting microglia or LPS-activated cells with 20 µM of Curcumin, migration into the cell-free scratch area was documented. Representative microscopic images clearly showed that Curcumin-treated resting cells as well as activated BV-2 cells exhibit a highly reduced migratory potential (Fig. 17A).

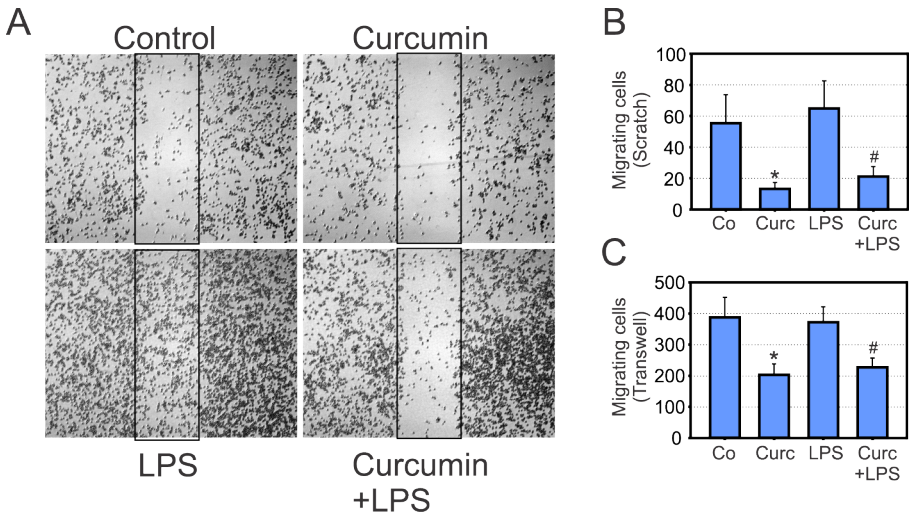

Figure 17 Curcumin reduces microglial migration. (A, B) Scratch assays in BV-2 microglia treated with solvent control, 20 µM Curcumin, 100 ng/ml LPS, or 20 µM Curcumin + 100 ng/ml LPS for 12 hours. (A) Micrographs from one representative experiment out of five independent experiments are shown. (B) Results of scratch assays are calculated mean values ± SEM from five independent experiments. (C) Transwell chamber migration of BV-2 microglial cells treated with solvent control, 20 µM Curcumin, 100 ng/ml LPS, or 20 µM Curcumin + 100 ng/ml LPS for 24 hours. The absolute number of migrating cells was counted in the lower chamber and mean values ± SEM are displayed. $p \leq 0.05$ for Curcumin vs. control, and # $p \leq 0.05$ for Curcumin + LPS vs. LPS, Student's t test.

The statistical analysis of five independent experiments revealed a significantly reduced number of migrating cells when Curcumin was present in the culture medium (Fig. 17B). As an independent measure of microglial cell motility and to study the long term effects of Curcumin, we performed transwell migration assays over a period of 24 hours. Similar as in the scratch assays, the migratory capacity of BV-2 cells was not changed by the activation agent LPS alone (Fig. 17C). In both, the resting and the activated microglial phenotype, Curcumin caused a significant attenuation of microglial migration (Fig. 17C). These results indicate that Curcumin-mediated signaling events have functional consequences related to microglial motility.

Curcumin inhibits LPS-induced microglial neurotoxicity

To test whether the transcriptomic changes in Curcumin-stimulated cells influence microglial neurotoxicity, 661W photoreceptor cells were incubated with conditioned medium from BV-2 cells. 661W is a retinoblastoma-derived cell line, which represents an established model to study microglial neurotoxicity in the special context of retinal degeneration (Dirscherl et al. 2010; Ebert et al. 2008; al-Ubaidi et al. 1992).

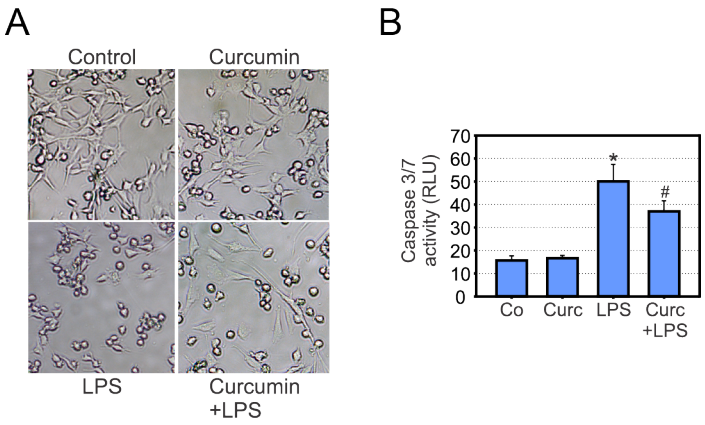

Figure 18 Curcumin reduces microglial neurotoxicity on photoreceptors. (A) Phase contrast micrographs showing morphological changes of 661W photoreceptor cell cultures treated with conditioned media from BV-2 cells for 48 hours. The supernatant from control-stimulated, 20 µM Curcumin-treated, 100 ng/ml LPS-treated, or 20 µM Curcumin + 100 ng/ml LPS-treated cells was added to 661W photoreceptor cells, respectively. The micrographs shown are from one representative experiment out of three independent experiments with the same tendencies. (B) Apoptosis-related caspase 3/7 activation in 661W photoreceptor cells incubated with conditioned media from control-stimulated, 20 µM Curcumin-treated, 100 ng/ml LPS-treated, or 20 µM Curcumin + 100 ng/ml LPS-treated BV-2 cells. Results are calculated from three independent experiments performed in duplicate measurements. * $p \leq 0.05$ for LPS vs. control and # $p \leq 0.05$ for Curcumin + LPS vs. LPS, respectively, Mann-Whitney Rank Sum test. RLU, relative luciferase units.

661W cells were incubated for 48 h with culture supernatants from unstimulated, Curcumin-, LPS- or LPS + Curcumin-treated BV-2 cells and 661W photoreceptor cell morphology was assessed by phase contrast microscopy. 661W cells in their own medium grew in a spindle-like shape with only few rounded apoptotic cells (Fig. 18A). Conditioned media from control- or Curcumin-treated microglial cells did not affect this morphology (Fig. 18A). In contrast, 661W cells incubated with LPS-stimulated BV-2 supernatant appeared apoptotic, leading to larger cell-free areas in the culture (Fig. 18A). When conditioned media from LPS + Curcumin-stimulated BV-2 cells was used, a nearly normal 661W cell morphology was retained (Fig. 18A). Direct incubation of 661W cells with Curcumin, LPS, or both had no effects on the cell

cultures (data not shown), demonstrating that the observed changes in 661W cell characteristics stem from secreted microglial compounds.

To corroborate these morphological findings with further functional data, we analyzed the influence of microglia-derived products on caspase-related apoptotic cell death. 661W cells cultured with supernatants from LPS-stimulated BV-2 cells showed a significant induction of caspase 3/7 activity (Fig. 18B). When using conditioned media from microglial cells co-treated with LPS + Curcumin, 661W apoptosis was still present but was significantly diminished (Fig. 18B). These data clearly implicate that Curcumin may limit the production of pro-apoptotic compounds in activated microglial cells or even promote the release of neurotrophic factors.

Discussion

Oxidative stress and neuroinflammation are major factors in the pathogenesis of neurodegenerative disorders (Hirsch & Hunot 2009). Therefore, antioxidant and anti-inflammatory compounds like Curcumin may be treatment options for this group of diseases (Ray & Lahiri 2009). However, only few experimental data are available that report on Curcumin-triggered transcriptional mechanisms and direct signaling targets in microglia.

Our transcriptomic analysis in BV-2 cells sheds some light on target genes and potential signaling mechanisms. We identified a prominent transcriptional response of resting as well as LPS-activated microglial cells after Curcumin treatment. Distinct gene clusters were detected that reflect up-regulated and suppressed transcripts in both microglial phenotypes. We identifed and validated six genes that were constistently induced in resting as well as activated BV-2 cells that have not been described as Curcumin targets before. Among these, four Curcumin target genes are related to cell migration. *Netrin G1* is a lipid-anchored protein that is structurally related to the netrin family of axon guidance molecules (J. C. Lin et al. 2003). It regulates synaptic interactions between neurons by binding to transmembrane netrin G ligands (Woo et al. 2009). Interestingly, the related *Netrin 1* molecule is a broad inhibitor of leukocyte chemotaxis (Ly et al. 2005) and Netrin G1 may have a similar function in microglia. The adhesion molecule PECAM1 is also directly involved in monocyte/macrophage migration (Jackson 2003). Another migration-related gene induced by Curcumin is *Plasma cell endoplasmic reticulum protein 1*. PERP 1 is a molecular chaperone required for proper folding and secretion of immunoglobulins in B-cells (Shimizu et al. 2009; van Anken et al. 2009). Related to our study, a recent report linked PERP 1 (alias MZB1) to calcium signaling, activation of integrins and cell adhesion (Flach et al. 2010). Expression of the *Notch-ligand Delta-like 1* has been demonstrated in BV-2 cells and primary rat brain microglial cells, where Notch-1 signaling negatively regulates TNF release (Cao et al. 2008). Our data show that basal Dll1 expression in resting microglial cells can be potently induced by Curcumin, which could potentially trigger Notch-signaling to prevent migration associated with pro-inflammatory priming of BV-2 cells.

These transcriptomic data of Curcumin-treatment promoted us to analyze its effects on microglial motility. Both types of assays, the wound healing assays and the transwell migration experiments, showed that BV-2 cell migration was significantly inhibited by 20 µM Curcumin over a period of 12 hours to 24 hours. These findings are in good agreement with papers reporting reduced migration of tumor cells, endothelial cells, and dendritic cells after treatment with comparable doses of Curcumin (Senft et al. 2010; Sameermahmood et al. 2008; Shirley et al. 2008). In the homeostatic state, microglia constantly scan their environment with their long protrusions without movement of the somata (Nimmerjahn et al. 2005). In contrast, migration of microglial cells is a hallmark of pro-inflammatory and chronic activation during early phases of neurodegeneration. Thus, Curcumin may support the homeostatic state of microglia and prevent their early and excessive transformation into migrating phagocytes.

It is well known that Curcumin broadly inhibits pro-inflammatory gene expression by targeting different signal pathways and transcriptional regulators including NFkB, AP1, EGR1, and STAT3 (Shishodia et al. 2007). Our microarray data corroborate these findings especially in LPS-activated BV-2 cells by showing Curcumin-triggered suppression of Ptgs2, Ccl2, Il6, and Nos2, which are NFkB, AP1, and STAT3 target genes (Maheshwari et al. 2006). Moreover, the Curcumin-regulated transcriptomic profiles revealed lower gene expression of *toll-like receptor 2* in resting microglia and *complement factor 3* in activated cells. These two factors broadly support the conversion of microglial cells to the pro-inflammatory state (H.-Y. Lin et al. 2010; R. Fan et al. 2007) and hence Curcumin signaling may abrogate both pathways. Our data also showed diminished mRNA expression of the transcription factors Egr2 and Stat1 following Curcumin-treatment. This indicates that Curcumin may further dampen microglial activation by interfering with two other key transcription factors expressed in activated microglial cells. In addition to its inhibitory effects on pro-inflammatory signaling, two well known anti-inflammatory molecules, PPARα and IL4, were significantly induced by Curcumin. PPARα and IL4 both specifically inhibit pro-inflammatory activation of microglial cells (J. Xu et al. 2005; Lyons et al. 2009) and some of the immune-dampening effects of Curcumin may be mediated via this signaling axis.

The cell culture experiments with conditioned media from BV-2 cells showed that Curcumin significantly reduced LPS-triggered microglial neurotoxicity on 661W photoreceptor cells. We hypothesize that the strong suppression of LPS-induced Nos2 transcription by Curcumin is a major pathway responsible for this phenomenon. In this context, Mandal *et al.* have recently demonstrated that Curcumin protects 661W cells from hydrogen peroxide-induced cell death (Mandal et al. 2009). This effect is very likely mediated by the antioxidant and radical-scavenging capacity of Curcumin. In a model of light-induced retinal degeneration, Curcumin also suppressed inflammatory marker expression *in vivo* (Mandal et al. 2009), which could be potentially mediated by its attenuating effect on retinal microglia.

Conclusions

We have shown that Curcumin triggered global changes in the transcriptome of resting and LPS-activated microglial cells. In addition to its known function in blocking pro-inflammatory gene expression via interference with NFkB signaling, Curcumin induced novel anti-inflammatory targets in microglia. Curcumin also significantly inhibited microglial migration and cytotoxicity, which are key features of neuroinflammation. Our publicly available dataset provides a basis to understand the pleiotropic beneficial effects of Curcumin on microglia as key innate immune cells of the nervous system. Moreover, the results of this study also underscore the importance of Curcumin as a promising dietary compound for the treatment of various neurodegenerative disorders associated with inflammation.

Acknowledgments

This work was supported by grants from the German Research Foundation (FOR1075 Project 4), the Elite Network of Bavaria, and the Pro Retina Foundation. The authors thank Prof. Muayyad Al Ubaidi for providing the 661W photoreceptor cell line.

Authors' contributions

MK, EL, and YW carried out cell culture stimulations and qRT-PCR experiments. MK and EL analyzed qRT-PCR and functional data. CM performed microarray analysis.

AA performed scratch assays. MM critically read and corrected the paper. TL designed the study, obtained funding, carried out biostatistical analyses of microarrays and wrote the manuscript. All authors read and approved the final manuscript.

2.3 Chapter 3 – Luteolin (Dirscherl et al. 2010)

Luteolin triggers global changes in the microglial transcriptome leading to a unique anti-inflammatory and neuroprotective phenotype

Konstantin Dirscherl*, Marcus Karlstetter*, Stefanie Ebert*, Dominik Kraus, Julia Hlawatsch, Yana Walczak, Christoph Moehle, Rudolf Fuchshofer, and Thomas Langmann

* Authors contributed equally to this work

Published in the Journal of Neuroinflammation. 2010 Jan 14;7:3.

Abstract

Background

Luteolin, a plant derived flavonoid, exerts a variety of pharmacological activities and anti-oxidant properties associated with its capacity to scavenge oxygen and nitrogen species. Luteolin also shows potent anti-inflammatory activities by inhibiting nuclear factor kappa B (NFkB) signaling in immune cells. To better understand the immuno-modulatory effects of this important flavonoid, we performed a genome-wide expression analysis in pro-inflammatory challenged microglia treated with Luteolin and conducted a phenotypic and functional characterization.

Methods

Resting and LPS-activated BV-2 microglia were treated with Luteolin in various concentrations and mRNA levels of pro-inflammatory markers were determined. DNA microarray experiments and bioinformatic data mining were performed to capture global transcriptomic changes following Luteolin stimulation of microglia. Extensive qRT-PCR analyses were carried out for an independent confirmation of newly identified Luteolin-regulated transcripts. The activation state of Luteolin-treated microglia was assessed by morphological characterization. Microglia-mediated neurotoxicity was assessed by quantifying secreted nitric oxide levels and apoptosis of 661W photoreceptors cultured in microglia-conditioned medium.

Results

Luteolin dose-dependently suppressed pro-inflammatory marker expression in LPS-activated microglia and triggered global changes in the microglial transcriptome with more than 50 differentially expressed transcripts. Pro-inflammatory and pro-apoptotic gene expression was effectively blocked by Luteolin. In contrast, mRNA levels of genes related to anti-oxidant metabolism, phagocytic uptake, ramification, and chemotaxis were significantly induced. Luteolin treatment had a major effect on microglial morphology leading to ramification of formerly amoeboid cells associated with the formation of long filopodia. When co-incubated with Luteolin, LPS-activated microglia showed strongly reduced NO secretion and significantly decreased neurotoxicity on 661W photoreceptor cultures.

Conclusions

Our findings confirm the inhibitory effects of Luteolin on pro-inflammatory cytokine expression in microglia. Moreover, our transcriptomic data suggest that this flavonoid is a potent modulator of microglial activation and affects several signaling pathways leading to a unique phenotype with anti-inflammatory, anti-oxidative, and neuroprotective characteristics. With the identification of several novel Luteolin-regulated genes, our findings provide a molecular basis to understand the versatile effects of Luteolin on microglial homeostasis. The data also suggest that Luteolin could be a promising candidate to develop immuno-modulatory and neuroprotective therapies for the treatment of neurodegenerative disorders.

Background

Microglia, the resident macrophages of the nervous system, have important roles in immune regulation (Hanisch 2002; Hanisch & Kettenmann 2007) and neuronal homeostasis (Streit 2002; Streit 2005). Microglia belong to the mononuclear phagocyte system but their special localization in the fragile neuronal environment and their morphological features clearly distinguish them from other peripheral macrophages (Ransohoff & Perry 2009; Giulian et al. 1995). Ramified microglia perform a very active and continuous surveillance function with their long protrusions (Davalos et al. 2005; Nimmerjahn et al. 2005). They receive permanent tonic inhibitory inputs from neurons to prevent microglial neurotoxicity (Broderick et al. 2002; Cardona et al. 2006). Loss of microglia-neuron cross-talk (Dick 2003), local danger signals such as extracellular ATP (Haynes et al. 2006), or neurotransmitter gradients (Ransohoff & Perry 2009) rapidly lead to a functional transformation of ramified microglia with a variety of effector functions.

Microglia activation is a protective mechanism regulating tissue repair and recovery in the early phase of neurodegeneration (Streit 2005). However, excessive or sustained activation of microglia often contributes to acute and chronic neuro-inflammatory responses in the brain and the retina (Hanisch & Kettenmann 2007). Activated microglia in the vicinity of degenerating neurons have been identified in a broad spectrum of neurodegenerative disorders including *Alzheimer's disease* (Khoury & Luster 2008), *Parkinson's disease* (Orr et al. 2002), *amyotrophic lateral*

sclerosis (Sargsyan et al. 2005), *multiple sclerosis* (Raivich & Banati 2004), and inherited photoreceptor dystrophies (Langmann 2007; Schuetz & Thanos 2004).

Macrophage heterogeneity and plasticity is very large and the set of marker combinations and sub-populations is essentially infinite (Hume 2008). To define a simplified conceptual framework, classification into polarized functional categories, called M1 and M2 macrophages has been proposed (Gordon & Taylor 2005; Mosser 2003). M1 or 'classically activated' macrophages produce high levels of oxidative metabolites and pro-inflammatory cytokines but also cause damage to healthy tissue as side effect (Martinez et al. 2008). M2 or 'alternatively activated' macrophages promote tissue remodeling and generally suppress destructive immune reactions. Information on microglial subsets in the nervous system are relatively scarce compared to other tissue macrophages. Nevertheless, recent findings from *in vitro* cultures of the murine microglial cell line MMGT12 (Michelucci et al. 2009) and hippocampal microglia from the PS1xAPP Alzheimer´s mouse model (Jimenez et al. 2008) implicate that microglia have the ability to differentiate into M1 and M2 polarized phenotypes. A co-existence of neurotoxic M1 microglia and regenerative M2 microglia has been recently documented in the injured mouse spinal cord (Kigerl et al. 2009). Microarray-based quantitation of M1 and M2 markers as well as functional tests on axonal regrowth after injury demonstrated that a transient anti-inflammatory and neuroprotective M2 response was rapidly overwhelmed by a neurotoxic M1 microglial response (Kigerl et al. 2009). A similar but age-dependent switch from alternative to classical activation was shown in PS1xAPP Alzheimer's mice (Jimenez et al. 2008), indicating a common phenomenon in neurodegenerative disorders. Compounds that induce the switch of microglia from inflammatory M1 type to anti-inflammatory M2 type could therefore be a potential therapeutic agent to attenuate neuronal inflammation and boost neuronal recovery (Zhang et al. 2009).

Several anti-inflammatory drugs have been shown to diminish neuroinflammation, but only a few direct functional effects on microglial activity have been elucidated (Lleo et al. 2007). Among the naturally occuring immuno-modulators, the flavonoid Luteolin (3´,4´,5,7-tetrahydroxyflavone), abundant in parsley, green pepper, celery, perilla leaf, and chamomile tea, exerts prominent anti-inflammatory and anti-oxidant activities (López-Lázaro 2009). Luteolin suppressed pro-inflammatory cytokine

production in macrophages by blocking *nuclear factor kappa B* (NFkB) and *activator protein 1* (AP1) signaling pathways (C. Chen et al. 2007) and inhibited the production of nitric oxide (Hu & Kitts 2004) and pro-inflammatory eicosanoids (Harris et al. 2006). Luteolin also diminshed the release of Tnf and superoxide anions in LPS or Interferon-γ treated microglial cell cultures (H.-Q. Chen et al. 2008; Rezai-Zadeh et al. 2008) and reduced the LPS-induced IL-6 production in brain microglia *in vivo* (Jang et al. 2008).

Although the inhibitory function of Luteolin on NFkB and a few selected cytokines is well documented in macrophages, a genome-wide search for further molecular targets in microglia has not yet been published. Furthermore, the immuno-modulatory effects of Luteolin related to the stimulation of distinct functional microglial phenotypes has not been investigated before. Therefore, this study investigated the global transcriptomic effects of Luteolin at near physiological concentrations (Shimoi et al. 1998) alone or in combination with LPS in pure BV-2 microglial cultures. We further validated the Luteolin-regulated expression of novel pro- and anti-inflammtory microglial transcripts, analyzed microglial morphology, and studied the consequences of microglia-conditioned media for photoreceptor viability.

Methods

Reagents

Luteolin (3´,4´,5,7-tetrahydroxyflavone) and *E.coli* 0111:B4 lipopolysaccharide were purchased from Sigma Aldrich (Steinheim, Germany). Luteolin was dissolved in DMSO and added in concentrations that did not exceed 0.05% of the total volume in any of the cell culture experiments.

Animals

C57BL/6 mice were purchased from Charles River Laboratories. Mice were kept in an air-conditioned barrier environment at constant temperature of 20-22°C on a 12h light-dark schedule, and had free access to food and water. The health of the animals was regularly monitored, and all procedures were approved by the University of Regensburg animal rights committee and complied with the German Law on Animal Protection and the Institute for Laboratory Animal Research Guide for the Care and Use of Laboratory Animals, 1999.

Cell culture

Brain microglia were isolated and cultured as described earlier (Ebert et al. 2009). BV-2 microglia-like cells were provided by Professor Ralph Lucius (Clinic of Neurology, Christian Albrechts University, Kiel, Germany). BV-2 cells were cultured in RPMI/5% FCS supplemented with 2mM L-Glutamine and 195 nM β-mercaptoethanol. Primary brain microglia or BV-2 cells were stimulated with 10 ng/ml or 50 ng/ml LPS and various concentrations of Luteolin for 24 h. 661W photoreceptor-like cells were a gift from Prof. Muayyad Al-Ubaidi (University of Illinois, Chicago, IL) and the culture conditions have been described elsewhere (Ebert et al. 2008).

Phalloidin staining

BV-2 cells were plated overnight on coverslips, fixed with 3.7% paraformaldehyde for 10 min at 37°C, permeabilized with 0.2% Triton X-100 for 5 min, blocked with 5% non-fat milk, 0.2% Triton X-100, and stained with DAPI for 10 min at room

temperature (0.1 µg/ml in PBS, 4',6-diamidino-2-phenylindol, Molecular Probes). Filamentous actin was stained by addition of 1.5 µM TRITC-conjugated phalloidin (Sigma). The coverslips were mounted on microscopic glass slides and viewed with a Axioskop 2 fluorescence microscope equipped with an Eclipse digital analyzer (Carl Zeiss).

NO measurement

NO concentrations were determined by measuring the amount of nitrite secreted by BV-2 cells into the culture medium using the Griess reagent system (Promega). 50 µl cell culture supernatant was collected and an equal volume of Griess reagent was added to each well. After incubation for 15 min at room temperature, the absorbance was read at 540 nm on a BMG FluoStar Optima plate reader (Labtech, Offenburg, Germany). The concentration of nitrite for each sample was calculated from a sodium nitrite standard curve.

Apoptosis assay

Apoptotic cell death of 661W cells was determined with the Caspase-Glo® 3/7 Assay (Promega). Cells were lysed and incubated with a luminogenic caspase-3/7 substrate, which contains the tetrapeptide sequence DEVD. Luminescence was then generated by addition of recombinant luciferase and was proportional to the amount of caspase activity present. The luminescent signal was read on a BMG FluoStar Optima plate reader (Labtech, Offenburg, Germany). A blank reaction was used to measure background luminescence associated with the cell culture system and Caspase-Glo® 3/7 Reagent. The value for the blank reaction was subtracted from all experimental values. Negative control reactions were performed to determine the basal caspase activity of 661W cells.

RNA isolation and reverse transcription

Total RNA was extracted from cultured microglia according to the manufacturer's instructions using the RNeasy Protect Mini Kit (Qiagen, Hilden, Germany). Purity and integrity of the RNA was assessed on the Agilent 2100 bioanalyzer with the RNA 6000 Nano LabChip® reagent set (Agilent Technologies, Böblingen, Germany).

The RNA was quantified spectrophotometrically and then stored at −80 °C. First-strand cDNA synthesis was performed with RevertAid™ H Minus First Strand cDNA Synthesis Kit (Fermentas, St. Leon-Rot, Germany).

DNA microarray analysis

Triplicate microarrays were carried out with three independent RNAs from non-stimulated BV-2 microglia or cultures treated for 24 h with 50 µM Luteolin, 50 ng/ml LPS, or 50 µM LPS + 50 ng/ml LPS, respectively. Generation of double-stranded cDNA, preparation and labeling of cRNA, hybridization to Affymetrix 430 2.0 mouse genome arrays, washing, and scanning were performed according to the Affymetrix standard protocol. Minimum information about a microarray experiment (MIAME) criteria were met (Brazma et al. 2001). The microarray datasets of this study are publicly available at the National Center for Biotechnology Information Gene Expression Omnibus (http://www.ncbi.nlm.nih.gov/geo/) as series record GSE18740.

Bioinformatic data analysis

The Affymetrix Expression Console Software Version 1.0 was used to create summarized expression values (CHP-files) from 3’ expression array feature intensities (CEL-files) using the Robust Multichip Analysis (RMA) algorithm. Integrative analysis of genome-wide expression activities from BV-2 cells was performed with the Gene Expression Dynamics Inspector (GEDI), a Matlab (Mathworks, Natick, MA) freeware program which uses self-organizing maps (SOMs) to translate high-dimensional data into a 2D mosaic (Eichler et al. 2003). Each tile of the mosaic represents an individual SOM cluster and is color-coded to represent high or low expression of the cluster's genes, thus identifying the underlying pattern.

Differentially regulated transcripts in 24 h Luteolin stimulated versus non-treated and Luteolin + LPS versus LPS-treated BV-2 cells, respectively, were retrieved with the Genomatix ChipInspector program (Genomatix Software GmbH, Munich, Germany), applying the Significance Analysis of Microarray (SAM) algorithm using a false-discovery rate of 0.1% and a minimum coverage of 3 independent probes. Functional annotation of transcripts was performed using the Database for

Annotation, Visualization, and Integrated Discovery (DAVID) (Dennis et al. 2003) and the Bibliosphere pathway edition (Genomatix).

Table 4 Primer pairs and Roche library probes for real time qRT-PCR validation

Gene	F-Primer (5'-3')	R-Primer (5'-3')	Roche Library Probe
AA467197	aaatggtggatcctactcaacc	gttgccctccggactttt	17
Blvrb	tcctcggagttctcagcttt	gcaccgtcacctcataacct	81
C3	accttacctcggcaagtttct	ttgtagagctgctggtcagg	76
CD36	ttgaaaagtctcggacattgag	tcagatccgaacacagcgta	6
CD83	gctctcctatgcagtgtcctg	ggatcgtcagggaataggc	2
Cfb	ctcgaacctgcagatccac	tcaaagtcctgcggtcgt	1
Cst7	atgtcagcaaagccctggta	ggtcttcctgcatgtagttcg	67
Cxcl10	gctgccgtcattttctgc	tctcactggcccgtcatc	3
Ddit3	ccaccacacctgaaagcag	tcctcataccaggcttcca	33
Gbp2	tgtagaccaaaagttccagacaga	gataaaggcatctcgcttgg	62
Gbp3	aagattgagctgggctacca	gaaactcttgagaacctcttttgc	73
Gclm	tggagcagctgtatcagtgg	caaaggcagtcaaatctggtg	18
Gusb	gtgggcattgtgctacctg	atttttgtcccggcgaac	25
Hmox1	ctgctagcctggtgcaaga	ccaacaggaagctgagagtga	25
Hp	ccctgggagctgttgtca	ctttgggcagctgtcatctt	15
Hprt1	tcctcctcagaccgctttt	cctggttcatcatcgctaatc	95
Ifi44	ctgattacaaaagaagacatgacagac	aggcaaaaccaaagactcca	78
Ifitm3	aacatgcccagagaggtgtc	accatcttccgatccctagac	84
Ifitm6	ccggatcacattacctggtc	catgtcgcccaccatctt	27
IL-6	gatggatgctaccaaactggat	ccaggtagctatggtactccaga	6
iNos	ctttgccacggacgagac	tcattgtactctgagggctga	13
Irf7	cttcagcactttcttccgaga	tgtagtgtggtgacccttgc	25
Kdr	cagtggtactggcagctagaag	acaagcatacgggcttgttt	68
Lcn2	atgtcacctccatcctggtc	cctgtgcatatttcccagagt	1
Lpcat1	aatgtgaggcgtgtcatgg	ggcagtcctcaaatgtatagtcg	81
Marco	cagagggagagcacttagcag	gccccgacaattcacatt	20
Mpeg1	cacagtgagcctgcacttaca	gcgctttcccaatagcttta	69
Nupr1-F	gatggaatcctggatgaatatga	gtccgacctttccgacct	64
Rnf145	catggacttctggcttctcat	aataaaaagtgttcccagaacctg	67
Saa3	atgctcgggggaactatgat	acagcctctctggcatcg	26
Slpi	gtgaatcctgttcccattcg	cctgagttttgacgcacctc	69
Srxn1	gctatgccacacagagaccata	gtgggaaagctggtgtcct	33
Trib3	gctatcgagccctgcact	acatgctggtgggtaggc	98

Quantitative real-time RT-PCR

Amplifications of 50 ng cDNA were performed with an ABI7900HT machine (Applied Biosystems) in triplicates in 10 µl reaction mixtures containing 1×TaqMan

Universal PCR Master Mix (Applied Biosystems), 200nM of primers and 0.25 µl dual-labeled probe (Roche ProbeLibrary). The reaction parameters were as follows: 2-min 50 °C hold, 30-min 60 °C hold, and 5-min 95 °C hold, followed by 45 cycles of 20-s 94 °C melt and 1-min 60 °C anneal/extension. Measurements were performed in triplicate. Results were analyzed with an ABI sequence detector software version 2.3 using the ΔΔCt method for relative quantitation. Primer sequences and Roche Library Probe numbers are listed in table 4.

Statistical analysis

Statistical analysis were performed on ΔΔCt data using analysis of variance with a two-sample Student's t test ($P < 0.05$) unless otherwise indicated. Quantitative data are expressed as mean ± SEM. The levels of gene expression in treated BV-2 cells are shown relative to control cells.

Results

Effects of Luteolin on selected pro-inflammatory markers

As a basis to study the genome-wide transcriptional effects of Luteolin on activated microglia and to validate our cell culture system, we initially performed a dose-response curve for Luteolin. Four pro-inflammatory microglia markers with different expression levels and ranges of induction were selected as positive controls for qRT-PCR analyses.

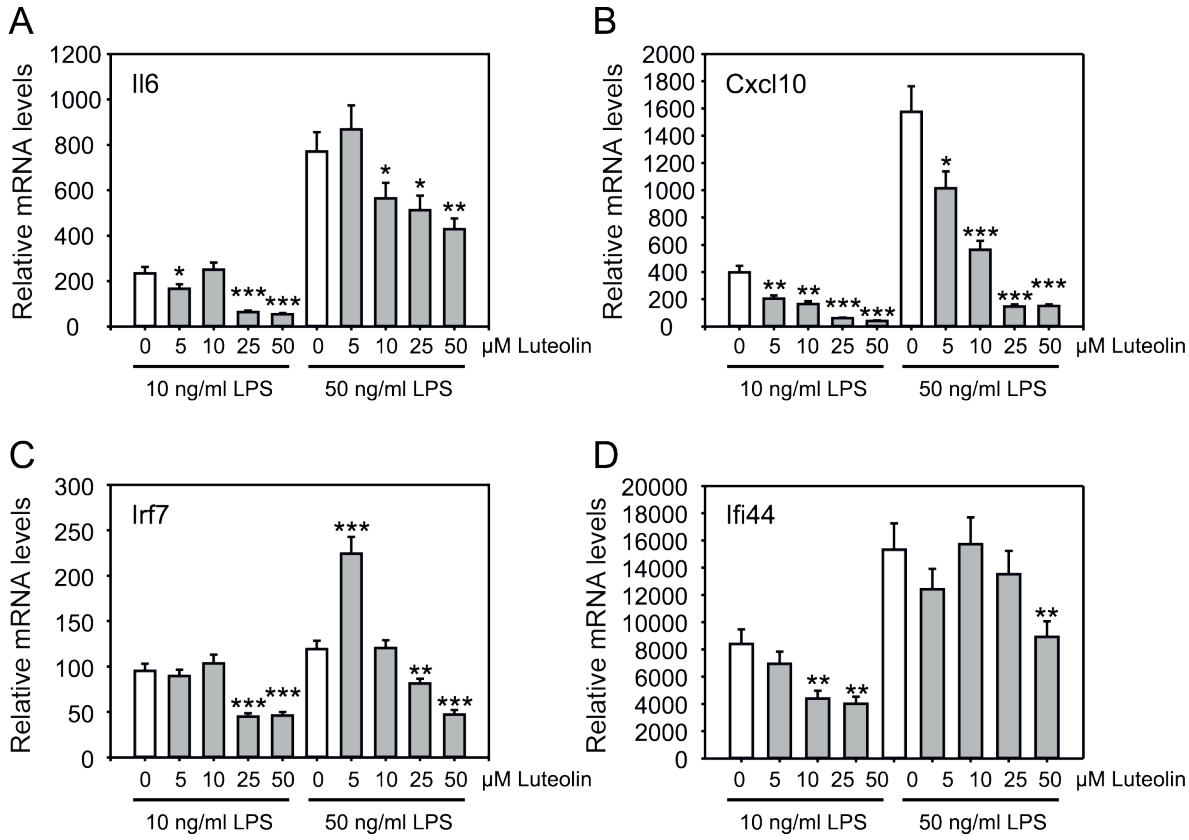

Figure 19 Dose-dependent suppression of LPS-induced pro-inflammatory gene expression in BV-2 microglia. BV-2 microglia were treated with the indicated concentrations of Luteolin for 1 h and then stimulated with 10 ng/ml or 50 ng/ml LPS for 24 h. Gene expression levels of (A) interleukin 6 (Il6), (B) chemokine (C-X-C motif) ligand 10 (Cxcl10), (C) interferon-regulatory factor 7 (Irf7), and (D) interferon-induced gene 44 (Ifi) were analyzed with real-time qRT-PCR. Expression was normalized to the control gene Gusb and mRNA levels (+/- SEM) are graphed relative to mock-treated control cells. Results are calculated from three independent experiments performed in triplicate measurements. * $p \leq 0.05$, ** $p \leq 0.01$, and *** $p \leq 0.001$ for Luteolin + LPS vs. LPS, respectively.

Interleukin 6 (Il6) is a well known pro-inflammatory cytokine target of Luteolin (Jang et al. 2008), *chemokine (C-X-C motif) ligand 10* (Cxcl10), *interferon-regulatory factor 7* (Irf7), and *interferon-inducible protein 44* (Ifi44) are LPS-sensitive genes in

microglia (Ebert et al. 2008). BV-2 microglia were pre-treated with different concentrations of Luteolin (0, 5, 10, 25, and 50 µM) for 1 h and then stimulated with LPS (10 ng/ml and 50 ng/ml) for a further 24 h period. Neither LPS nor Luteolin changed the proliferation rate or cell survival at the concentration levels applied to the cells (data not shown). mRNA levels of Il6 (Fig. 19A), Cxcl10 (Fig. 19B), Irf7 (Fig. 19C), and Ifi44 (Fig. 19D), which were all induced by 10 ng/ml LPS and further increased by 50 ng/ml LPS, were dose-dependently reduced by Luteolin (Fig. 19A-D). Luteolin's effects on the four genes were most prominent at 50 µM (Fig. 19A-D) and therefore this concentration was used in all further experiments.

Luteolin triggers global changes in the microglial transcriptome

Our next goal was to capture and compare the transcriptional profile of non-activated and LPS-activated BV-2 microgli treated each with 50 µM Luteolin for 24 h using Affymetrix Mouse Genome 430 2.0 GeneChips. Twelve microarray analyses from three independent stimulation experiments were performed and high stringency criteria with a minimal signal intensity of 50 fluorescence units were used. The complete microarray RMA datasets and all raw data (Affymetrix CEL-files) were stored in the NCBI GEO repository as record GSE18740. We used the Gene Expression Dynamics Inspector (GEDI) to determine the global patterns of gene expression in the four different conditions, untreated, Luteolin-treated, LPS-treated, and Luteolin + LPS-treated microglia. GEDI is based on self-organizing maps to identify genome-wide transcriptome activity via 'gestalt' recognition (Eichler et al. 2003). GEDI is sample-oriented rather than gene-oriented, which facilitates the identification of genome-wide patterns. Each mosaic tile in the GEDI map represents a gene group or cluster that is expressed at similar levels, with blue color indicating a low level and red corresponding to high expression. The four GEDI maps clearly show a dynamic regulation of gene expression in stimulated versus non-stimulated microglia (Fig. 20). Especially the upper right positions in the control dataset and more pronounced in the LPS-treated dataset display an inverse regulation of the gene clusters following Luteolin stimulation (Fig. 20A, white circles).

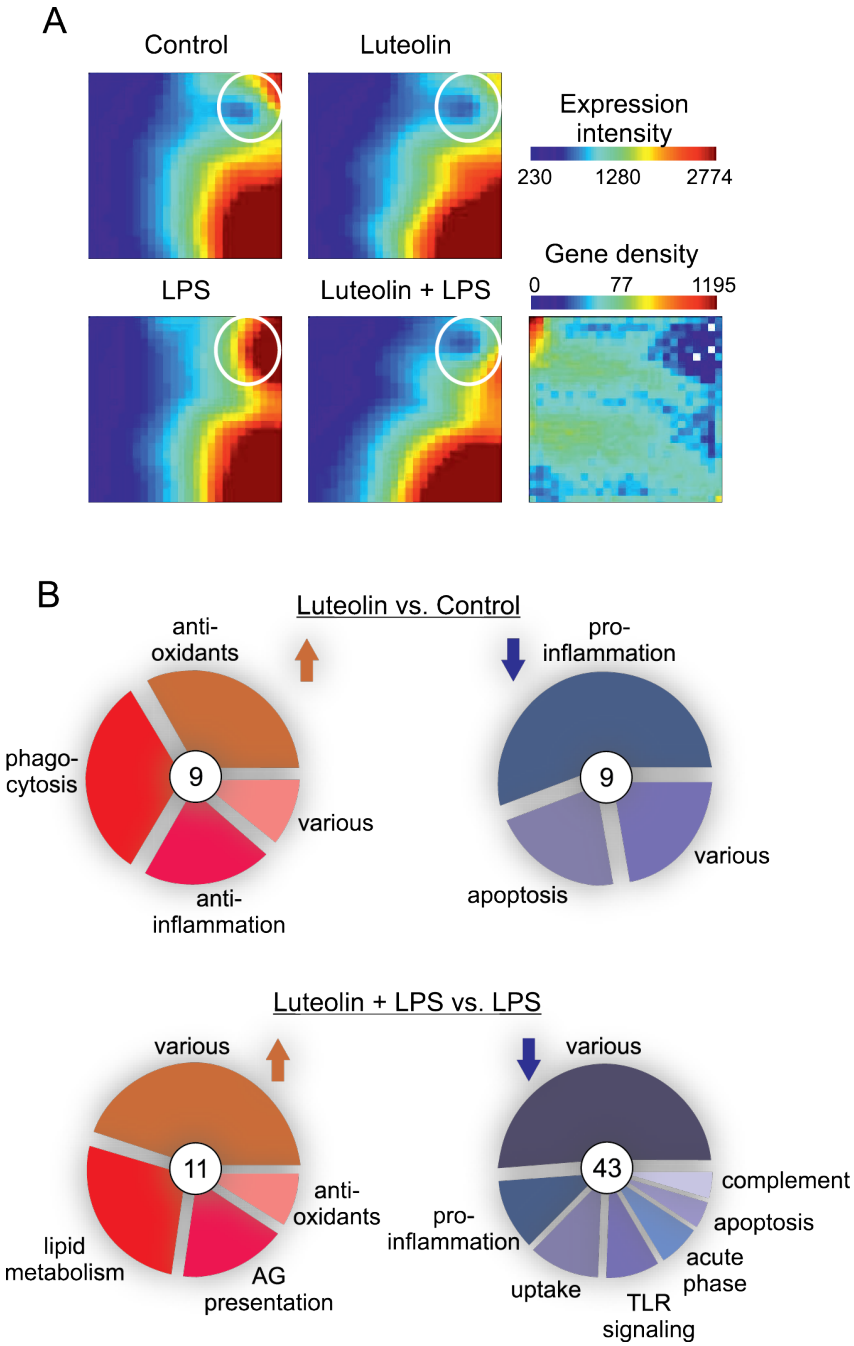

Figure 20 Luteolin triggers global transcriptomic changes in non-activated and LPS-activated BV-2 microglia. (A) Comparative Gene Expression Dynamics Inspector (GEDI) analysis of DNA-microarray datasets from control BV-2 cells or cells treated with 50 µM Luteolin, 50 ng/ml LPS, or 50 µM Luteolin + 50 ng/ml LPS. The white circle denotes the most prominent expression changes in several corresponding gene clusters. (B) Genomatix ChipInspector single probe analysis of differentially expressed transcripts in Luteolin versus control-treated cells (top) or Luteolin + LPS treated cells versus LPS stimulated cells. Triplicate Affymetrix Mouse 430 2.0 GeneChips were analyzed with a false-discovery-rate (FDR) <0.1%, 3 significant probes and log2 ratios >1. Differentially expressed transcrips from both comparisons were subjected to pathway analysis and clusters with ≥ 3 genes were defined as an independent group. Up-regulated genes are shown on the left side in red and down-regulated genes are displayed on the right side in blue. The total numbers of significantly up- or down-regulated genes from both comparions are indicated in circles placed in the centers of individual pie charts. All differentially expressed genes are listed in Tables 5 and 6, respectively.

These results demonstrate that stimulation with Luteolin has a major impact on the global pattern of gene expression notably in activated microglia and to a lower extent in resting cells. We have previously shown that a single probe analysis of Affymetrix microarrays using the Genomatix ChipInspector tool with the Significance Analysis of Microarray (SAM) algorithm improves detection of regulated transcripts (Weigelt et al. 2009). We therefore used ChipInspector to analyze our dataset applying a false discovery rate (FDR) of 0.1%, a minimal probe coverage of 3, and a minimum log2 ratio of 1 (fold change of 2.0). Thereby, 18 significantly regulated genes were identified in Luteolin-treated versus non-treated microglia (Table 5) and 54 differentially expressed genes were detected in Luteolin + LPS versus LPS-stimulated cells (Table 6).

Table 5 Differentially expressed transcripts after 24 h stimulation of BV-2 cells with 50 µM Luteolin.

Nr	ID	Symbol	Gene Name	FC*	Cov
UP-REGULATED					
1	74315	Rnf145	Ring finger protein 145	2.87	11
2	76650	Srxn1	Sulfiredoxin 1 homolog	2.38	5
3	19252	Dusp1	Dual specificity phosphatase 1	2.35	10
4	12267	C3ar1	Complement component 3a receptor 1	2.30	22
5	12491	Cd36	CD36 antigen	2.28	10
6	12475	Cd14	CD14 antigen	2.25	10
7	233016	Blvrb	Biliverdin reductase B	2.22	9
8	15368	Hmox1	Heme oxygenase 1	2.17	10
9	210992	Lpcat1	Lysophosphatidylcholine acyltransferase 1	2.13	11
DOWN-REGULATED					
1	13198	Ddit3	DNA-damage inducible transcript 3	-5.21	11
2	12862	Cox6a2	Cytochrome c oxidase, subunit VI a, polypeptide 2	-2.89	9
3	228775	Trib3	Tribbles homolog 3	-2.62	22
4	56312	Nupr1	Nuclear protein 1	-2.36	15
5	13011	Cst7	Cystatin F	-2.19	9
6	223920	Soat2	Sterol O-acyltransferase 2	-2.16	8
7	16149	Cd74	CD74 antigen	-2.10	8
8	17064	Cd93	CD93 antigen	-2.08	11
9	213002	Ifitm6	Interferon induced transmembrane protein 6	-2.06	8

Significance analysis of triplicate microarrays was performed with a false discovery rate of 0.1% and a minimum probe coverage of 3. ID, Entrez Gene ID; FC: Fold change; Cov: probe coverage; * validated by Taqman realtime RT-PCR.

Table 6 Differentially expressed transcripts after 24 h stimulation with 50 µM Luteolin + 50 ng/ml LPS versus 50 ng/ml LPS

Nr	ID	Symbol	Gene Name	FC*	Cov
UP-REGULATED					
1	74315	Rnf145	Ring finger protein 145	3.27	11
2	210992	Lpcat1	Lysophosphatidylcholine acyltransferase 1	2.55	11
3	12522	Cd83	CD83 antigen	2.51	11
4	14630	Gclm	Glutamate-cysteine ligase , modifier subunit	2.46	10
5	16889	Lipa	Lysosomal acid lipase A	2.31	6
6	56336	B4galt5	UDP-Gal:betaGlcNAc beta 1,4-galactosyltransferase, polypeptide 5	2.30	8
7	14950	H13	Histocompatibility 13	2.30	7
8	14104	Fasn	Fatty acid synthase	2.28	4
9	12125	Bcl2l11	BCL2-like 11	2.16	14
10	16542	Kdr	Kinase insert domain protein receptor	2.16	9
11	216345	Ccdc131	Coiled-coil domain containing 131	2.11	7
DOWN-REGULATED					
1	66141	Ifitm3	Interferon induced transmembrane protein 3	-13.74	9
2	433470	AA467197	Expressed sequence AA467197, miR-147	-9.32	9
3	16819	Lcn2	Lipocalin 2	-6.87	10
4	14469	Gbp2	Guanylate binding protein 2	-6.41	16
5	14962	Cfb	Complement factor B	-5.94	8
6	13198	Ddit3	DNA-damage inducible transcript 3	-5.58	11
7	16181	Il1rn	Interleukin 1 receptor antagonist	-5.28	33
8	55932	Gbp3	Guanylate binding protein 3	-4.72	10
9	56312	Nupr1	Nuclear protein 1	-4.35	15
10	75345	Slamf7	SLAM family member 7	-4.14	9
11	20210	Saa3	Serum amyloid A 3	-3.78	7
12	17386	Mmp13	Matrix metallopeptidase 13	-3.63	11
13	15439	Hp	Haptoglobin	-3.56	11
14	17167	Marco	Macrophage receptor with collagenous structure	-3.34	8
15	12266	C3	Complement component 3	-3.29	6
16	12870	Cp	Ceruloplasmin	-3.05	5
17	13011	Cst7	Cystatin F	-3.03	9
18	23882	Gadd45g	Growth arrest and DNA-damage-inducible 45 gamma	-2.95	11
19	242341	Atp6v0d2	ATPase, H+ transporting, lysosomal V0 subunit D2	-2.81	13
20	68774	Ms4a6d	Membrane-spanning 4-domains, subfamily A, member 6D	-2.75	19
21	83673	Snhg1	Small nucleolar RNA host gene 1	-2.75	24
22	12494	Cd38	CD38 antigen	-2.73	6
23	19655	Rbmx	RNA binding motif protein, X chromosome	-2.73	11
24	56405	Dusp14	Dual specificity phosphatase 14	-2.68	10
25	213002	Ifitm6	Interferon induced transmembrane protein 6	-2.57	8
26	12517	Cd72	CD72 antigen	-2.55	9
27	14129	Fcgr1	Fc receptor, IgG, high affinity I	-2.55	11

Table 6 Differentially expressed transcripts after 24 h stimulation with 50 µM Luteolin + 50 ng/ml LPS versus 50 ng/ml LPS

Nr	ID	Symbol	Gene Name	FC*	Cov
DOWN-REGULATED					
28	14130	Fcgr2b	Fc receptor, IgG, low affinity IIb	-2.48	27
29	231532	Arhgap24	Rho GTPase activating protein 24	-2.46	8
30	29818	Hspb7	Heat shock protein family, member 7 (cardiovascular)	-2.45	5
31	17476	Mpeg1	Macrophage expressed gene 1	-2.43	6
32	66222	Serpinb1a	Serine peptidase inhibitor, clade B, member 1a	-2.41	10
33	78771	Mctp1	Multiple C2 domains, transmembrane 1	-2.39	8
34	20568	Slpi	Secretory leukocyte protease inhibitor	-2.39	9
35	12507	Cd5	CD5 antigen	-2.35	9
36	50778	Rgs1	Regulator of G-protein signaling 1	-2.35	11
37	21897	Tlr1	Toll-like receptor 1	-2.20	5
38	16149	Cd74	CD74 antigen	-2.17	5
39	73167	Arhgap8	Rho GTPase activating protein 8	-2.13	8
40	15064	Mr1	Major histocompatibility complex, class I-related	-2.06	7
41	347722	Centg2	Centaurin, gamma 2	-2.04	11
42	98365	Slamf9	SLAM family member 9	-2.04	8
43	72999	Insig2	Insulin induced gene 2	-2.00	8

Significance analysis of triplicate microarrays was performed with a false discovery rate of 0.1% and a minimum probe coverage of 3. ID, Entrez Gene ID; FC: Fold change; Cov: probe coverage; * validated by Taqman realtime RT-PCR.

Comparison of the total number of differentially expressed genes indicated that the effects of Luteolin were more pronounced in LPS-activated BV-2 cells than in resting microglia. Also, the overall fold change range was higher in the LPS-treated microglia than in the resting BV-2 cells when stimulated with Luteolin. These finding correlate with the gene cluster patterns observed in GEDI analysis and implicate that Luteolin is an effective counter-player of pro-inflammatory microglial activation.

Luteolin regulates important immune pathways and changes the microglial transcriptional phenotype

Our next aim was to put the newly identified Luteolin-regulated expression patterns into a specific biological context. We used all differentially expressed genes to perform a classification into functional categories with the Database for Annotation, Visualization, and Integrated Discovery (DAVID). The major enriched functional categories in Luteolin-treated resting microglia were *anti-oxidants*, *phagocytosis*, and *anti-inflammation* for up-regulated genes and *pro-inflammation* and *apoptosis* for

down-regulated genes (Fig. 20B, upper part). These pathways indicate that Luteolin stimulated anti-oxidant and anti-inflammatory transcriptional programs which could potentially reflect M2 macrophage polarization. Moreover, basal pro-inflammatory and pro-apoptotic gene expression was blocked in non-activated BV-2 microglia. In Luteolin + LPS co-treated versus LPS-treated cells, 11 induced transcripts represented pathways of *lipid metabolism*, *antigen presentation*, and *anti-oxidants* (Fig. 20B, bottom left). Interestingly, a large number of down-regulated genes covered the pathway categories *pro-inflammation*, *toll-like receptor* (TLR) *signaling*, *acute phase response*, *apoptosis*, and *complement factors* (Fig. 20B, bottom right). These results implicate that Luteolin-induced transcriptomic changes promote a stable anti-inflammatory, anti-oxidant, and anti-apoptotic microglial phenotype reminescent of M2 macrophages. Our microarray data also identified a significant number of genes that could not be grouped into larger immune-related pathways and that have not been previously connected to microglial activation or flavonoid stimulation (Tables 5 and 6).

Microarray validation by qRT-PCR confirms novel Luteolin-regulated target genes

To validate a significant portion of the DNA microarray results, real-time qRT-PCR analyses were carried out with RNA samples from three independent BV-2 replicate experiments. We focused on representative candidates from different biological pathways which have not been previously described as flavonoid targets. 22 genes fulfilled these criteria and were analyzed with qRT-PCR. In the first set of experiments, mRNA levels of genes up-regulated by Luteolin treatment were assessed (Fig. 21). Transcripts of *Sulfirexodin 1* (Srxn1), *Biliverdin reductase B* (Blvrb), *Heme oxigenase 1* (Hmox1), and *Glutamate-cysteine ligase* (Gclm) are components of the cellular anti-oxidant response (Wegiel et al. 2009; Doi et al. 2009; Bea et al. 2003) and were all induced by Luteolin treatment (Fig. 21A-D). We could further validate increased levels of *Lysophosphatidylcholine acyltransferase* (Lpcat1), *Ring finger protein 145* (Rnf145), Cd36 antigen, *Kinase insert domain receptor* (Kdr, alias Vegfr2), and Cd83 antigen. Lpcat1 catalyzes the inactivation of inflammatory lipids (Cheng et al. 2009), whereas Cd36 and Kdr are surface receptors required for phagocytic uptake and chemotactic migration, respectively (Koenigsknecht & Landreth 2004; Ryu et al. 2009). The function of Rnf145 is currently unknown.

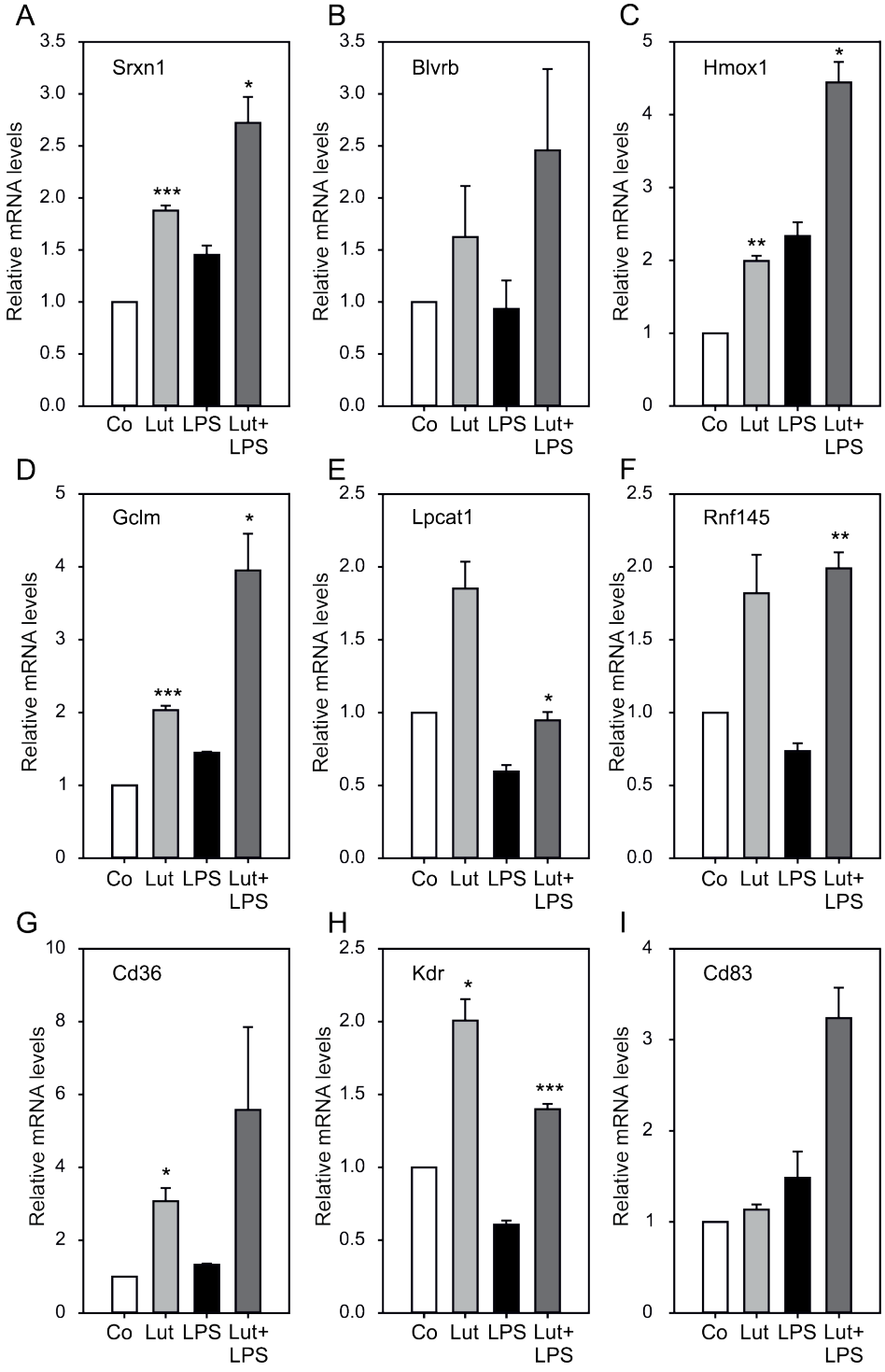

Figure 21 Luteolin induces anti-oxidant, anti-inflammtory, and survival pathways. Real-time qRT-PCR validation of transcripts in BV-2 microglia stimulated with 50 µM Luteolin, 50 ng/ml LPS, or 50 µM Luteolin + 50 ng/ml LPS. Relative mRNA levels were quantified for (A) Sulfiredoxin 1 (Srxn1), (B) Biliverdin reductase b (Blvrb), (C) Heme oxigenase 1 (Hmox1), (D) Glutamate-cysteine ligase modifier subunit (Gclm), (E) Lysophosphatidylcholine acyltransferase 1 (Lpcat1), (F) Ring finger protein 145 (Rnf145), (G) Cd36 antigen (Cd36), (H) Kinase insert domain protein receptor (Kdr), and (I) Cd83 antigen (Cd83). Expression was normalized to the control gene Gusb and mRNA levels (+/- SEM) are graphed relative to mock-treated control cells. Results are calculated from three independent experiments performed in triplicate measurements. * $p \leq 0.05$, ** $p \leq 0.01$, *** $p \leq 0.001$ for Luteolin vs. control and Luteolin + LPS vs. LPS, respectively.

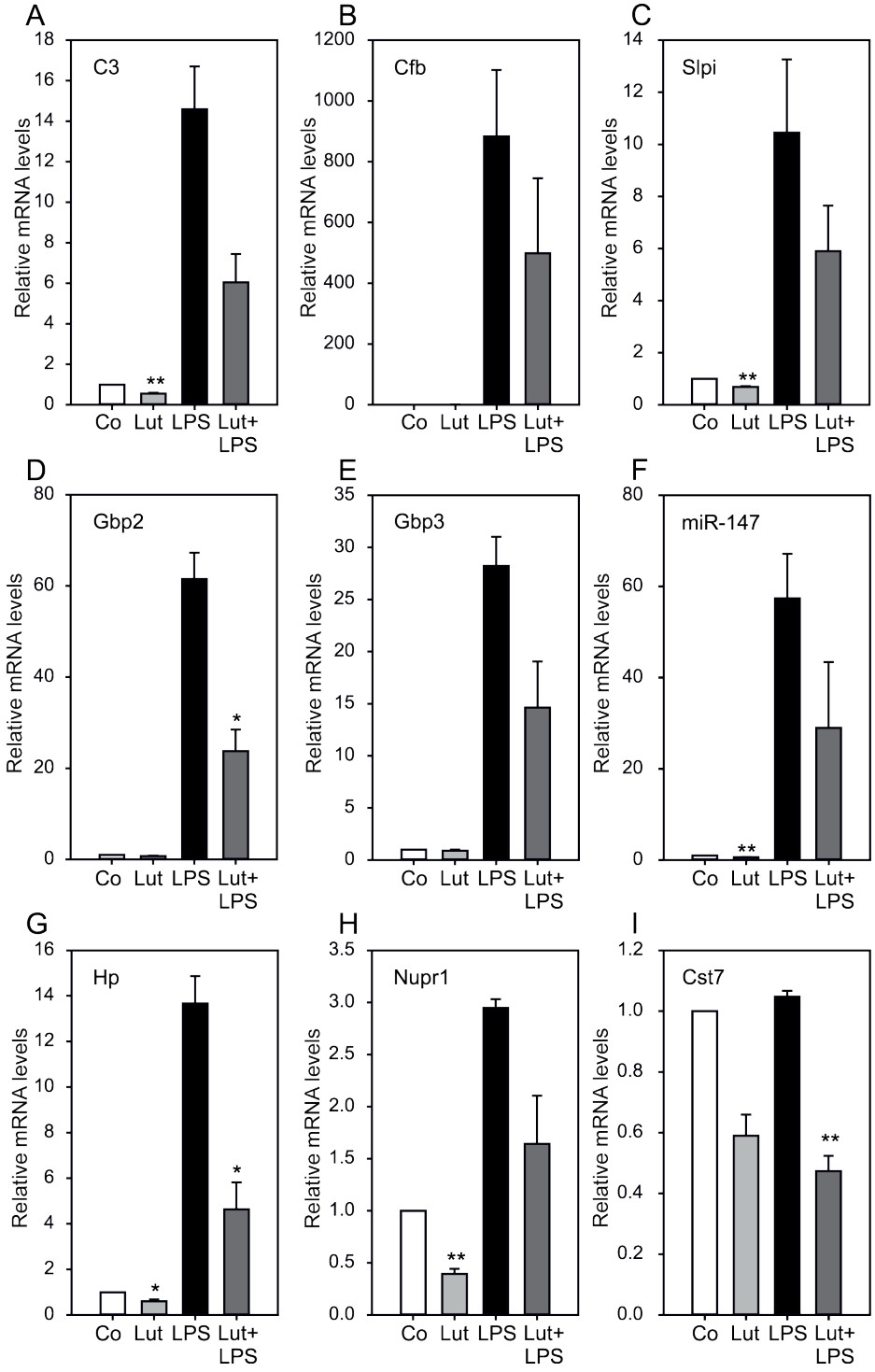

Figure 22 Luteolin inhibits pro-inflammatory and stress-related pathways. Real-time qRT-PCR validation of transcripts in BV-2 microglia stimulated with 50 µM Luteolin, 50 ng/ml LPS, or 50 µM Luteolin + 50 ng/ml LPS. Relative mRNA levels were quantified for (A) Complement component 3 (C3), (B) Complement factor B (Cfb), (C) Serine leukocyte peptidase inhibitor (Spli), (D) Guanylate binding protein 2 (Gnbp2), (E) Guanylate binding protein 3 (Gnbp3), (F) micro RNA 147 (miR-147), (G) Haptoglobin (Hp), (H) Nuclear protein 1 (Nupr1), and (I) Cystatin F (Cst7). Expression was normalized to the control gene Gusb and mRNA levels (+/- SEM) are graphed relative to mock-treated control cells. Results are calculated from three independent experiments performed in triplicate measurements. * $p \leq 0.05$, ** $p \leq 0.01$ for Luteolin vs. control and Luteolin + LPS vs. LPS, respectively.

In the next set of qRT-PCR experiments, down-regulated transcripts involved in pro-inflammatory activation and acute phase response were analyzed. *Complement factor C3* (C3), *Complement factor b* (Cfb), *Secretory leukocyte protease inhibitor* (Slpi), and the pro-inflammatory *Guanylate binding proteins 2* (Gbp2) and Gbp3 (Shenoy et al. 2007) showed diminished mRNA levels in Luteolin-treated samples (Fig. 22A-D). The same tendency was seen in the newly identified microRNA miR-147, which is involved in toll-like receptor signaling (Liu et al. 2009), the acute phase gene *Haptoglobin* (Hp), the stress-related gene *Nuclear protein 1* (Nupr1, alias p8) (Plant et al. 2006), and *Cystatin 7* (Cst7) (Fig. 22F-I).

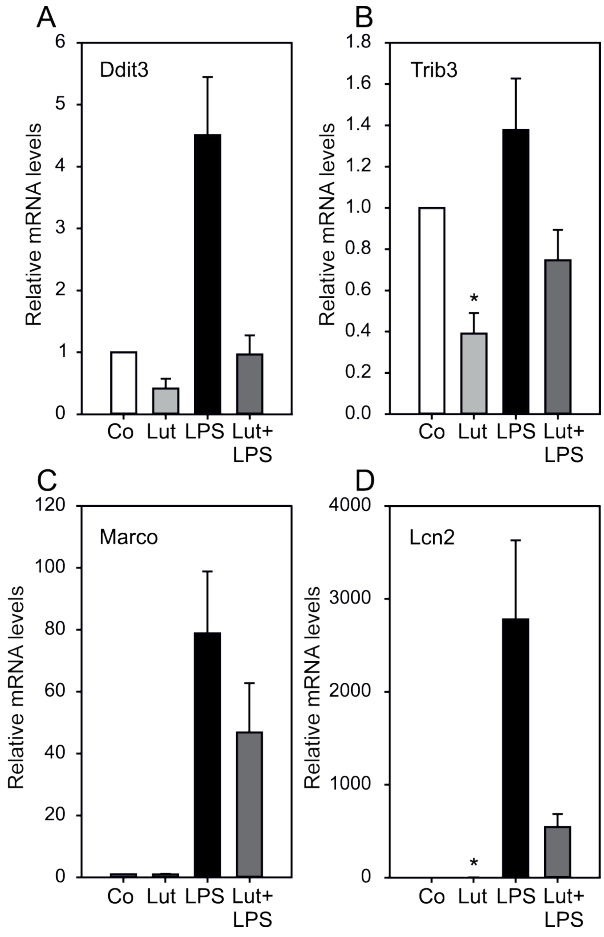

Figure 23 Luteolin inhibits apoptosis-related pathways and reduces de-ramification genes. Real-time qRT-PCR validation of transcripts in BV-2 microglia stimulated with 50 µM Luteolin, 50 ng/ml LPS, or 50 µM Luteolin + 50 ng/ml LPS. Relative mRNA levels were quantified for (A) DNA-damage inducible transcript 3 (Ddit3), (B) Tribbles homolog 3 (Trib3), (C) Macrophage receptor with collagenous structure (Marco), and (D) lipocalin 2 (Lcn2). Expression was normalized to the control gene Gusb and mRNA levels (+/- SEM) are graphed relative to mock-treated control cells. Results are calculated from three independent experiments performed in triplicate measurements. * $p \leq 0.05$ for Luteolin vs. control and Luteolin + LPS vs. LPS, respectively.

As third group of genes validated by qRT-PCR, four Luteolin-repressed genes related to apoptosis and microglial shape formation were studied (Fig. 23A-D). The apoptotic mediators *DNA-damage inducible transcript 3* (Ddit3, alias Chop, Gadd153) and *Tribbles homolog 3* (Gotoh et al. 2002; Shang et al. 2009) were down-regulated by Luteolin in non-activated as well as LPS-activated microglia (Fig. 23A, B), indicating anti-apoptotic protection mechanisms elicited by Luteolin. In line with these findings, we also observed reduced expression of the *Macrophage receptor with collagenous structure* (Marco) and *Lipocalin 2* (Lcn2), two molecules with dual roles in apoptosis and de-ramification of activated microglia (S. Lee et al. 2007; Granucci et al. 2003).

Luteolin changes microglial morphology and inhibits NO secretion

To assess whether the particular gene expression profiles measured in Luteolin-stimulated microglia translate into detectable functional properties, phenotypic characterization was performed. The general activation state and morphological phenotype of microglia is particularly reflected by their cell shape and cytoskeletal organization. To detected morphological changes and for visualization of filopodia we performed phalloidin staining. Conventional BV-2 microglia cultures were low level activated cells with a flat shape and some filopodia (Fig. 24A). Culture of BV-2 cells in the presence of Luteolin lead to considerable ramification and formation of long protrusions (Fig. 24B), indicating induction of a surveillance state. LPS-activation of BV-2 cells caused formation of a round cell shape with retracted filopodia (Fig. 24C). In contrast, co-incubation of LPS-treated cells with Luteolin sustained the ramified microglial morphology (Fig. 24D). A similar effect was seen in primary mouse microglia, where Luteolin increased the length of filopodia in non-activated cells (Fig. 24E, F) and caused flattening and ramification of LPS-treated cells (Fig. 24G, H). To test the direct effect of Luteolin on microglial secretion of toxic metabolites, NO levels were determined in the supernatant of BV-2 cells. Treatment of BV-2 cells with Luteolin alone did not result in increased NO concentrations (Fig. 24I), whereas stimulation with LPS markedly increased secreted NO levels. Co-incubation of LPS-activated cells with Luteolin nearly completely abolished NO secretion (Fig. 24I).

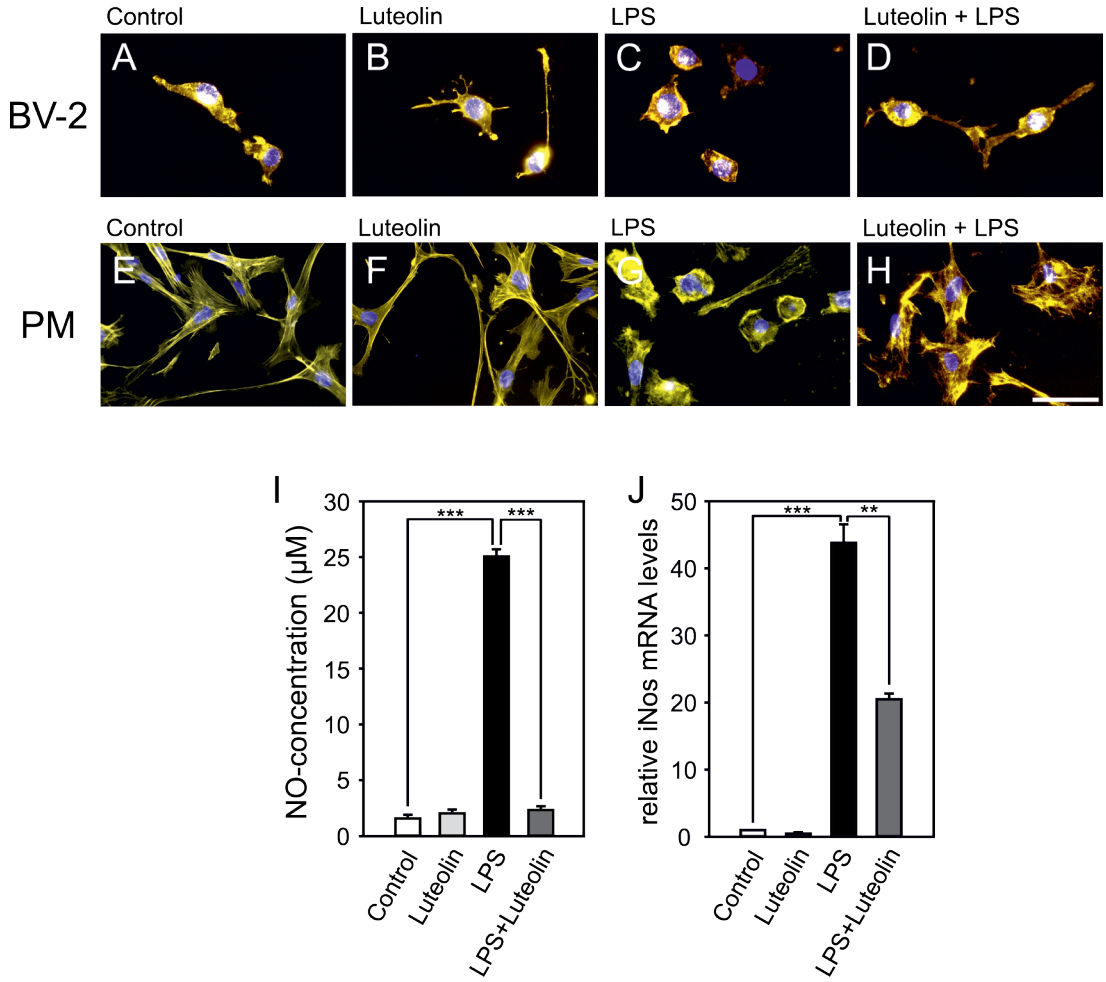

Figure 24 Luteolin promotes ramification of microglia and inhibits NO-synthesis. Effects of Luteolin, LPS and Luteolin + LPS on BV-2 (A-D) and primary brain microglia (E-H) cell morphology and actin cytoskeleton. Phallodin-TRITC-staining of F-actin bundles and DAPI co-staining reveals that 24 h treatment with 50 µM Luteolin in non-activated (B, F) or LPS-activated microglia (D, H) supports ramification. (I) NO release from BV-2 cells treated for 24 h with 50 µM Luteolin, 50 ng/ml LPS, or LPS + Luteolin. The micrographs and data shown are from one representative experiment out of three independent experiments with the same tendencies. Scale bar, 50 µM. (J) Real-time qRT-PCR analysis of iNos transcripts in BV-2 microglia stimulated with 50 µM Luteolin, 50 ng/ml LPS, or 50 µM Luteolin + 50 ng/ml LPS. Expression was normalized to the control gene Gusb and mRNA levels (+/- SEM) are graphed relative to mock-treated control cells. Results are calculated from two independent experiments performed in triplicate measurements. *** $p \leq 0.001$, ** $p \leq 0.01$ for LPS vs. control and Luteolin + LPS vs. LPS, respectively.

These data indicate that Luteolin favors the ramified surveillance state of microglia and effectively inhibits cytotoxic NO formation. Kim *et al.* previously reported that Luteolin triggered a blockade of NO secretion in LPS-stimulated BV-2 microglia, which was mediated by inhibition of *inducible NO synthase* (iNos) protein expression (J. Kim et al. 2006). To independently verify these data by qRT-PCR, we analyzed iNos mRNA levels in BV-2 cells treated with Luteolin, LPS, or both simultaneously. LPS caused a more than 40-fold increase in iNos transcripts and Luteolin

co-treatment significantly reduced iNos levels more than 2-fold. Thus, our expression data corroborate the findings by Kim *et al.* and provide a reasonable explanation for reduced NO secretion levels (J. Kim et al. 2006).

To test the hypothesis that Luteolin leads to decreased microglial neurotoxicity, a culture system of 661W photoreceptor cells with conditioned medium (CM) from BV-2 cells or primary microglia was established. 661W, a retina-derived cell line (al-Ubaidi et al. 1992), represents a valuable model to study microglial neurotoxicity in the special context of retinal degeneration (Ebert et al. 2008).

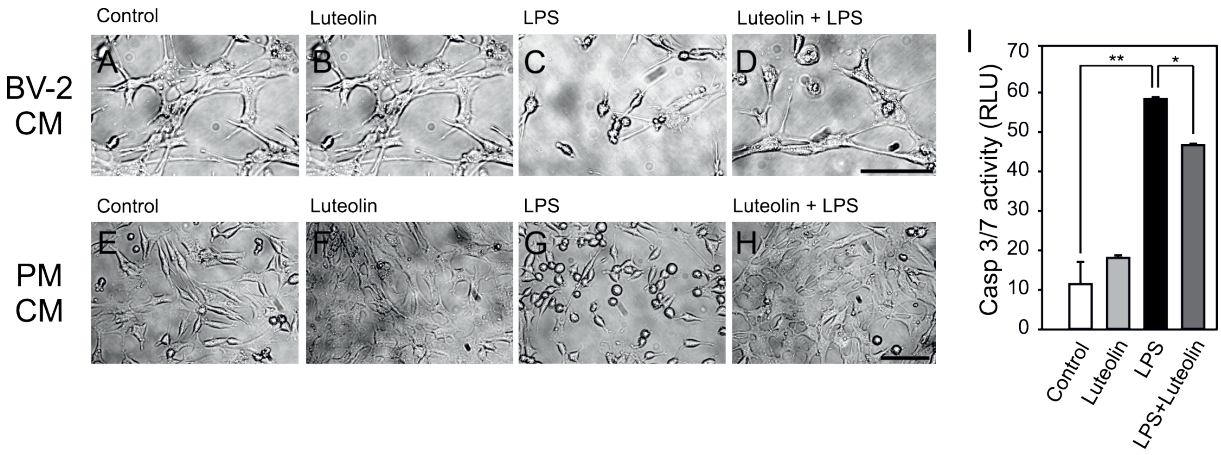

Figure 25 Luteolin inhibits microglial neurotoxicity on photoreceptors. Phase contrast micrographs showing morphological changes of 661W photoreceptor cultures treated with conditioned media from BV-2 cells (A-D) or primary brain microglia (E-H). The supernatant from control-stimulated (A, E), 50 µM Luteolin-treated (B, F), 50 ng/ml LPS-treated (C, G), or 50 µM Luteolin + 50 ng/ml LPS-treated cells (D, H) was added to 661W photoreceptor cells, respectively. The micrographs shown are from one representative experiment out of three independent experiments with the same tendencies. Scale bar, 50 µM. (I) Apoptosis-related caspase 3/7 activation in 661W photoreceptor cells incubated with conditioned media from control-stimulated, 50 µM Luteolin-treated, 50 ng/ml LPS-treated, or 50 µM Luteolin + 50 ng/ml LPS-treated BV-2 cells. Results are calculated from two independent experiments performed in triplicate measurements. ** $p \leq 0.01$, * $p \leq 0.05$ for LPS vs. control and Luteolin + LPS vs. LPS, respectively.

661W cells were incubated for 24 h with culture supernatants from unstimulated, Luteolin-, LPS- or LPS + Luteolin-treated cells and 661W photoreceptor cell morphology was assessed by phase contrast microscopy. 661W cells in their own medium grew confluent after 24 h and the presence of CM from control- or Luteolin-treated BV-2 cells did not affect cell morphology (Fig. 25A, B). As described previously (Tan et al. 2004), confluent 661W cells flattened out and often multiple cells were connected to each other through their projected extensions (Fig. 25A, B). In contrast, 661W cells co-incubated with LPS-stimulated BV-2 supernatant appeared

elongated and smaller, leading to prominent cell-free areas present in the culture (Fig. 25C). When adding CM from LPS + Luteolin-stimulated BV-2 cells, nearly normal cell characteristics were retained (Fig. 25D). Similar morphological changes of 661W cells were observed when cultured in the presence of primary microglia CM (Fig. 25E-H). Direct incubation of photoreceptor cells with LPS, Luteolin, or both had no effects on cell morphology (data not shown), indicating that the observed changes in 661W cell growth arise from secreted microglial compounds.

To correlate the microscopic findings with functional data, we next studied the influence of microglia-secreted products on caspase-related apoptotic signaling in the neuronal cell model. 661W cells cultured in the presence of CM from LPS-stimulated BV-2 cells displayed a strong induction of caspase 3/7 activity (Fig. 25I). When CM from microglia co-treated with LPS + Luteolin was used, 661W apoptosis was still present but was significantly diminished (Fig. 25I). Culture media from BV-2 cells kept in the presence of Luteolin alone had no effect on 661W apoptosis. These findings implicate that Luteolin either stimulates microglia to produce less pro-apoptotic substances or actively promotes the release of survival signals.

Discussion

Like other plant-derived flavonoids, Luteolin has a variety of biological activities including well-known anti-mutagenic and anti-tumorigenic properties (Ross & Kasum 2002). Moreover, this flavone possesses direct anti-oxidant activity, which is attributed to structural features of all flavonoids, which favor scavenging of reactive oxygen and nitrogen species (Rice-Evans et al. 1996). Although the anti-oxidant and anti-inflammatory activities of Luteolin may be also useful in the treatment of many chronic inflammatory diseases including neurodegeneration, only little information is available about Luteolin-mediated transcriptional mechanisms or molecular targets in microglia (Seelinger et al. 2008).

We have therefore performed the first genome-wide study of Luteolin-mediated transcriptional effects in microglia. To our surprise, Luteolin treatment did not only change expression levels of a few transcripts but had a broad and strong impact on the transcriptome of resting and particularly of LPS-activated microglia. The microarray dataset and the qRT-PCR validations revealed several Luteolin-regulated pathways. Luteolin caused simultaneous up-regulation of four important anti-oxidant enzymes Srxn1, Blvrb, Gclm, and Hmox1. These data are consistent with earlier findings demonstrating increased Hmox1 transcription in RAW264.7 macrophages after Luteolin treatment (Li et al. 2000). Stimulation with the flavonoid induced binding of the transcription factor *NF-E2-related factor 2* (Nrf2) to *anti-oxidant response elements* (ARE) in the Hmox1 promoter region (Li et al. 2000). Luteolin is a potent activator of Nrf2 (Lim et al. 2007) and the majority of anti-oxidant enzymes contain ARE in their regulatory regions, including Srxn1 (Singh et al. 2009). Moreover, mouse embryonic fibroblasts derived from $Nrf2^{-/-}$ mice showed significantly lower Blvrb and Gclm mRNA levels upon Diquat induction (Osburn et al. 2006). Therefore, we speculate that increased microglial expression of Srxn1, Blvrb, and Gclm is also mediated by activation of Nrf2. This hypothesis is further corroborated by the protective functions of Nrf2 in several microglia-related neurodegenerative disorders (de Vries et al. 2008).

Luteolin significantly enhanced mRNA synthesis of five other genes involved in different biological pathways. Lpcat1 is a lysophospholipid acyltransferase implicated in anti-inflammatory responses by converting *lyso-platelet activation factor* (lyso-PAF)

to PAF and *lyso-phosphatidylcholine* (lyso-PC) to PC (Harayama et al. 2008). LPC exerts considerable neuroinflammatory reactivity in the brain and inhibition of LPC signaling in astrocytes and microglia confers neuroprotection (Harayama et al. 2008). Lpcat1 is also highly expressed in the retina (Cheng et al. 2009), indicating that Luteolin-induced Lpcat1 levels could lead to diminished LPC levels in retinal microglia. Rnf145 was also up-regulated by Luteolin but the function of this protein remains to be determined. Cd36 and Kdr (alias Vegfr2) were also significantly induced by Luteolin in non-activated as well as activated microglia. The pattern recognition receptor Cd36 signals to the actin cytoskeleton and regulates microglial migration and phagocytosis (Stuart et al. 2007), whereas Kdr is involved in the chemotactic response of microglia (Ryu et al. 2009). We thus speculate that Luteolin-mediated expression of both genes could result in increased phagocytic responses of microglia without inducing inflammation.

Several reports have demonstrated that Luteolin inhibits pro-inflammatory cytokine expression in various cell types by blocking NFkB (reviewed in López-Lázaro 2009). Our microarray data confirmed these findings and revealed further NFkB target genes including the recently discovered microRNA miR-147 (Liu et al. 2009). Recently, Jang et al. showed that Luteolin reduced Il6 production mainly by inhibiting JNK signaling and AP1 activation (Jang et al. 2008). Luteolin did not affect IkB-α degradation or NFkB DNA binding in brain microglia, implicating that Luteolin-mediated effects in microglia are not solely dependent on NFkB blockade (Jang et al. 2008). In line with this notion, our Luteolin-regulated expression profiles identified several genes with NFkB-independent promoter control. Likewise, Luteolin down-regulated *complement factor 3*, which is regulated by AP1 (Martin et al. 2007) and blocked expression of Slpi, which is a target of *interferon regulatory factor 1* (IRF1) (Nguyen et al. 1999). Luteolin also diminished mRNA levels of the pro-inflammatory GTPase Gbp2 and the acute phase protein *Haptoglobin*, which are both regulated by *signal transducers and activators of transcription* (STATs) (Ramsauer et al. 2007; Zauberman et al. 2001). These data clearly show that Luteolin dampens microglia activation by interfering with several divergent signaling pathways.

The Luteolin-regulated differential expression patterns also revealed genes involved in microglial apoptosis and ramification. Microglia are more susceptible than macrophages to apoptosis (White et al. 1998) and recent evidence indicates that microglial apoptosis and senescence may precede neurodegeneration (Streit et al. 2009). Ddit 3 and Trib3, which were both induced by LPS and suppressed by Luteolin, support stress and NO-mediated apoptosis (Gotoh et al. 2002; Shang et al. 2009). We therefore hypothesize that Luteolin could promote the survival of activated and stressed microglia in an environment of early neurodegeneration. Our expression data also revealed the unexpected finding that Luteolin down-regulated Lcn2 and Marco, two molecules involved in microglial ramification and formation of filopodia. Lee *et al.* demonstrated that stable expression of Lcn in BV-2 microglia, the same cell line we used in our experiments, induced a round cell shape with a loss of processes (S. Lee et al. 2007). In line with this, over-expression of the scavenger receptor Marco in dendritic cells caused rounding of cells and down-regulated antigen uptake (Granucci et al. 2003). Thus, we hypothesized that the observed changes in mRNA levels of both genes might also translate into different morphological characters.

The morphological and functional assays fully supported the implications from gene expression profiles and revealed a direct effect of Luteolin on the microglial phenotype. Luteolin stimulated the formation of filopodia and caused ramification of BV-2 cells and primary microglia even in the setting of strong LPS activation. Moreover, NO secretion was completely blocked in LPS-activated microglia upon co-incubation with Luteolin. We studied the effects of conditioned media from microglia on cultured photoreceptor-like 661W cells and demonstrated that Luteolin-treatment effectively protected 661W cells from LPS-induced microglial toxicity. Since NO and other reactive oxygen species are the major radicals secreted from microglia, we speculate that Luteolin directly inhibits the secretion of these cytotoxic radicals. Our hypothesis is corroborated by recent data demonstrating that Luteolin concentration-dependently attenuated LPS-induced dopaminergic neuron loss by blocking NO secretion from cultured rat microglia (H.-Q. Chen et al. 2008).

Conclusions

We have shown that the flavonoid Luteolin is a potent modulator of microglial activation, cell shape, and effector functions. Luteolin induced global changes in the transcriptome of resting or LPS-activated microglia leading to a polarized M2-like phenotype with anti-inflammatory and neuroprotective characteristics. Luteolin's mechanisms of action appear to target several independent pathways independent of NFkB. Our results provide a basis to develop immuno-modulatory and neuroprotective therapies for the treatment of neurodegenerative disorders.

Acknowledgements

This work was supported by grants from the German Research Foundation (FOR1075 Project 4), the Elite Network of Bavaria, and the Pro Retina Foundation. The authors thank Prof. Muayyad Al Ubaidi for providing the 661W photoreceptor cell line.

Authors' contributions

KD, SE, and DK carried out all cell cultures and qRT-PCR experiments. MK, JH, and YW analyzed qRT-PCR and functional data. CM performed microarray hybridizations and raw data analyses. RF analyzed microarray data and critically read the manuscript. TL designed the study, obtained funding, carried out biostatistical analyses of microarrays and wrote the manuscript. All authors read and approved the final manuscript.

3 Discussion

Microgliosis is a common response to injury and accompanies various pathological conditions of the CNS. Therefore, microglial cells represent a broad target for therapy options. Modulation of microglia towards a neuroprotective phenotype represents a promising approach, yet the interpretation of the altered phenotype and the benefits of such a cellular therapy are difficult to evaluate. As one aspect of the complexity of microglial biology, there is still little knowledge about microglial subpopulations. The results shown and discussed in this work, describe the application of novel experimental strategies with the aim to characterize microglial subpopulations occuring in retinal degeneration. This concept includes the identification of selective marker genes and the elucidation of the phenotypic functional diversity of microglial populations to develop and interpret therapeutic strategies.

3.1 The concept of microglial subpopulations

The phenotypic diversity of microglia is a local specific response to a multitude of microenvironmental conditions. Several reports observed profound and persistent retinal microgliosis under dystrophic conditions, suggesting a predominant participation of classically (M1) activated microglia. However, identification of M2-marker transcripts during acute neuronal injury and retinal degeneration, indicates the co-existence of regulatory, alternatively (M2) activated microglia even in severe phases of neuroinflammation (Gehrig et al. 2007; Eter et al. 2008). The local distribution of alternatively and classically activated microglia in the degenerating tissue, seems to be a critical determinant of tissue integrity. Alternatively activated microglial cells exhibit functions mainly beneficial for neuronal tissue regeneration (Kigerl et al. 2009). However, neuroprotective features have also been described for moderately M1-activated microglia (Li et al. 2007), which reflects the situation during onset of retinal degeneration. Ongoing retinal degeneration is accompanied by consecutive release of pro-inflammatory triggers from apoptotic cells, leading to a stepwise increment of classically activated microglial cells. In cell culture experiments, time-delayed challenge of microglia with different pro-inflammatory stimuli, induces stronger activation than co-application of stimuli simultaneously

(Hausler et al. 2002). This suggests a stepwise ‘priming’ of alternatively activated microglia during early phases of degeneration, which could explain the rapid switch to an overwhelming presence of classicaly activated microglia at later stages. Activated microglia can actively induce apoptosis in photoreceptors, which further exacerbates retinal degeneration (Roque et al. 1999). Therefore, microglia may reside in a chronically overactivated state during the resolution phase and may overwhelm the regulatory capacity of the alternatively activated microglia fraction (Langmann 2007). While signaling pathways leading to the final commitment of chronic neurotoxic activation are still poorly understood, therapeutic prevention or rescue from this stage could possibly inhibit degeneration processes. It is obvious that microglial activation involves multiple transient states/phenotypes, including naïve, ‘primed’, activated and overactivated microglia and this concept should be considered, when developing new therapeutic strategies.

Apart from the above described microglial subpopulations, an age-related microglial type was recently described. Senescent microglia from old healthy mice, exhibit shorter, less branched processes and slower process motility. In addition, senescent microglia had a slower migratory potential towards an injury spot and impaired disaggregation in the resolution phase (Damani et al. 2011). These results are in line with earlier observations in brain tissue from AD patients, indicating a significant co-localization of senescent microglia with degenerating neuronal structures (Streit et al. 2009). In contrast to chronically activated microglia, less toxic senescent microglia may sustain a permanent low-grade inflammation which is relevant in the pathogenesis of age-related disorders like AMD. The impact of prolonged microglial dysfunction has been studied recently, describing autosomal-dominant mutations in the *macrophage colony stimulating factor 1 receptor* (CSFR1) gene as the genetic cause for *hereditary diffuse leukoencephalopathy with spheroids* (HDLS) (Rademakers et al. 2011). HDLS patients suffer from behavioral changes, dementia, depression and parkinsonism at ages 40-50 years and die within 6 years of onset. Interestingly, microglia are exclusively expressing CSFR1 in the CNS and CSFR1 downstream signaling is crucially involved in microglial proliferation and differentiation (Rademakers et al. 2011). The molecular characterization for this phenotype may

elucidate how disruption of CSFR1 signaling leads to microglial dysfunction, which in this case is highly associated with a severe and sustained CNS pathology.

3.2 Identification and characterization of microglial subpopulations

Discrimination of heterogeneous microglial types during various pathological conditions requires the application of novel experimental strategies and techniques to allow an individual molecular characterization. Identification of specific neuroprotective mechanisms in alternatively activated microglia could deliver tools for altering pro-inflammatory microglial activation. Mouse models with microglia-specific reporter transgenes offered a detailed insight into the morphological transformation and migration of microglia in dystrophic retinas (Ebert et al. 2009). Morphological observations enable gross discrimination of microglial phenotypes (e.g. ramified versus amoeboid). However, these studies hardly allow an estimation of the relative M1/M2 phenotype distribution. In order to discriminate and quantify microglia subsets during retinal degeneration, reporter transgenes controlled by M1- and M2-specific markers would represent a valuable tool for refined molecular characterization of distinct cell populations *in situ*.

Single markers adopted from macrophage classification are currently used to describe polarized activation phenotypes of microglia. However, it is generally questionable, whether single markers are sufficient to discriminate the fine tuned variety of microglial subsets. In contrast, genome-wide transcription profiling provides a comprehensive view and offers the possibility to discriminate distinct microglial cell types, by unique gene expression signatures. Transcriptomic profiling also allows identification of common activation/attenuation gene clusters as ‘fingerprints’ for microglial phenotypes. Data presented in this work, led to the identification of various novel M2-related gene clusters by genome-wide transcript analysis of cultured microglia. These datasets include transcriptomic profiles modulated with the plant-derived polyphenols Curcumin and Luteolin (Dirscherl et al. 2010; Karlstetter et al. 2011). An earlier transcript profiling approach provided evidence of a regulatory network under the control of the transcription factor PU.1 in a microglial population, isolated from dystrophic retinas (Weigelt et al. 2007). The subsequent functional characterization of selected PU.1 target genes has then led to the

identification of novel microglial markers and activation mechanisms, which will be discussed later (Karlstetter et al. 2010a; Stoecker et al. 2009). In the future, cross-comparison of many global expression datasets may help to dissect common mechanisms and novel specific markers of microglial activation.

3.3 Microglial phenotype modulation as therapeutic option for retinal dystrophies

Chronic microglial activation is a frequently observed phenomenon in severe stages of retinal dystrophies, preceded by sequential steps of activation. Bioactive compounds and endogenous factors, preventing or reprogramming neurotoxic over-activation of microglia, may be a promising tool to slow down the progression of retinal degeneration.

3.3.1 AMWAP, a counter-regulator of neuroinflammation

To identify mechanisms involved in microglial activation, the novel transcript AMWAP was selected from our retinal microglia gene expression dataset for detailed functional analysis (Weigelt et al. 2007). Like other whey acidic proteins, AMWAP expression was activated during pro-inflammatory microglial activation and showed anti-microbial, protease-inhibitory and anti-inflammatory potential. This suggests that AMWAP may be a feed-back regulator of pro-inflammatory microglial activation. In our experiments, AMWAP expression induced alternative activation markers Arg1 and Cd206 (Karlstetter et al. 2010a) (Chapter 1). Based on these findings we assumed, that AMWAP is a secreted factor for neuroprotective microglial modulation *in vivo*. This hypothesis is currently being tested in our lab by virus-mediated over-expression of AMWAP in the laser-damaged mouse retina. We assume a paracrine effect of secreted AMWAP on all retinal microglia, as it has been described for the whey acidic protein SLPI in brain injury after ischemic stroke (Wang et al. 2003). Thus, paracrine action would allow a broad local application of recombinant AMWAP protein to the diseased retina and circumvents many problems associated with a cell specific gene therapeutic approach. Attenuation of microglial activation by AMWAP *in vivo* would be a proof of concept that the identification of

further microglial factors by genome-wide expression profiling can highlight novel treatment concepts.

3.3.2 Curcumin and Luteolin induce neuroprotective phenotypes in microglia

Plant-derived polyphenols show pleiotropic biological activities including anti-allergic, anti-carcinogenic, anti-oxidant and anti-septic capacities (Maheshwari et al. 2006; Seelinger et al. 2008). Apart from studies investigating only single hallmarks of inflammation (Seelinger et al. 2008; Jagetia & Aggarwal 2007), our work described the modulatory effect of these substances on the global inflammatory transcriptome (Karlstetter et al. 2011; Dirscherl et al. 2010) (Chapter 2 & 3). In particular, Curcumin and Luteolin potently attenuated pro-inflammatory gene expression via multiple signaling pathways. In line with these findings, earlier studies indicated that Curcumin interacts with pro-inflammatory transcription factors and chromatin factors, which would explain the broad impact on gene expression (Shishodia et al. 2007; Reuter et al. 2011). Luteolin exhibits a related mode of action (Jang et al. 2008). Both, Luteolin and Curcumin induced the expression of distinct anti-inflammatory gene clusters. A gene cluster associated with M2-functions like phagocytic uptake, ramification and chemotaxis was characteristic for the Luteolin-stimulated phenotype. In contrast, Curcumin induced a gene set involving different anti-inflammatory genes and transcripts related to adhesion and migration, which led to decreased microglial migration capacity. Despite general neuroprotective effects, each substance had a unique gene expression signature. Based on these findings, Luteolin and Curcumin may present valuable therapeutic agents to prevent chronic microglial activation and slow down progression of neurodegeneration. Furthermore, the beneficial effects of Luteolin on ramification and chemotaxis could be relevant for the ‘rejuvenation’ of dysfunctional senescent microglia. For both compounds, it has to be considered whether they can be administered via dietary supplementation, which depends on the ability to cross the BBB/BRB for enrichment in the CNS/retina. There is good evidence that the flavonoids Naringenin and Quercetin can well penetrate into the brain (Youdim et al. 2004), but this still needs to be determined for Luteolin. Curcumin has been detected in the forebrain of mice after systemic injection,

which led to downregulation of pro-inflammatory markers after light-induced retinal degeneration (Purkayastha et al. 2009). Experiments by Mandal et al. also indicate that Curcumin enrichment reaches bioactive levels in the retina after dietary supplementation, however Curcumin accumulation has not been experimentally proven in the retina (Mandal et al. 2009). The fact that certain bioactive substances can not penetrate the brain, could be potentially circumvented by chemical modification or packaging. Curcumin loaded nanoparticles for instance, can enhance half-life of Curcumin in neuronal tissue and improve the efficacy of BBB penetration (Tsai et al. 2011).

3.4 Perspectives

Although valuable insight into microglia biology has been gained from mouse models, the functions of human microglia have been hardly elucidated. This is due to the fact, that human tissue is hard to obtain and microglia from *postmortem* retinas are difficult to isolate. It is obvious that investigations of human microglia are required to validate the findings from animal studies in a clinical context. Recently, the establishment of a protocol for generation of human microglia derived from induced pluripotent stem cells (iPS) has been reported (pending European patent EP2010_055731). These iPS-derived human microglia open a broad field of study and will help to gain profound data for human therapy. Primary human microglia from iPS cells are available in high numbers, which allows wide-range screening of pharmacological substances, transcriptional phenotyping and functional characterization, as described in this work for mouse cells. Moreover, primary microglia from patients carrying mutations that cause microglial dysfunction would allow particular determination of the functional consequences of the respective dysfunction and the development of individualized therapeutic strategies. Detailed knowledge about the mode of action of bioactive compounds on microglia (e.g. induction of phagocytosis or process movement) may also allow a rescue from the individual underlying ‘microgliopathy’.

Clinical studies represent a further important step to test microglia-modulating substances in retinal dystrophies. At the moment, the effect of Curcumin is being investigated in clinical studies with general neurodegenerative disorders like AD (clinicaltrials.gov), but studies for retinal disorders have not been initiatied yet. In this

regard, the immuno-modulatory effect on microglia can be only assessed by clinical parameters like visual function, providing rather indirect evidence. To directly monitor microglial activation in human subjects, radio-labeled ligands for the mitochondrial protein TSPO represent a feasible tool to visualize microglial activation via positron emission tomography (PET). Several studies have shown that TSPO radioligands selectively bind to activated microglia and profound microglial activation was detected in disease conditions in humans (Banati 2002). Microglial activation along the optic nerve and the retina have been also observed by PET scan in patients suffering from intranuclear ophtalmoplegia, underscoring that this technique is adequate of visualizing microglial activation in the retina (Cagnin et al. 2007; Banati et al. 2000). This technology would allow the imaging of microglial activation in human subjects, in order to track microglial activation after application of therapeutic compounds.

In conclusion, the recent association of microglial dysfunction with human disease and microglial activation as common phenomenon of CNS pathology, necessitates the clinical translation of therapeutic strategies developed in animal models to alleviate human degenerative diseases.

4 Summary

Microglia are the sentinel cells of the retina, where they are involved in surveillance of tissue integrity and clearance of cellular debris. The innate immune functions of microglia are tightly controlled by retinal neurons via the secretion of suppressing factors to prevent harmful pro-inflammatory activation. Progressive retinal cell death is a common sink of all inherited retinal diseases, causing perturbance of the retinal tissue homeostasis. This leads to pro-inflammatory microglial activation, a mutual event of all retinal dystrophies. Sustained microglial activation is considered to exacerbate the progression of retinal disease. Gene therapy is a current strategy aiming to cure inherited retinal degenerative diseases. In contrast to this individualized approach, modulation of microglial activity is independent of the causative genetic defect and therefore provides a broad therapeutic range. Local application of microglia-regulating proteins or the supplementation of anti-inflammatory plant-derived compounds could be envisioned for the treatment of degenerative retinal diseases.

Transcriptional profiling of retinal microglia led to the identification of the novel whey acidic protein AMWAP. Based on the known properties of other myeloid-derived whey acidic proteins, we assumed that AMWAP could modulate microglial activity. Functional analyses then revealed that AMWAP has several immuno-regulatory effects. AMWAP effectively inhibts serine-proteases, has broad anti-microbial potential and dampens transcript levels of pro-inflammatory marker genes. AMWAP also induces expression of alternative marker genes associated with neurotrophic functions. The results presented in this work propose that AMWAP could be a potential therapeutic tool to dampen microglial activation and attenuate retinal degeneration.

Compounds from plant extracts like Curcumin and Luteolin have been widely used in traditional chinese medicine, because they have well known anti-inflammatory and radical scavenging activities. As part of this work, we analyzed the modulatory effects of Curcumin and Luteolin on pro-inflammatory activated microglial cells by transcriptomic profiling. The assessment of global gene expression showed indications for reprogramming of the pro-inflammatory activated microglia phenotype.

Curcumin and Luteolin attenuated pro-inflammatory activation of microglia and concurrently induced the expression of neuroprotective markers with substance-specific gene signatures. Subsequent functional analysis of microglia treated with both compounds *in vitro* revealed profound neuroprotective features. In conclusion, both plant-derived polyphenolic compounds may be promising tools to counter-act neurotoxic microglial activation in retinal disease.

5 Zusammenfassung

Mikrogliazellen erfüllen wichtige Überwachungsfunktionen in der gesunden Netzhaut und tragen wesentlich zur Aufrechterhaltung der Gewebshomöostase bei. Mikrogliale Immunmechanismen werden aktiv durch die Präsentation und Sekretion suppressiver Faktoren von retinalen Neuronen kontrolliert, um eine überschießende Mikrogliaaktivierung zu verhindern. Fortschreitender Zelltod stellt einen gemeinsamen Endpunkt aller retinalen Degenerationskrankheiten dar, wodurch eine Störung der Gewebshomöostase ausgelöst wird. Die einhergehende pro-inflammatorische Mikrogliaaktivierung gilt somit als gemeinsames Merkmal retinaler Dystrophien. Es wird angenommen, dass eine chronische Mikrogliaaktivierung zu einem schnelleren Fortschreiten von Degenerationsprozessen beiträgt. Als Therapiemöglichkeiten wurden bisher hauptsächlich gentherapeutische Ansätze erforscht, die darauf abzielen den jeweils kausalen genetischen Defekt zu beheben. Unabhängig von der genetischen Ursache, stellt die Modulation der Mikrogliaaktivierung einen breiten symptomatischen Behandlungsansatz dar. Die Beeinflussung entzündlicher Mikrogliazellen könnte das Fortschreiten der Degenerationserkrankung verlangsamen. Lokale Applikation von entzündungsdämpfenden Proteinen oder die orale Verabreichung von anti-entzündlichen sekundären Pflanzenstoffen stellen sehr vielversprechende Therapieansätze dar.

Das neuartige *whey acidic protein* AMWAP wurde basierend auf Daten eines genomweiten Genexpressionsprofils aus aktivierten retinalen Mikrogliazellen, zur weiteren funktionellen Charakterisierung ausgewählt. Aufgrund der entzündungshemmenden Eigenschaften von Peptiden der *whey acidc protein* Familie, wurde die Hypothese aufgestellt, dass auch AMWAP ähnliche Eigenschaften aufweist. Die in dieser Arbeit vorgestellten Ergebnisse der funktionellen Analyse von AMWAP haben gezeigt, dass AMWAP Entzündungsmechanismen auf verschiedene Weise beeinflusst und somit die inflammatorische Mikgrogliaaktivierung abschwächt. Im Detail wirkte AMWAP Protease-hemmend, anti-mikrobiell und verminderte die Expression pro-inflammatorischer Gene. Zusätzlich erhöhte AMWAP die Produktion von Markern der alternativen Aktivierung, was auf eine Induktion neuroprotektiver Mechanismen

hindeutet. Aufgrund dieser Befunde könnte AMWAP einen Kandidaten zur Modulation der Mikrogliaaktivierung bei Netzhautdegeneration darstellen.

Bioaktive sekundäre Pflanzenstoffe wie Curcumin oder Luteolin finden aufgrund ihrer entzündungshemmenden und anti-oxidativen Eigenschaften breite Anwendung in der traditionellen chinesischen Medizin. In dieser Arbeit sollte der immunregulatorische Einfluss der Pflanzenstoffe Curcumin und Luteolin auf aktivierte Mikrogliazellen durch genomweite Transkriptprofilierung untersucht werden. Die ganzheitliche Erfassung des Transkriptoms der modulierten Mikrogliazellen zeigte eine globale Beeinflussung des aktivierten Zellstatus. Behandlung der Mikrogliazellen mit Curcumin und Luteolin führten zur potenten Suppression der pro-inflammatorischen Aktivierung und zugleich zur Induktion von Genclustern mit neuroprotektiven Markern. Vergleichend zeigten Curcumin und Luteolin die Induktion unterschiedlicher neuroprotektiver Gene. Durch funktionelle Analyse wurden für beide Substanzen eindeutige neuroprotektive Eigenschaften in Zellkulturexperimenten mit Photorezeptorzellen nachgewiesen. Zusammenfassend kann gefolgert werden, dass Curcumin und Luteolin das Expressionsmuster aktivierter Mikrogliazellen merklich beeinflussen und beide Substanzen durch ein breites Wirkungsspektrum mögliche experimentelle Therapieansätze für retinale Degenerationserkrankungen darstellen könnten.

6 References

Ajami, B. et al., 2007. Local self-renewal can sustain CNS microglia maintenance and function throughout adult life. *Nature Neuroscience*, 10(12), pp.1538–1543.

al-Ubaidi, M.R. et al., 1992. Bilateral retinal and brain tumors in transgenic mice expressing simian virus 40 large T antigen under control of the human interphotoreceptor retinoid-binding protein promoter. *The Journal of cell biology*, 119(6), pp.1681–1687.

Ambrosini, E. & Aloisi, F., 2004. Chemokines and glial cells: a complex network in the central nervous system. *Neurochemical research*, 29(5), pp.1017–1038.

Ammon, H. & Wahl, M., 1991. Pharmacology of Curcuma-Longa. *Planta Medica*, 57(1), pp.1–7.

Antonietta Ajmone-Cat, M. et al., 2011. Docosahexaenoic acid modulates inflammatory and antineurogenic functions of activated microglial cells. *Journal of neuroscience research*.

Ashkenazi, A. & Dixit, V.M., 1998. Death receptors: signaling and modulation. *Science*, 281(5381), pp.1305–1308.

Banati, R.B., 2002. Visualising microglial activation in vivo. *Glia*, 40(2), pp.206–217.

Banati, R.B. et al., 2000. The peripheral benzodiazepine binding site in the brain in multiple sclerosis: quantitative in vivo imaging of microglia as a measure of disease activity. *Brain : a journal of neurology*, 123 (Pt 11), pp.2321–2337.

Bea, F. et al., 2003. Induction of glutathione synthesis in macrophages by oxidized low-density lipoproteins is mediated by consensus antioxidant response elements. *Circulation research*, 92(4), pp.386–393.

Benveniste, E.N., 1997. Role of macrophages/microglia in multiple sclerosis and experimental allergic encephalomyelitis. *Journal of molecular medicine*, 75(3), pp.165–173.

Bingle, C.D. & Vyakarnam, A., 2008. Novel innate immune functions of the whey acidic protein family. *Trends in immunology*, 29(9), pp.444–453.

Brambilla, R. et al., 2003. P2Y receptors in brain astroglial cells: Identification of a gliotic P2Y receptor coupled to activation of a calcium-independent ras/ERK1/2 pathway. *Drug Development Research*, 59(1), pp.161–170.

Brazma, A. et al., 2001. Minimum information about a microarray experiment (MIAME)-toward standards for microarray data. *Nature genetics*, 29(4), pp.365–371.

Brenner, D. & Mak, T.W., 2009. Mitochondrial cell death effectors. *Current Opinion in Cell Biology*, 21(6), pp.871–877.

Bringmann, A. et al., 2006. Müller cells in the healthy and diseased retina. *Progress in retinal and eye research*, 25(4), pp.397–424.

Broderick, C. et al., 2002. Constitutive retinal CD200 expression regulates resident microglia and activation state of inflammatory cells during experimental autoimmune uveoretinitis. *The American journal of pathology*, 161(5), pp.1669–1677.

Cagnin, A. et al., 2007. Positron emission tomography imaging of neuroinflammation. *Neurotherapeutics*, 4(3), pp.443–452.

Campbell, N.A. et al., 2010. *Biology*, Benjamin-Cummings Pub Co.

Cao, Q. et al., 2008. Expression of Notch-1 receptor and its ligands Jagged-1 and Delta-1 in amoeboid microglia in postnatal rat brain and murine BV-2 cells. *Glia*, 56(11), pp.1224–1237.

Cardona, A. et al., 2006. Control of microglial neurotoxicity by the fractalkine receptor. *Nature Neuroscience*, 9(7), pp.917–924.

Carter, D.A. & Dick, A.D., 2004. CD200 maintains microglial potential to migrate in adult human retinal explant model. *Current Eye Research*, 28(6), pp.427–436.

Chaigne-Delalande, B., Moreau, J.-F. & Legembre, P., 2008. Rewinding the DISC. *Archivum immunologiae et therapiae experimentalis*, 56(1), pp.9–14.

Chang, G. & Hao, Y., 1993. Apoptosis: Final common pathway of photoreceptor death in rd, rds, and mutant mice. *Neuron*.

Chen, C., Peng, W. & Tsai, K., 2007. Luteolin suppresses inflammation-associated gene expression by blocking NF-[kappa] B and AP-1 activation pathway in mouse alveolar macrophages. *Life sciences*.

Chen, H.-Q. et al., 2008. Luteolin protects dopaminergic neurons from inflammation-induced injury through inhibition of microglial activation. *Neuroscience Letters*, 448(2), pp.175–179.

Cheng, L., Han, X. & Shi, Y., 2009. A regulatory role of LPCAT1 in the synthesis of inflammatory lipids, PAF and LPC, in the retina of diabetic mice. *American journal of physiology. Endocrinology and metabolism*, 297(6), pp.E1276–E1282.

Choi, D.K., Koppula, S. & Suk, K., 2011. Inhibitors of Microglial Neurotoxicity: Focus on Natural Products. *Molecules*, 16(2), pp.1021–1043.

Cole, G.M., Ma, Q.-L. & Frautschy, S.A., 2010. Dietary fatty acids and the aging brain. *Nutrition Reviews*, 68, pp.S102–S111.

Colobran, R. et al., 2007. The chemokine network. I. How the genomic organization of chemokines contains clues for deciphering their functional complexity. *Clinical and experimental immunology*, 148(2), pp.208–217.

Combadière, C. et al., 2007. CX3CR1-dependent subretinal microglia cell accumulation is associated with cardinal features of age-related macular degeneration. *The Journal of clinical investigation*, 117(10), pp.2920–2928.

Damani, M.R. et al., 2011. Age-related alterations in the dynamic behavior of microglia. *Aging cell*, 10(2), pp.263–276.

Davalos, D. et al., 2005. ATP mediates rapid microglial response to local brain injury in vivo. *Nature Neuroscience*, 8(6), pp.752–758.

Davis-Bruno, K. & Tassinari, M.S., 2011. Essential fatty acid supplementation of DHA and ARA and effects on neurodevelopment across animal species: a review of the literature. *Birth Defects Research Part B: Developmental and Reproductive Toxicology*, 92(3), pp.240–250.

De Simone, R. et al., 2007. NGF promotes microglial migration through the activation of its high affinity receptor: Modulation by TGF-β. *Journal of neuroimmunology*, 190(1), pp.53–60.

de Vries, H.E. et al., 2008. Nrf2-induced antioxidant Protection: A Promising target to counteract ROS-mediated damage in neurodegenerative disease? *Free Radical Biology and Medicine*, 45(10), pp.1375–1383.

Dear, T., Ramshaw, I. & Kefford, R., 1988. Differential Expression of a Novel Gene, Wdnm1, in Nonmetastatic Rat Mammary Adenocarcinoma Cells. *Cancer research*, 48(18), pp.5203–5209.

Dear, T.N., McDonald, D.A. & Kefford, R.F., 1989. Transcriptional down-regulation of a rat gene, WDNM2, in metastatic DMBA-8 cells. *Cancer research*, 49(19), pp.5323–5328.

Dennis, G. et al., 2003. DAVID: Database for Annotation, Visualization, and Integrated Discovery. *Genome Biology*, 4(5), p.P3.

Dick, A.D., 2003. Control of myeloid activity during retinal inflammation. *Journal of leukocyte biology*, 74(2), pp.161–166.

Dirscherl, K. et al., 2010. Luteolin triggers global changes in the microglial transcriptome leading to a unique anti-inflammatory and neuroprotective phenotype. *Journal of neuroinflammation*, 7, p.3.

Doi, Y. et al., 2009. Microglia activated with the toll-like receptor 9 ligand CpG attenuate oligomeric amyloid {beta} neurotoxicity in in vitro and in vivo models of Alzheimer's disease. *The American journal of pathology*, 175(5), pp.2121–2132.

Doumas, S., Kolokotronis, A. & Stefanopoulos, P., 2005. Anti-inflammatory and antimicrobial roles of secretory leukocyte protease inhibitor. *Infection and immunity*, 73(3), pp.1271–1274.

Dunaief, J.L. et al., 2002. The role of apoptosis in age-related macular degeneration. *Archives of ophthalmology*, 120(11), pp.1435–1442.

Ebert, S. et al., 2008. Chondroitin sulfate disaccharide stimulates microglia to adopt a novel regulatory phenotype. *Journal of leukocyte biology*, 84(3), pp.736–740.

Ebert, S. et al., 2009. Docosahexaenoic acid attenuates microglial activation and delays early retinal degeneration. *Journal of Neurochemistry*, 110(6), pp.1863–1875.

Eichler, G.S., Huang, S. & Ingber, D.E., 2003. Gene Expression Dynamics Inspector (GEDI): for integrative analysis of expression profiles. *Bioinformatics (Oxford, England)*, 19(17), pp.2321–2322.

Essner, E., 1979. An electron microscopic study of macrophages in rats with inherited retinal dystrophy. *Investigative ophthalmology & visual science*.

Eter, N. et al., 2008. In Vivo Visualization of Dendritic Cells, Macrophages, and Microglial Cells Responding to Laser-Induced Damage in the Fundus of the Eye. *Investigative ophthalmology & visual science*, 49(8), pp.3649–3658.

Fan, R., DeFilippis, K. & Van Nostrand, W.E., 2007. Induction of complement proteins in a mouse model for cerebral microvascular A beta deposition. *Journal of neuroinflammation*, 4, pp.22–.

Fan, W. et al., 2010. Early Involvement of Immune/Inflammatory Response Genes in Retinal Degeneration in DBA/2J Mice. *Ophthalmology and eye diseases*, 1, pp.23–41.

Ferreira, R. et al., 2010. Neuropeptide Y modulation of interleukin-1 beta (IL-1beta)-induced nitric oxide production in microglia. *Journal of Biological Chemistry*, 285(53), pp.41921–41934.

Flach, H. et al., 2010. Mzb1 Protein Regulates Calcium Homeostasis, Antibody Secretion, and Integrin Activation in Innate-like B Cells. *Immunity*, 33(5), pp.723–735.

Gao, H.-M. et al., 2011. HMGB1 acts on microglia Mac1 to mediate chronic neuroinflammation that drives progressive neurodegeneration. *The Journal of neuroscience : the official journal of the Society for Neuroscience*, 31(3), pp.1081–1092.

Gehrig, A. et al., 2007. Genome-wide expression profiling of the retinoschisin-deficient retina in early postnatal mouse development. *Investigative ophthalmology & visual science*, 48(2), pp.891–900.

Ginhoux, F. et al., 2010. Fate mapping analysis reveals that adult microglia derive from primitive macrophages. *Science (New York, N.Y.)*, 330(6005), pp.841–845.

Girard, C. et al., 2012. Axonal Regeneration and Neuroinflammation: Roles for the Translocator Protein 18 kDa. *Journal of neuroendocrinology*, 24(1), pp.71–81.

Giulian, D. et al., 1995. Cell surface morphology identifies microglia as a distinct class of mononuclear phagocyte. *The Journal of Neuroscience*, 15(11), pp.7712–7726.

Gordon, S. & Taylor, P.R., 2005. Monocyte and macrophage heterogeneity. *Nature reviews. Immunology*, 5(12), pp.953–964.

Gotoh, T. et al., 2002. Nitric oxide-induced apoptosis in RAW 264.7 macrophages is mediated by endoplasmic reticulum stress pathway involving ATF6 and CHOP. *The Journal of biological chemistry*, 277(14), pp.12343–12350.

Graeber, M.B. & Streit, W.J., 2009. Microglia: biology and pathology. *Acta Neuropathologica*, 119(1), pp.89–105.

Granucci, F. et al., 2003. The scavenger receptor MARCO mediates cytoskeleton rearrangements in dendritic cells and microglia. *Blood*, 102(8), pp.2940–2947.

Gupta, N., Brown, K.E. & Milam, A.H., 2003. Activated microglia in human retinitis pigmentosa, late-onset retinal degeneration, and age-related macular degeneration. *Experimental eye research*, 76(4), pp.463–471.

Hagiwara, K. et al., 2003. Mouse SWAM1 and SWAM2 are antibacterial proteins composed of a single whey acidic protein motif. *Journal of immunology (Baltimore, Md. : 1950)*, 170(4), pp.1973–1979.

Hanisch, U.-K., 2002. Microglia as a source and target of cytokines. *Glia*, 40(2), pp.140–155.

Hanisch, U.-K. & Kettenmann, H., 2007. Microglia: active sensor and versatile effector cells in the normal and pathologic brain. *Nature Neuroscience*, 10(11), pp.1387–1394.

Harayama, T. et al., 2008. Identification of a novel noninflammatory biosynthetic pathway of platelet-activating factor. *The Journal of biological chemistry*, 283(17), pp.11097–11106.

Harris, G.K. et al., 2006. Luteolin and chrysin differentially inhibit cyclooxygenase-2 expression and scavenge reactive oxygen species but similarly inhibit prostaglandin-E2 formation in RAW 264.7 cells. *The Journal of nutrition*, 136(6), pp.1517–1521.

Hausler, K.G. et al., 2002. Interferon-gamma differentially modulates the release of cytokines and chemokines in lipopolysaccharide- and pneumococcal cell wall-stimulated mouse microglia and macrophages. *European Journal of Neuroscience*, 16(11), pp.2113–2122.

Haynes, S.E. et al., 2006. The P2Y12 receptor regulates microglial activation by extracellular nucleotides. *Nature Neuroscience*, 9(12), pp.1512–1519.

He, L.-F. et al., 2010. Curcumin protects pre-oligodendrocytes from activated microglia in vitro and in vivo. *Brain research*, 1339, pp.60–69.

Hickey, W. & Kimura, H., 1988. Perivascular microglial cells of the CNS are bone marrow-derived and present antigen in vivo. *Science (New York, N.Y.)*, 239(4837), pp.290–292.

Hiemstra, P.S. et al., 1996. Antibacterial activity of antileukoprotease. *Infection and immunity*, 64(11), pp.4520–4524.

Hinojosa, A.E. et al., 2011. CCL2/MCP-1 modulation of microglial activation and proliferation. *Journal of neuroinflammation*, 8(1), p.77.

Hirsch, E.C. & Hunot, S., 2009. Neuroinflammation in Parkinson's disease: a target for neuroprotection? *Lancet neurology*, 8(4), pp.382–397.

Hoek, R.M., 2000. Down-Regulation of the Macrophage Lineage Through Interaction with OX2 (CD200). *Science (New York, N.Y.)*, 290(5497), pp.1768–1771.

Hong, S.H. et al., 2006. Mitochondrial ligand inhibits store□operated calcium influx and COX2 production in human microglia. *Journal of neuroscience research*, 83(7), pp.1293–1298.

Hu, C. & Kitts, D.D., 2004. Luteolin and luteolin-7-O-glucoside from dandelion flower suppress iNOS and COX-2 in RAW264.7 cells. *Molecular and cellular biochemistry*, 265(1-2), pp.107–113.

Hume, D.A., 2008. Differentiation and heterogeneity in the mononuclear phagocyte system. *Mucosal Immunology*, 1(6), pp.432–441.

Hume, D.A., 1983. Immunohistochemical localization of a macrophage-specific antigen in developing mouse retina: phagocytosis of dying neurons and differentiation of microglial cells to form a regular array in the plexiform layers. *The Journal of cell biology*, 97(1), pp.253–257.

Inoue, K., Koizumi, S. & Tsuda, M., 2007. The role of nucleotides in the neuron-glia communication responsible for the brain functions. *Journal of Neurochemistry*, 102(5), pp.1447–1458.

Jackson, D.E., 2003. The unfolding tale of PECAM-1. *FEBS Letters*, 540(1-3), pp.7–14.

Jager, R.D., Mieler, W.F. & Miller, J.W., 2008. Age-related macular degeneration. *New England Journal of Medicine*, 358(24), pp.2606–2617.

Jagetia, G.C. & Aggarwal, B.B., 2007. “Spicing up” of the immune system by curcumin. *Journal of clinical immunology*, 27(1), pp.19–35.

Jang, S. & Johnson, R.W., 2010. Can consuming flavonoids restore old microglia to their youthful state? *Nutrition Reviews*, 68(12), pp.719–728.

Jang, S., Kelley, K.W. & Johnson, R.W., 2008. Luteolin reduces IL-6 production in microglia by inhibiting JNK phosphorylation and activation of AP-1. *Proceedings of the National Academy of Sciences of the United States of America*, 105(21), pp.7534–7539.

Jimenez, S. et al., 2008. Inflammatory response in the hippocampus of PS1M146L/APP751SL mouse model of Alzheimer's disease: age-dependent switch in the microglial phenotype from alternative to classic. *The Journal of neuroscience : the official journal of the Society for Neuroscience*, 28(45), pp.11650–11661.

Jin, C.-Y. et al., 2007a. Curcumin attenuates the release of pro-inflammatory cytokines in lipopolysaccharide-stimulated BV2 microglia. *Acta Pharmacologica Sinica*, 28(10), pp.1645–1651.

Jin, F.Y. et al., 1997. Secretory leukocyte protease inhibitor: a macrophage product induced by and antagonistic to bacterial lipopolysaccharide. *Cell*, 88(3), pp.417–426.

Jin, S. et al., 2007b. Interferon-beta is neuroprotective against the toxicity induced by activated microglia. *Brain research*, 1179, pp.140–146.

Jung, D., Bong, J. & Baik, M., 2004. Extracellular proteinase inhibitor-accelerated apoptosis is associated with B cell activating factor in mammary epithelial cells. *Experimental cell research*, 292(1), pp.115–122.

Jung, K.K. et al., 2006. Inhibitory effect of curcumin on nitric oxide production from lipopolysaccharide-activated primary microglia. *Life sciences*, 79(21), pp.2022–2031.

Kaneko, H. et al., 2008. Characteristics of Bone Marrow-Derived Microglia in the Normal and Injured Retina. *Investigative ophthalmology & visual science*, 49(9), pp.4162–4168.

Kang, G. et al., 2004. Curcumin suppresses lipopolysaccharide-induced cyclooxygenase-2 expression by inhibiting activator protein 1 and nuclear factor kappa B bindings in BV2 microglial cells. *Journal of Pharmacological Sciences*, 94(3), pp.325–328.

Karlstetter, M. et al., 2011. Curcumin is a potent modulator of microglial gene expression and migration. *Journal of neuroinflammation*, 8, p.125.

Karlstetter, M., Walczak, Y., Weigelt, K., Ebert, S., et al., 2010a. The novel activated microglia/macrophage WAP domain protein, AMWAP, acts as a counter-regulator of proinflammatory response. *Journal of immunology (Baltimore, Md. : 1950)*, 185(6), pp.3379–3390.

Karlstetter, M., Ebert, S. & Langmann, T., 2010b. Microglia in the healthy and degenerating retina: Insights from novel mouse models. *Immunobiology*, 215(9-10), pp.685–691.

Kezic, J. & McMenamin, P.G., 2008. Differential turnover rates of monocyte-derived cells in varied ocular tissue microenvironments. *Journal of leukocyte biology*, 84(3), pp.721–729.

Khoury, El, J. & Luster, A.D., 2008. Mechanisms of microglia accumulation in Alzheimer's disease: therapeutic implications. *Trends in pharmacological sciences*, 29(12), pp.626–632.

Kigerl, K.A. et al., 2009. Identification of two distinct macrophage subsets with divergent effects causing either neurotoxicity or regeneration in the injured mouse spinal cord. *The Journal of neuroscience : the official journal of the Society for Neuroscience*, 29(43), pp.13435–13444.

Kim, H. et al., 2003. Curcumin suppresses janus kinase-STAT inflammatory signaling through activation of Src homology 2 domain-containing tyrosine phosphatase 2 in brain microglia. *Journal of immunology (Baltimore, Md. : 1950)*, 171(11), pp.6072–6079.

Kim, J. et al., 2006. Luteolin inhibits LPS-stimulated inducible nitric oxide synthase expression in BV-2 microglial cells. *Planta Medica*, 72(1), pp.65–68.

Klesney-Tait, J., Turnbull, I.R. & Colonna, M., 2006. The TREM receptor family and signal integration. *Nature immunology*, 7(12), pp.1266–1273.

Klinke, R., Bauer, C. & Silbernagl, S., 2003. *Lehrbuch der Physiologie*,

Klune, J.R. et al., 2008. HMGB1: endogenous danger signaling. *Molecular medicine (Cambridge, Mass.)*, 14(7-8), pp.476–484.

Koenigsknecht, J. & Landreth, G., 2004. Microglial phagocytosis of fibrillar beta-amyloid through a beta1 integrin-dependent mechanism. *The Journal of neuroscience : the official journal of the Society for Neuroscience*, 24(44), pp.9838–9846.

Krady, J.K. et al., 2008. Ciliary neurotrophic factor and interleukin-6 differentially activate microglia. *Journal of neuroscience research*, 86(7), pp.1538–1547.

Langmann, T., 2007. Microglia activation in retinal degeneration. *Journal of leukocyte biology*, 81(6), pp.1345–1351.

Langmann, T. et al., 2009. Induction of Early Growth Response-1 Mediates Microglia Activation In Vitro But is Dispensable In Vivo. *NeuroMolecular Medicine*, 11(2), pp.87–96.

Laslo, P. et al., 2006. Multilineage transcriptional priming and determination of alternate hematopoietic cell fates. *Cell*, 126(4), pp.755–766.

Lavrik, I.N., 2010. Systems biology of apoptosis signaling networks. *Current opinion in biotechnology*, 21(4), pp.551–555.

Lawson, L.J. et al., 1990. Heterogeneity in the distribution and morphology of microglia in the normal adult mouse brain. *Neuroscience*, 39(1), pp.151–170.

Lee, J.E. et al., 2008. Ex vivo dynamic imaging of retinal microglia using time-lapse confocal microscopy. *Investigative ophthalmology & visual science*, 49(9), pp.4169–4176.

Lee, S. et al., 2007. A dual role of lipocalin 2 in the apoptosis and deramification of activated microglia. *Journal of immunology (Baltimore, Md. : 1950)*, 179(5), pp.3231–3241.

Li, L. et al., 2007. The function of microglia, either neuroprotection or neurotoxicity, is determined by the equilibrium among factors released from activated microglia in vitro. *Brain research*, 1159, pp.8–17.

Li, N. et al., 2000. Induction of heme oxygenase-1 expression in macrophages by diesel exhaust particle chemicals and quinones via the antioxidant-responsive element. *Journal of immunology (Baltimore, Md. : 1950)*, 165(6), pp.3393–3401.

Liebner, S., Czupalla, C.J. & Wolburg, H., 2011. Current concepts of blood-brain barrier development. *The International Journal of Developmental Biology*, 55(4-5), pp.467–476.

Lim, J.H. et al., 2007. Isoorientin induces Nrf2 pathway-driven antioxidant response through phosphatidylinositol 3-kinase signaling. *Archives of pharmacal research*, 30(12), pp.1590–1598.

Lin, H.-Y. et al., 2010. Peptidoglycan enhances proinflammatory cytokine expression through the TLR2 receptor, MyD88, phosphatidylinositol 3-kinase/AKT and NF-kappaB pathways in BV-2 microglia. *International immunopharmacology*, 10(8), pp.883–891.

Lin, J.C. et al., 2003. The netrin-G1 ligand NGL-1 promotes the outgrowth of thalamocortical axons. *Nature Neuroscience*, 6(12), pp.1270–1276.

Liu, G. et al., 2009. miR-147, a microRNA that is induced upon Toll-like receptor stimulation, regulates murine macrophage inflammatory responses. *Proceedings of the National Academy of Sciences of the United States of America*, 106(37), pp.15819–15824.

Lleo, A., Galea, E. & Sastre, M., 2007. Molecular targets of non-steroidal anti-inflammatory drugs in neurodegenerative diseases. *Cellular and molecular life sciences : CMLS*, 64(11), pp.1403–1418.

Lo, A.C.Y. et al., 2011. Apoptosis and other cell death mechanisms after retinal detachment: implications for photoreceptor rescue. *Ophthalmologica. Journal international d'ophtalmologie. International journal of ophthalmology. Zeitschrift für Augenheilkunde*, 226 Suppl 1, pp.10–17.

Lohr, H.R. et al., 2006. Multiple, parallel cellular suicide mechanisms participate in photoreceptor cell death. *Experimental eye research*, 83(2), pp.380–389.

Lotze, M.T. & Tracey, K.J., 2005. High-mobility group box 1 protein (HMGB1): nuclear weapon in the immune arsenal. *Nature reviews. Immunology*, 5(4), pp.331–342.

López-Lázaro, M., 2009. Distribution and biological activities of the flavonoid luteolin. *Mini reviews in medicinal chemistry*, 9(1), pp.31–59.

Lutz, M.B. et al., 1999. An advanced culture method for generating large quantities of highly pure dendritic cells from mouse bone marrow. *Journal of immunological methods*, 223(1), pp.77–92.

Ly, N.P. et al., 2005. Netrin-1 inhibits leukocyte migration in vitro and in vivo. *Proceedings of the National Academy of Sciences of the United States of America*, 102(41), pp.14729–14734.

Lyons, A. et al., 2009. Decreased neuronal CD200 expression in IL-4-deficient mice results in increased neuroinflammation in response to lipopolysaccharide. *Brain, behavior, and immunity*, 23(7), pp.1020–1027.

Maheshwari, R.K. et al., 2006. Multiple biological activities of curcumin: a short review. *Life sciences*, 78(18), pp.2081–2087.

Mandal, M.N.A. et al., 2009. Curcumin protects retinal cells from light-and oxidant stress-induced cell death. *Free Radical Biology and Medicine*, 46(5), pp.672–679.

Martin, C.B., Ingersoll, S.A. & Martin, B.K., 2007. Transcriptional control of the C3a receptor gene in glial cells: Dependence upon AP-1 but not Ets. *Molecular immunology*, 44(5), pp.703–712.

Martinez, F., Sica, A. & Mantovani, A., 2008. Macrophage activation and polarization. *Frontiers in Bioscience*, pp.453–461.

Masland, R., 2001. The fundamental plan of the retina. *Nature Neuroscience*, 4(9), pp.877–886.

Mauerer, R., Walczak, Y. & Langmann, T., 2009. Comprehensive mRNA profiling of lipid-related genes in microglia and macrophages using taqman arrays. *Methods in molecular biology (Clifton, N.J.)*, 580, pp.187–201.

Michelucci, A. et al., 2009. Characterization of the microglial phenotype under specific pro-inflammatory and anti-inflammatory conditions: Effects of oligomeric and fibrillar amyloid-beta. *Journal of neuroimmunology*, 210(1-2), pp.3–12.

Mildner, A. et al., 2007. Microglia in the adult brain arise from Ly-6ChiCCR2+ monocytes only under defined host conditions. *Nature Neuroscience*, 10(12), pp.1544–1553.

Mohlin, C., Liljekvist-Soltic, I. & Johansson, K., 2011. Further assessment of neuropathology in retinal explants and neuroprotection by human neural progenitor cells. *Journal of neural engineering*, 8(6), p.066012.

Molhuizen, H. & Schalkwijk, J., 1995. Structural, Biochemical, and Cell Biological Aspects of the Serine Proteinase-Inhibitor Skalp/Elafin/Esi. *Biological Chemistry Hoppe-Seyler*, 376(1), pp.1–7.

Moreau, T. et al., 2008. Multifaceted roles of human elafin and secretory leukocyte proteinase inhibitor (SLPI), two serine protease inhibitors of the chelonianin family. *Biochimie*, 90(2), pp.284–295.

Mosser, D., 2003. The many faces of macrophage activation. *Journal of leukocyte biology*.

Mueller, A.M. et al., 2008. Novel role for SLPI in MOG-induced EAE revealed by spinal cord expression analysis. *Journal of neuroinflammation*, 5, p.20.

Mukherjee, P.K. et al., 2007. Neurotrophins enhance retinal pigment epithelial cell survival through neuroprotectin D1 signaling. *Proceedings of the National Academy of Sciences of the United States of America*, 104(32), pp.13152–13157.

Muzio, L., Martino, G. & Furlan, R., 2007. Multifaceted aspects of inflammation in multiple sclerosis: The role of microglia. *Journal of neuroimmunology*, 191(1-2), pp.39–44.

Nakamura, A. et al., 2003. Increased susceptibility to LPS-induced endotoxin shock in secretory leukoprotease inhibitor (SLPI)-deficient mice. *The Journal of experimental medicine*, 197(5), pp.669–674.

Nguyen, H. et al., 1999. Identification of the secretory leukocyte protease inhibitor (SLPI) as a target of IRF-1 regulation. *Oncogene*, 18(39), pp.5455–5463.

Nimmerjahn, A., Kirchhoff, F. & Helmchen, F., 2005. Resting microglial cells are highly dynamic surveillants of brain parenchyma in vivo. *Science (New York, N.Y.)*, 308(5726), pp.1314–1318.

Nukumi, N. et al., 2007. Reduction of tumorigenesis and invasion of human breast cancer cells by whey acidic protein (WAP). *Cancer letters*, 252(1), pp.65–74.

Odaka, C. et al., 2003. Murine macrophages produce secretory leukocyte protease inhibitor during clearance of apoptotic cells: implications for resolution of the inflammatory response. *Journal of immunology (Baltimore, Md. : 1950)*, 171(3), pp.1507–1514.

Oppenheim, J.J. & Yang, D., 2005. Alarmins: chemotactic activators of immune responses. *Current Opinion in Immunology*, 17(4), pp.359–365.

Orr, C.F., Rowe, D.B. & Halliday, G.M., 2002. An inflammatory review of Parkinson's disease. *Progress in Neurobiology*, 68(5), pp.325–340.

Osburn, W.O. et al., 2006. Nrf2 regulates an adaptive response protecting against oxidative damage following diquat-mediated formation of superoxide anion. *Archives of biochemistry and biophysics*, 454(1), pp.7–15.

Paglinawan, R. et al., 2003. TGFβ directs gene expression of activated microglia to an anti‐inflammatory phenotype strongly focusing on chemokine genes and cell migratory genes. *Glia*, 44(3), pp.219–231.

Park, J.S., 2003. Involvement of Toll-like Receptors 2 and 4 in Cellular Activation by High Mobility Group Box 1 Protein. *Journal of Biological Chemistry*, 279(9), pp.7370–7377.

Penfold, P.L., Killingsworth, M.C. & Sarks, S.H., 1985. Senile macular degeneration: The involvement of immunocompetent cells. *Graefe's Archive for Clinical and Experimental Ophthalmology*, 223(2), pp.69–76.

Perry, V., Hume, D. & Gordon, S., 1985. Immunohistochemical localization of macrophages and microglia in the adult and developing mouse brain. *Neuroscience*, 15(2), pp.313–326.

Perry, V.H. & Gordon, S., 1988. Macrophages and microglia in the nervous system. *Trends in neurosciences*, 11(6), pp.273–277.

Plant, S. et al., 2006. Upregulation of the stress-associated gene p8 in mouse models of demyelination and in multiple sclerosis tissues. *Glia*, 53(5), pp.529–537.

Ponomarev, E.D. et al., 2010. MicroRNA-124 promotes microglia quiescence and suppresses EAE by deactivating macrophages via the C/EBP-α–PU.1 pathway. *Nature Medicine*, pp.1–8.

Prinz, M. et al., 2008. Distinct and nonredundant in vivo functions of IFNAR on myeloid cells limit autoimmunity in the central nervous system. *Immunity*, 28(5), pp.675–686.

Purkayastha, S. et al., 2009. Curcumin blocks brain tumor formation. *Brain research*, 1266, pp.130–138.

Rademakers, R. et al., 2011. Mutations in the colony stimulating factor 1 receptor (CSF1R) gene cause hereditary diffuse leukoencephalopathy with spheroids. *Nature genetics*.

Raivich, G. & Banati, R., 2004. Brain microglia and blood-derived macrophages: molecular profiles and functional roles in multiple sclerosis and animal models of autoimmune demyelinating disease. *Brain research. Brain research reviews*, 46(3), pp.261–281.

Ramsauer, K. et al., 2007. Distinct modes of action applied by transcription factors STAT1 and IRF1 to initiate transcription of the IFN-gamma-inducible gbp2 gene. *Proceedings of the National Academy of Sciences of the United States of America*, 104(8), pp.2849–2854.

Ranganathan, S. et al., 1999. The whey acidic protein family: a new signature motif and three-dimensional structure by comparative modeling1. *Journal of Molecular Graphics and Modelling*, 17(2), pp.106–113.

Ransohoff, R., LiPing, L. & Cardona, E., 2007. *Chemokines and Chemokine Receptors: Multiporpose Players in Neuroinflammation*, Elsevier.

Ransohoff, R.M., 2007. Microgliosis: the questions shape the answers. *Nature Neuroscience*, 10(12), pp.1507–1509.

Ransohoff, R.M. & Perry, V.H., 2009. Microglial Physiology: Unique Stimuli, Specialized Responses. *Annual review of immunology*, 27(1), pp.119–145.

Ray, B. & Lahiri, D.K., 2009. Neuroinflammation in Alzheimer's disease: different molecular targets and potential therapeutic agents including curcumin. *Current Opinion in Pharmacology*, 9(4), pp.434–444.

Reuter, S. et al., 2011. Epigenetic changes induced by curcumin and other natural compounds. *Genes & nutrition*, 6(2), pp.93–108.

Rezai-Zadeh, K. et al., 2008. Apigenin and luteolin modulate microglial activation via inhibition of STAT1-induced CD40 expression. *Journal of neuroinflammation*, 5, p.41.

Rice-Evans, C.A., Miller, N.J. & Paganga, G., 1996. Structure-antioxidant activity relationships of flavonoids and phenolic acids. *Free Radical Biology and Medicine*, 20(7), pp.933–956.

Rio-Hortega, P.D., 1939. THE MICROGLIA. *The Lancet*, 233(6036), pp.1023–1026.

Rohrer, B. et al., 2004. Multidestructive pathways triggered in photoreceptor cell death of the RD mouse as determined through gene expression profiling. *The Journal of biological chemistry*, 279(40), pp.41903–41910.

Roque, R.S. et al., 1999. Retina-derived microglial cells induce photoreceptor cell death in vitro. *Brain research*, 836(1-2), pp.110–119.

Ross, J.A. & Kasum, C.M., 2002. Dietary flavonoids: bioavailability, metabolic effects, and safety. *Annual review of nutrition*, 22, pp.19–34.

Rowell, E., Merkenschlager, M. & Wilson, C.B., 2008. Long-range regulation of cytokine gene expression. *Current Opinion in Immunology*, 20(3), pp.272–280.

Rubartelli, A. & Lotze, M.T., 2007. Inside, outside, upside down: damage-associated molecular-pattern molecules (DAMPs) and redox. *Trends in immunology*, 28(10), pp.429–436.

Rupprecht, R. et al., 2009. Translocator Protein (18 kD) as Target for Anxiolytics Without Benzodiazepine-Like Side Effects. *Science (New York, N.Y.)*, 325(5939), pp.490–493.

Ryu, J.K. et al., 2009. Microglial VEGF receptor response is an integral chemotactic component in Alzheimer's disease pathology. *The Journal of neuroscience : the official journal of the Society for Neuroscience*, 29(1), pp.3–13.

Sameermahmood, Z. et al., 2008. Curcumin modulates SDF-1alpha/CXCR4-induced migration of human retinal endothelial cells (HRECs). *Investigative ophthalmology & visual science*, 49(8), pp.3305–3311.

Sano, Y. et al., 2006. Photoreceptor cell apoptosis in the retinal degeneration of Uchl3-deficient mice. *The American journal of pathology*, 169(1), pp.132–141.

Sargsyan, S., Monk, P. & Shaw, P., 2005. Microglia as potential contributors to motor neuron injury in amyotrophic lateral sclerosis. *Glia*, 51(4), pp.241–253.

Sasahara, M. et al., 2008. Activation of Bone Marrow-Derived Microglia Promotes Photoreceptor Survival in Inherited Retinal Degeneration. *The American journal of pathology*, 172(6), pp.1693–1703.

Sasmono, R.T., 2002. A macrophage colony-stimulating factor receptor-green fluorescent protein transgene is expressed throughout the mononuclear phagocyte system of the mouse. *Blood*, 101(3), pp.1155–1163.

Scheibner, K.A. et al., 2006. Hyaluronan fragments act as an endogenous danger signal by engaging TLR2. *Journal of immunology (Baltimore, Md. : 1950)*, 177(2), p.1272.

Schuetz, E. & Thanos, S., 2004. Microglia-Targeted Pharmacotherapy in Retinal Neurodegenerative Diseases. *Current Drug Targets*, 5(7), pp.619–627.

Schwartz, M., 2007. Modulating the immune system: a vaccine for glaucoma? *Canadian journal of ophthalmology. Journal canadien d'ophtalmologie*, 42(3), pp.439–441.

Schwartz, M. et al., 2006. Microglial phenotype: is the commitment reversible? *Trends in neurosciences*, 29(2), pp.68–74.

Seelinger, G., Merfort, I. & Schempp, C.M., 2008. Anti-oxidant, anti-inflammatory and anti-allergic activities of luteolin. *Planta Medica*, 74(14), pp.1667–1677.

Senft, C. et al., 2010. The nontoxic natural compound Curcumin exerts anti-proliferative, anti-migratory, and anti-invasive properties against malignant gliomas. *BMC Cancer*, 10(1), p.491.

Shai, Y., 2002. Mode of action of membrane active antimicrobial peptides. *Biopolymers*, 66(4), pp.236–248.

Shang, Y.-Y. et al., 2009. TRB3, upregulated by ox-LDL, mediates human monocyte-derived macrophage apoptosis. *Febs Journal*, 276(10), pp.2752–2761.

Sheehan, J.J. et al., 2007. Proteolytic activation of monocyte chemoattractant protein-1 by plasmin underlies excitotoxic neurodegeneration in mice. *The Journal of neuroscience : the official journal of the Society for Neuroscience*, 27(7), pp.1738–1745.

Shenoy, A.R. et al., 2007. Emerging themes in IFN-gamma-induced macrophage immunity by the p47 and p65 GTPase families. *Immunobiology*, 212(9-10), pp.771–784.

Shimizu, Y., Meunier, L. & Hendershot, L.M., 2009. pERp1 is significantly up-regulated during plasma cell differentiation and contributes to the oxidative folding of immunoglobulin. *Proceedings of the National Academy of Sciences of the United States of America*, 106(40), pp.17013–17018.

Shimoi, K. et al., 1998. Intestinal absorption of luteolin and luteolin 7-O-beta-glucoside in rats and humans. *FEBS Letters*, 438(3), pp.220–224.

Shirley, S.A. et al., 2008. Curcumin prevents human dendritic cell response to immune stimulants. *Biochemical and biophysical research communications*, 374(3), pp.431–436.

Shishodia, S., Singh, T. & Chaturvedi, M.M., 2007. Modulation of transcription factors by curcumin. *Advances in experimental medicine and biology*, 595, pp.127–148.

Simpson, A. et al., 1999. Elafin (elastase-specific inhibitor) has anti-microbial activity against Gram-positive and Gram-negative respiratory pathogens. *FEBS Letters*, 452(3), pp.309–313.

Singh, A. et al., 2009. Nrf2-dependent sulfiredoxin-1 expression protects against cigarette smoke-induced oxidative stress in lungs. *Free Radical Biology and Medicine*, 46(3), pp.376–386.

Soulet, D. & Rivest, S., 2008. Bone-marrow-derived microglia: myth or reality? *Current Opinion in Pharmacology*, 8(4), pp.508–518.

Stoecker, K. et al., 2009. Induction of STAP-1 promotes neurotoxic activation of microglia. *Biochemical and biophysical research communications*, 379(1), pp.121–126.

Stoehr, H. et al., 2004. Membrane-associated guanylate kinase proteins MPP4 and MPP5 associate with Veli3 at distinct intercellular junctions of the neurosensory retina. *The Journal of Comparative Neurology*, 481(1), pp.31–41.

Stone, J. et al., 1999. Mechanisms of photoreceptor death and survival in mammalian retina. *Progress in retinal and eye research*, 18(6), pp.689–736.

Streit, W.J., 2005. Microglia and neuroprotection: implications for Alzheimer's disease. *Brain research. Brain research reviews*, 48(2), pp.234–239.

Streit, W.J., 2002. Microglia as neuroprotective, immunocompetent cells of the CNS. *Glia*, 40(2), pp.133–139.

Streit, W.J. et al., 2009. Dystrophic (senescent) rather than activated microglial cells are associated with tau pathology and likely precede neurodegeneration in Alzheimer's disease. *Acta Neuropathologica*, 118(4), pp.475–485.

Stuart, L.M. et al., 2007. CD36 signals to the actin cytoskeleton and regulates microglial migration via a p130Cas complex. *The Journal of biological chemistry*, 282(37), pp.27392–27401.

Swaroop, A. et al., 2007. Genetic susceptibility to age-related macular degeneration: a paradigm for dissecting complex disease traits. *Human Molecular Genetics*, 16(R2), p.R174.

Taggart, C.C., 2002. Secretory Leucoprotease Inhibitor Prevents Lipopolysaccharide-induced Ikappa Balpha Degradation without Affecting Phosphorylation or Ubiquitination. *Journal of Biological Chemistry*, 277(37), pp.33648–33653.

Taggart, C.C. et al., 2005. Secretory leucoprotease inhibitor binds to NF-kappaB binding sites in monocytes and inhibits p65 binding. *The Journal of experimental medicine*, 202(12), pp.1659–1668.

Takahashi, K., 2005. Clearance of apoptotic neurons without inflammation by microglial triggering receptor expressed on myeloid cells-2. *Journal of Experimental Medicine*, 201(4), pp.647–657.

Tan, E. et al., 2004. Expression of cone-photoreceptor-specific antigens in a cell line derived from retinal tumors in transgenic mice. *Investigative ophthalmology & visual science*, 45(3), pp.764–768.

Thanos, S., 1991. The Relationship of Microglial Cells to Dying Neurons During Natural Neuronal Cell-Death and Axotomy-Induced Degeneration of the Rat Retina. *European Journal of Neuroscience*, 3(12), pp.1189–1207.

Tsai, Y.-M. et al., 2011. Curcumin and its nano-formulation: the kinetics of tissue distribution and blood-brain barrier penetration. *International journal of pharmaceutics*, 416(1), pp.331–338.

Tso, M.O. et al., 1994. Apoptosis leads to photoreceptor degeneration in inherited retinal dystrophy of RCS rats. *Investigative ophthalmology & visual science*, 35(6), pp.2693–2699.

van Anken, E. et al., 2009. Efficient IgM assembly and secretion require the plasma cell induced endoplasmic reticulum protein pERp1. *Proceedings of the National Academy of Sciences of the United States of America*, 106(40), pp.17019–17024.

Veiga, S. et al., 2007. Translocator protein (18 kDa) is involved in the regulation of reactive gliosis. *Glia*, 55(14), pp.1426–1436.

Wake, H. et al., 2009. Resting microglia directly monitor the functional state of synapses in vivo and determine the fate of ischemic terminals. *The Journal of neuroscience : the official journal of the Society for Neuroscience*, 29(13), pp.3974–3980.

Walton, M.R. et al., 2000. PU.1 expression in microglia. *Journal of neuroimmunology*, 104(2), pp.109–115.

Wang, X. et al., 2003. Up-regulation of secretory leukocyte protease inhibitor (SLPI) in the brain after ischemic stroke: Adenoviral expression of SLPI protects brain from ischemic injury. *Molecular Pharmacology*, 64(4), pp.833–840.

Weber, B.H.F., 2002. Inactivation of the murine X-linked juvenile retinoschisis gene, Rs1h, suggests a role of retinoschisin in retinal cell layer organization and synaptic structure. *Proceedings of the National Academy of Sciences*, 99(9), pp.6222–6227.

Wegiel, B. et al., 2009. Cell surface biliverdin reductase mediates biliverdin-induced anti-inflammatory effects via phosphatidylinositol 3-kinase and Akt. *The Journal of biological chemistry*, 284(32), pp.21369–21378.

Weigelt, K. et al., 2008. An integrated workflow for analysis of ChIP-chip data. *BioTechniques*, 45(2), pp.131–2, 134, 136 passim.

Weigelt, K. et al., 2007. Dap12 expression in activated microglia from retinoschisin-deficient retina and its PU.1-dependent promoter regulation. *Journal of leukocyte biology*, 82(6), pp.1564–1574.

Weigelt, K. et al., 2009. Transcriptomic profiling identifies a PU.1 regulatory network in macrophages. *Biochemical and biophysical research communications*, 380(2), pp.308–312.

Weldon, S. et al., 2007. The role of secretory leucoprotease inhibitor in the resolution of inflammatory responses. In *Biochemical Society Transactions*. Biochemical Society Transactions. pp. 273–276.

White, C.A., McCombe, P.A. & Pender, M.P., 1998. Microglia are more susceptible than macrophages to apoptosis in the central nervous system in experimental autoimmune encephalomyelitis through a mechanism not involving Fas (CD95). *International immunology*, 10(7), pp.935–941.

Williams, S.E. et al., 2006. SLPI and elafin: one glove, many fingers. *Clinical Science*, 110(1), p.21.

Woo, J., Kwon, S.-K. & Kim, E., 2009. The NGL family of leucine-rich repeat-containing synaptic adhesion molecules. *Molecular and Cellular Neuroscience*, 42(1), pp.1–10.

Xu, H. et al., 2007. Turnover of resident retinal microglia in the normal adult mouse. *Glia*, 55(11), pp.1189–1198.

Xu, J. et al., 2005. Agonists for the peroxisome proliferator-activated receptor-alpha and the retinoid X receptor inhibit inflammatory responses of microglia. *Journal of neuroscience research*, 81(3), pp.403–411.

Yang, J. et al., 2005. Suppression of macrophage responses to bacterial lipopolysaccharide (LPS) by secretory leukocyte protease inhibitor (SLPI) is independent of its anti-protease function. *Biochimica et biophysica acta*, 1745(3), pp.310–317.

Yang, S. et al., 2008. Curcumin protects dopaminergic neuron against LPS induced neurotoxicity in primary rat neuron/glia culture. *Neurochemical research*, 33(10), pp.2044–2053.

Youdim, K.A. et al., 2004. Flavonoid permeability across an in situ model of the blood-brain barrier. *Free Radical Biology and Medicine*, 36(5), pp.592–604.

Yuhong Chen, M.B.K.Z., 2010. Age-related Macular Degeneration: Genetic and Environmental Factors of Disease. *Molecular Interventions*, 10(5), p.271.

Zasloff, M., 2002. Antimicrobial peptides of multicellular organisms. *Nature*.

Zauberman, A., Lapter, S. & Zipori, D., 2001. Smad proteins suppress CCAAT/enhancer-binding protein (C/EBP) beta- and STAT3-mediated transcriptional activation of the haptoglobin promoter. *The Journal of biological chemistry*, 276(27), pp.24719–24725.

Zeiss, C.J., 2004. Proliferation of Microglia, but not Photoreceptors, in the Outer Nuclear Layer of the rd-1 Mouse. *Investigative ophthalmology & visual science*, 45(3), pp.971–976.

Zeng, H. et al., 2005. Identification of sequential events and factors associated with microglial activation, migration, and cytotoxicity in retinal degeneration in rd mice. *Investigative ophthalmology & visual science*, 46(8), pp.2992–2999.

Zhang, Z., Zhang, Z.-Y. & Schluesener, H.J., 2009. Compound A, a plant origin ligand of glucocorticoid receptors, increases regulatory T cells and M2 macrophages to attenuate experimental autoimmune neuritis with reduced side effects. *Journal of immunology (Baltimore, Md. : 1950)*, 183(5), pp.3081–3091.

Zhu, J., Nathan, C. & Ding, A., 1999. Suppression of macrophage responses to bacterial lipopolysaccharide by a non-secretory form of secretory leukocyte protease inhibitor. *Biochimica et Biophysica Acta (BBA) - Molecular Cell Research*, 1451(2-3), pp.219–223.

Zlotnik, A., Yoshie, O. & Nomiyama, H., 2006. The chemokine and chemokine receptor superfamilies and their molecular evolution. *Genome Biology*, 7(12), p.243.

7 Appendix

Appendix 1

Supplementary data for chapter 1 (Karlstetter et al. 2010):

```
Org.: ATG AAG ACA GCC ACA GTC TTG TTT CTG GTG GCT TTG ATC ACT GTG
Opt.: ATG AAA ACC GCC ACC GTC CTG TTC CTG GTT GCG CTG ATT ACC GTG
AA:    M   K   T   A   T   V   L   F   L   V   A   L   I   T   V

Org.: GGG ATG AAC ACT ACC TAT GTA GTG TCT TGC CCC AAA GAA TTT GAA
Opt.: GGT ATG AAT ACA ACC TAT GTG GTG TCC TGT CCG AAA GAA TTT GAG
AA:    G   M   N   T   T   Y   V   V   S   C   P   K   E   F   E

Org.: AAA CCT GGA GCT TGT CCC AAG CCT TCA CCA GAA AGT GTT GGA ATT
Opt.: AAA CCG GGT GCC TGC CCG AAA CCG AGT CCG GAA TCG GTT GGC ATT
AA:    K   P   G   A   C   P   K   P   S   P   E   S   V   G   I

Org.: TGT GTT GAT CAA TGC TCA GGA GAT GGA TCC TGC CCT GGC AAC ATG
Opt.: TGT GTG GAC CAG TGT AGC GGC GAT GGC AGT TGT CCG GGC AAC ATG
AA:    C   V   D   Q   C   S   G   D   G   S   C   P   G   N   M

Org.: AAG TGC TGT AGC AAT AGC TGT GGT CAT GTC TGC AAA ACT CCT GTC
Opt.: AAA TGC TGC AGC AAT AGC TGC GGC CAT GTG TGC AAA ACC CCG GTG
AA:    K   C   C   S   N   S   C   G   H   V   C   K   T   P   V

Org.: TTT TAA
Opt.: TTT TAA
AA:    F   *
```

Figure S1 Comparison of the mouse AMWAP open reading frame (top) and the codon optimized version (bottom) used for inducible expression in *E. coli* BL21 cells. The codon adaption index was increased from 0.70 before optimization to 0.91 after optimization.

A

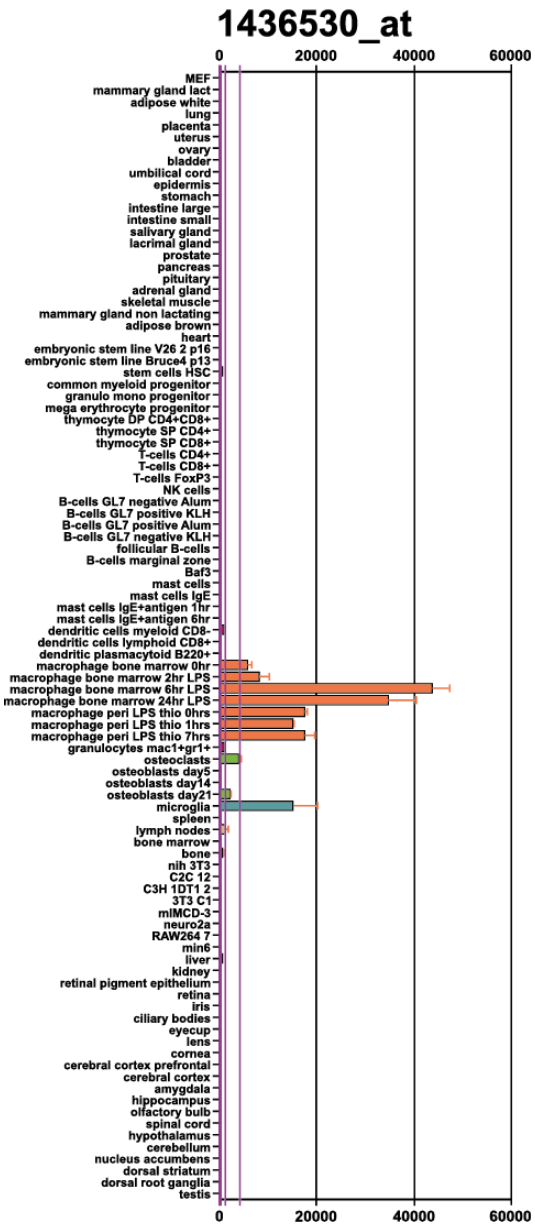

B

AMWAP (Mus musculus)

```
                                  CTTCCTCCCACACCCATAATTCTAGCTT

TACTGAGGCTATAAAATTATTTCATGAGTTCAGCCGAGCCAGAGCCAAC

1   ATGAAGACAGCCACAGTCTTGTTTCTGGTGGCTTTGATCACTGTG

46  GGGATGAACACTACCTATGTAGTGTCTTGCCCCAAAGAATTTGAA

91  AAACCTGGAGCTTGTCCCAAGCCTTCACCAGAAAGTGTTGGAATT

136 TGTGTTGATCAATGCTCAGGAGATGGATCCTGCCCTGGCAACATG

181 AAGTGCTGTAGCAATAGCTGTGGTCATGTCTGCAAAACTCCTGTC

226 TTTTAAATGGTTGACAGCCATGTGGAAGATGGATTCAATCTTCAT

AAACATGAATGATGGCCAGCCCCAGAAGATTTCTTCTGAATTCACAGAG

CCTGTGCTTGGCTACTTCCTAGCCCTAGAATTGCATTCTTGGACAAGGA

AGATCTATATTGTGGTGACAATGCCCTAATATGTCTGTGTCCAAAATAAA

CTACCCTTAGCATTCAAAAAAAAAAAAAAAA
```

Expi (Mus musculus)

```
                                                      A

CTGGAAAGCTGTTTTTTCTATATTTCCTGATTGACTGCCTCCTCCCACT

TTACTGAGGGTATAAATTGCTTCGTGAGTTCAACCCAGTCAGAGCCAAC

1   ATGAAGACAGCCACAGTCTTTGTTCTGGTAGCTTTGATTTTCATG

46  ACAATGACTACTGCCTGGGCTCTGTCTAACCCCAAAGAAAAACCT

91  GGCGCTTGTCCTAAGCCGCCCCCACGCAGTTTTGGAACTTGTGAT

136 GAACGATGCACAGGAGATGGATCGTGCTCTGGCAACATGAAGTGC

181 TGCAGCAATGGCTGTGGTCATGCCTGCAAACCTCCTGTCTTTTAA

CCATGTGGAAGATGGATCTTTATAAGCAGGACTGATGGCTAGCCCCAGA

AGATTTTTTTGAACCTACAGACCCCATGCTTGGCTCCTCCTTAGACCTA

GAATTGCATCCTTGGAAGAGGAAGATCTATACTGTGGTGACAGCTTCCT

AACGTGTTTGTGTCTAAAATAAACTATCCTTAGCATCCTTCCTGTTGAA

GAGTTCTTAAAAAAAAAAAAAAAAAAAAAAA
```

Figure S2 (A) Comprehensive expression profile of the AMWAP-specific Affymetrix probe set 1436530_at in various mouse tissues and cell types. Significant AMWAP transcript levels were specifically and exclusively detected in different macrophage populations and microglia. Data were obtained from the BioGPS database data (BioGPS, http://biogps.gnf.org and http://macrophages.com). (B) cDNA sequences of mouse AMWAP (top) and Expi (bottom) with underlined Affymetrix microarray probes. The probes used to detect AMWAP transcripts in isolated retinal microglia from wild-type and retinoschisin-deficient mice were highly specific for AMWAP and showed multiple gaps in the corresponding Expi cDNA sequence regions (indicated by gray shading).

Supplementary Table 1

Primer sequences and Roche Probe library IDs used for real-time qRT-PCR analysis

Gene	Accession No.	F-Primer (5'-3')	R-Primer (5'-3')	Probe ID
AMWAP	NM_001081957	TTTGATCACTGTGGGGATG	ACACTTTCTGGTGAAGGCTTG	1
CCL2	NM_011333	CATCCACGTGTTGGCTCA	GATCATCTTGCTGGTGAATGAGT	61
IL-1β	NM_008361	TGTAATGAAAGACGGCACACC	TCTTCTTTGGGTATTGCTTGG	78
IL-6	NM_031168	GATGGATGCTACCAAACTGGAT	CCAGGTAGCTATGGTACTCCAGA	6
CD206	NM_008625	GGACGAGCAGGTGCAGTT	CAACACATCCCGCCTTTC	47
Arginase 1	NM_007482.3	CCTGAAGGAACTGAAAGGAAAG	TTGGCAGATATGCAGGGAGT	2
PU.1	NM_32370	GGAGAAGCTGATGGCTTGG	CAGGCGAATCTTTTTCTTGC	94

Appendix 2

Abbreviations:

AcH3	Acetyl-histone H3
AD	Alzheimer's disease
AMD	Age-related macular degeneration
AMWAP	Activated Microglia/Macrophage WAP domain protein
Ap-1	Activator protein 1
Arg1	Arginase 1
ATP	Adenosin Triphosphate
B. subtilis	*Bacillus subtilis*
BBB	Blood brain barrier
Blvrb	Biliverdin reductase B
BM	Bone marrow
BRB	Blood retinal barrier
C3	Complement component 3
CAPE	Caffeic acid phenethyl ester
Casp	Caspase
Cbp	CREB-binding protein
Ccl2	Chemokine (C-C motif) ligand 2
Ccl3	Chemokine (C-C motif) ligand 3
Ccl4	Chemokine (C-C motif) ligand 4
Ccl5	Chemokine (C-C motif) ligand 5
Ccl6	Chemokine (C-C motif) ligand 6
Ccl9	Chemokine (C-C motif) ligand 9
Cd200	Cluster of differentiation 200
Cd200r	Cluster of differentiation 200 receptor
Cd206	Cluster of differentiation 206
Cd36	Cluster of differentiation 36
Cd83	Cluster of differentiation 83
Cfb	Complement factor b
ChIP	Chromatin Immunoprecipitation
Chop	C/EBP homologous protein
CHX	Cycloheximide
CM	Conditioned medium
cm^2	Square centimeters
CNS	Central nervous system
Cox2	Cyclooxygenase 2
CpG	CG-rich sequence
cRNA	Copy RNA
Csfr1	Colony stimulating factor receptor 1
CSPG-DS	Chondroitin sulfate disaccharide
Ct	Cycle threshold
CX3CL1	Chemokine (C-X3-C motif) ligand 1
CX3CR1	CX3C chemokine receptor 1
Cxcl10	C-X-C motif chemokine 10
Cy3	Cyanine 3
DAMP	Damage associated molecular patterns
DAPI	4',6-Diamidin-2-phenylindol
DAVID	Database for annotation, visualization and integrated genome discovery
Ddit	DNA damage-inducible transcript
ΔΔCt	Delta delta Cycle threshold
DHA	Docosahexaenoic acid
DISC	Death-inducing signaling complex
Dll1	Delta-like protein 1
DMEM	Dulbecco's modified eagle medium
DMSO	Dimethylsulfoxide
DNA	Deoxyribonucleic acid

E. coli	*Escherichia coli*
EGFP	Enhanced green fluorescent protein
Egr2	Early growth response protein 2
Expi	Extracellular proteinase inhibitor precursor
FAS	Tumor necrosis factor receptor superfamily, member 6
FCS	Fetal calf serum
FDR	False discovery rate
Fig	Figure
g	relative centrifuge force
Gadd153	Growth arrest and DNA damage induced-153
Gbp2	Guanylate binding protein 2
Gbp3	Guanylate binding protein 3
GCL	Glutamate cystein ligase
Gclm	Glutamate cystein ligase, modifier subunit
GEDI	Gene expression dynamics inspector
GEO	Gene expression omnibus
GFP	Green fluorescent protein
h	Hours
HDLS	Hereditary diffuse leukoencephalopathy with spheroids
HMGB1	High-mobility-group-protein b1
Hmox1	heme oxygenase-1
Hp	Haptoglobin
Ifi44	Interferon-induced protein 44
IFNAR	Interferon-α/β receptor
IFNβ	Interferon-β
IkBα	Nuclear factor of ‚kappa light polypeptide gene enhancer' in B-cells inhibitor, alpha
IL-1β	Interleukine-1β
IL-4	Interleukine-4
IL-6	Interleukine-6
IL-10	Interleukine-10
Inf-γ	Interferon-γ
INL	Inner nuclear layer
iNOS	Inducible nitric oxide synthase
IPL	Inner plexiform layer
iPS	Induced pluripotent stem cell
Irf7	Interferon regulatory factor 7
Kdr	Kinase insert domain receptor
LB medium	Luria broth medium
Lcn2	Lipocalin-2
LPC	Lysophosphatidylcholine
Lpcat	Lysophosphatidylcholine Acyltransferase
LPS	Lipopolysaccharide
Lyso-paf	*Lyso-platelet activation factor*
Lyso-pc	*Lyso-phosphatid*
Lyzs	Lysozyme
M-CSF	Macrophage colony-stimulating factor
Marco	Macrophage receptor with collagenous structure
mg	Milligram
min	Minute
miRNA	MicroRNA
ml	Milliliter
mm^2	Square millimeter
MMGT12	Murine cell line
mRNA	Messenger RNA
MS	Multiple Sclerosis
MTT	Methylthiazoletetrazolium
MZB1	Marginal zone B and B1 cell-specific protein
NFkB	Nuclear factor 'kappa-light-chain-enhancer' of activated B-cells
ng	Nanogram

nm	Nanometer
NO	Nitric oxide
Nos2	Nitric oxide synthase-2
Nrf2	NF-E2-related factor 2
Ntng1	Netrin-G1
Nupr1	Nuclear protein transcriptional regulator 1
OD	Optical density
OHT	Hydroxytamoxifen
ONL	Outer nuclear layer
OPL	Outer plexiform layer
OS	Outer segments
P. aeruginosa	Pseudomonas aeruginosa
P2Y12	Purinergic receptor P2Y, G-protein coupled, 12
PAM3CSK	Tripalmitoylated lipopetide Cysteine, Serine, Lysine 4
PBS	Phosphate buffered saline
PCR	Polymerase chain reaction
Pecam1	Platelet endothelial cell adhesion molecule 1
Perp1	Plasma cell-induced resident ER protein
PET	Positron emission tomography
PMSF	Phenylmethylsulfonylfluorid
PPARa	Peroxisome proliferator-activated receptor alpha
PS1	Presenilin 1
Ptgs	Prostaglandin-endoperoxide synthase 2
PU.1	Purine-rich box-1
qRT-PCR	Quantitative real-time PCR
Rd	Retinal degeneration
Rds	Retinal degeneration slow
Rho	Rhodopsin
RLM-RACE	RNA-ligase mediated rapid amplification of cDNA-ends
RMA	Robust multichip average
RNA	Ribonucleic acid
Rnf145	Ring finger protein 145
ROS	Reactive oxgen species
RP	Retinitis pigmentosa
RPE	Retinal pigment epithelium
Rpm	Rotations per minute
RPMI	Roswell park memorial institute
Rs1h	Retinoschisin murine homolog
SAM	Significance analysis of microarrays
SD	Standard deviation
SDS	Sodium dodecyl sulfate
siRNA	Small interfering RNA
SLPI	Secretory leukocyte protease inhibitor
SOM	Self-organizing maps
SPP1	Secreted phosphoprotein 1
Srxn1	Sulfiredoxin
STAP-1	Signal-transducing adaptor protein 1
STAT	Signal transducers and activators of transcription protein
SWAM1	Single WAP motif protein 1
TIFF	Tagged image file format
TLR	Toll-like receptor
TLR4	Toll-like receptor 4
TLR9	Toll-like receptor 9
TNF	Tumor necrosis factor
TNFR1	Tumor necrosis factor receptor-1
TREM2	Triggering receptor expressed on myeloid cells 2
TRITC	Tetramethylrhodamine-5-(and 6)-isothiocyanate
TSPO	Translocator protein
TUNEL	TdT-mediated dUTP-biotin nick end labeling

U	Unit
µm	Micrometer
Vegfr2	Vascular Endothelial Growth Factor Receptor 2
WAP	Whey acidic protein
wt	Wild-type

Appendix 3

Publications:

Karlstetter M, Lippe E, Walczak Y, Moehle C, Aslanidis A, Mirza M, Langmann T.Curcumin is a potent modulator of microglial gene expression and migration. *J Neuroinflammation*. 2011 Sep 29;8:125.

Kraus D, **Karlstetter M**, Walczak Y, Hilfinger D, Langmann T, Weber BH. Retinal expression of the X-linked juvenile retinoschisis (RS1) gene is controlled by an upstream CpG island and two opposing CRX-bound regions. *Biochim Biophys Acta*. 2011 Apr-Jun;1809(4-6):245-54.

Karlstetter M, Walczak Y, Weigelt K, Ebert S, Van den Brulle J, Schwer H, Fuchshofer R, Langmann T. The novel activated microglia/macrophage WAP domain protein, AMWAP, acts as a counter-regulator of proinflammatory response. *J Immunol*. 2010 Sep 15;185(6):3379-90.

Langmann T, Di Gioia SA, Rau I, Stöhr H, Maksimovic NS, Corbo JC, Renner AB, Zrenner E, Kumaramanickavel G, **Karlstetter M**, Arsenijevic Y, Weber BH, Gal A, Rivolta C. Nonsense mutations in FAM161A cause RP28-associated recessive retinitis pigmentosa. *Am J Hum Genet*. 2010 Sep 10;87(3):376-81.

Corbo JC, Lawrence KA, **Karlstetter M**, Myers CA, Abdelaziz M, Dirkes W, Weigelt K, Seifert M, Benes V, Fritsche LG, Weber BH, Langmann T. CRX ChIP-seq reveals the cis-regulatory architecture of mouse photoreceptors. *Genome Res*. 2010 Nov;20(11):1512-25.

Karlstetter M, Ebert S, Langmann T. Microglia in the healthy and degenerating retina: insights from novel mouse models. *Immunobiology*. 2010 Sep-Oct;215(9-10):685-91. Review.

Dirscherl K, **Karlstetter M**, Ebert S, Kraus D, Hlawatsch J, Walczak Y, Moehle C, Fuchshofer R, Langmann T. Luteolin triggers global changes in the microglial transcriptome leading to a unique anti-inflammatory and neuroprotective phenotype. *J Neuroinflammation*. 2010 Jan 14;7:3.

Stoecker K, Weigelt K, Ebert S, **Karlstetter M**, Walczak Y, Langmann T.Induction of STAP-1 promotes neurotoxic activation of microglia. *Biochem Biophys Res Commun*. 2009 Jan 30;379(1):121-6.

Appendix 4

Conference contributions:

2009

Pro Retina Research-Colloquium
Potsdam, Germany
The novel activated microglia WAP domain protein, AMWAP, is induced during microglia activation and acts as a negative regulator of the pro-inflammatory response (Poster)

Annual Meeting of the European Macrophage and Dendritic Cell Society (EMDS)
Regensburg, Germany
The novel activated microglia WAP domain protein, AMWAP, is induced during microglia activation and acts as a negative regulator of the pro-inflammatory response (Poster)

2010

Pro Retina Research-Colloquium
Potsdam, Germany
The novel activated microglia WAP domain protein, AMWAP, is induced during microglia activation and acts as a negative regulator of the pro-inflammatory response (Poster)

XIVth International Symposium on Retinal Degeneration
Mont Tremblant, Canada
The novel activated microglia WAP domain protein, AMWAP, is induced during microglia activation and acts as a negative regulator of the pro-inflammatory response (Poster)

Annual Meeting of the European Macrophage and Dendritic Cell Society (EMDS)
Edinburgh, UK
The novel activated microglia WAP domain protein, AMWAP, is induced during microglia activation and acts as a negative regulator of the pro-inflammatory response (Poster)

22nd Meeting of the German Society of Human Genetics
Regensburg, Germany
Transcriptional Regulation and retinal knock-down of Fam161a, the mouse ortholog of the human RP28 gene (Poster)

2011

Pro Retina Research-Colloquium
Potsdam, Germany
PU.1 and NFkB control Activated Macrophage/Microglia WAP domain protein (AMWAP) expression during microglial activation (Poster)

Gordon Research Conference Mammary Gland Biology
Newport, Rhode Island, USA
The novel whey acidic protein AMWAP acts as a negative regulator of the pro-inflammatory response (Poster)

10th European meeting on Glial Cells in Health and Disease
Prague, Czech Republic
The novel Activated Microglia/Macrophage WAP Domain Protein, AMWAP, is induced during microglial activation and acts as a negative regulator of the pro-inflammatory response (Poster)

Further projects associated with this thesis:

Medical thesis Konstantin Dirscherl

Medical thesis Elena Lippe

Curriculum vitae

Marcus Karlstetter, Diplom-Biologe

* 5. März 1982 in Passau

Promotion

seit 02/2009	Institut für Humangenetik, Universität Regensburg ‘Modulation and function of microglial phenotypes’
04/2011 bis 07/2011	Gastwissenschaftler, Labor Prof. Hennighausen, National Institutes of Health, Bethesda, USA

Studium

03/2008 bis 12/2008	Diplomarbeit AG Langmann, Institut für Humangenetik, Universität Regensburg
09/2006 bis 07/2007	Auslandsstudium University of Leicester, UK
10/2002 bis 12/2008	Studium der Biologie, Universität Regensburg Hauptfach: Zellbiologie Erstes Nebenfach: Biochemie Zweites Nebenfach: Entwicklungsbiologie
Okt. 2001 bis Okt. 2002	Studium der Pädagogik und Soziologie (M.A.), Universität Regensburg

Schule

Mai 2001	Abitur, Adalbert Stifter Gymnasium Passau

Stipendien

07/2010	Reisestipendium der Pro Retina Deutschland e.V., Retinal Degeneration Symposium, Mont Tremblant, Kanada
08/2009 bis 08/2011	Promotionsstipendium des Elitenetzwerk Bayern

Danksagung

Ein ganz besonderer Dank gilt meinem Doktorvater *Herrn Prof. Dr. Thomas Langmann*, der nicht nur die wissenschaftliche Betreuung meiner Doktorarbeit übernommen und dessen Voranschreiten durch seine hilfreichen Ratschläge und anregenden Diskussionen begleitete, sondern mich auch im Hinblick auf meine fachliche, berufliche und persönliche Weiterentwicklung stets gefördert hat.

Bedanken möchte ich mich auch bei *Herrn Prof. Dr. Stephan Schneuwly* für die Übernahme des Zweitgutachtens und seine ständige Hilfsbereitschaft während meines gesamten Studiums.

Ich danke *Herrn Prof. Dr. Wolf Hayo Castrop* und *Herrn Prof. Dr. Thomas Dresselhaus* sich als Drittprüfer bzw. Vorsitzender des Prüfungsausschusses zur Verfügung zu stellen.

Bei *Herrn Prof. Dr. Bernhard Weber* bedanke ich mich für die Bereitstellung des Arbeitsplatzes am Institut für Humangenetik.

Ich bedanke mich bei *Herrn Prof. Dr. Lothar Hennighausen*, dass ich drei Monate in seinem Labor am NIH arbeiten konnte.

Ein Großer Dank gilt an dieser Stelle auch *Yana Walczak* für die stets lustige Zeit, die gute Zusammenarbeit und ihre unermüdliche Unterstützung im Labor.

Nicht versäumen will ich es, mich bei allen momentanen und ehemaligen Kollegen der AG Langmann und dem Institut für Humangenetik zu bedanken. Für die angenehme Arbeitsatmosphäre und konstruktive Zusammenarbeit richte ich ein herzliches Dankeschön an *Stefanie Ebert*, *Tobias Härtinger*, *Alexander Aslanidis*, *Dominik Kraus*, *Julia Hlawatsch, Karin Weigelt* und *Konstantin Dirscherl*. Großer Dank gebührt auch *Jürgen Kaschkötö* für seine außerordentliche Unterstützung im EDV-Bereich. Für die stete Versorgung mit Espresso und den kurzweiligen Gesprächen danke ich den ‘Espresso-Club’-Mitgliedern *Lars Fritsche* und *Regina Gellner*. *Kerstin Rückl* und *Frank Zach* sei gedankt für ihre ständige Hilfsbereitschaft in proteinbiochemischen Fragen. Bei dem Team unserer Diagnostikabteilung bedanke ich mich für die immer zügige Abwicklung der Sequenzierungen.

Großer Dank gebührt auch allen meinen Freunden, die mich stets bei Laune gehalten haben und mir den nötigen Ausgleich zum Laboralltag verschafften.

Ein besonders herzlicher Dank gilt meiner Familie, insbesondere meinen Eltern *Rainer* und *Gudrun Karlstetter*, denen ich diese Arbeit widme. Sie haben mir meine akademische Ausbildung ermöglicht und mir stets uneingeschränkten Rückhalt gegeben.

Zu guter Letzt geht mein ganz persönlicher Dank an meine Freundin *Daniela Hilfinger*, die mich während meiner gesamten Doktorarbeit immerwährend motiviert hat, mir mit ihren wertvollen Ratschlägen zur Seite stand und mir zur richtigen Zeit die nötige Ruhe gab.